

CONJUGATED POLYMER BASED MATERIALS  
VIA THE INCORPORATION OF POLYMERIZABLE UNITS

by

HYUN A KANG

B.S. Chemistry  
Korea Advanced Institute of Science and Technology, 1998

Submitted to the Department of Chemistry  
in Partial Fulfillment of the Requirements for the Degree of

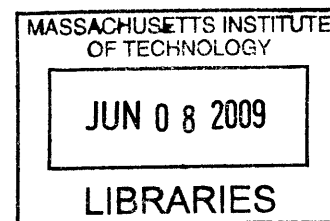
DOCTOR OF PHILOSOPHY IN CHEMISTRY

at the

MASSACHUSETTS INSTITUTE OF TECHNOLOGY

JUNE 2009

**ARCHIVES**



© 2009 Massachusetts Institute of Technology. All rights reserved.

Signature of Author: \_\_\_\_\_  
Department of Chemistry  
May 22, 2009

Certified by: \_\_\_\_\_  
Timothy M. Swager  
John D. MacArthur Professor of Chemistry  
Thesis Supervisor

Accepted by: \_\_\_\_\_  
Robert W. Field  
Haslam and Dewey Professor of Chemistry  
Chairman, Departmental Committee on Graduate Students

This doctoral thesis has been examined by a Committee of the Department of Chemistry as follows:

Professor Gregory C. Fu: \_\_\_\_\_  
Chairman

Professor Timothy M. Swager: \_\_\_\_\_  
Thesis Advisor

Professor Edwin L. Thomas: \_\_\_\_\_  
Department of Materials Science and Engineering



*Dedicated to My Family*

# Conjugated Polymer Based Materials via the Incorporation of Polymerizable Units

by

HYUN A KANG

Submitted to the Department of Chemistry on May 22, 2009  
in Partial Fulfillment of the requirements for the Degree of  
Doctor of Philosophy in Chemistry

## ABSTRACT

Since the discovery of conducting polymers (CPs), efforts have focused on synthesizing CPs with improved processability, and finding new applications for the unique conjugated structure of CPs. This Thesis details the development of new CP based materials by block copolymerization and/or end-capping with polymerizable units.

In Chapter 1, three different norbornene derivatives having phenylene-heterocyclic moieties were copolymerized with either norbornene or 7-oxanorbornene derivatives via ring-opening metathesis polymerization (ROMP). Block copolymers' stabilities and solubilities could be improved by hydrogenation of double bonds in the polymer backbone. The block copolymers were subsequently cross-linked by anodic electropolymerization of phenylene-heterocycle moieties, affording conducting polymers. All of these three block copolymers were readily deposited on the electrode substrates, and their cyclic voltammograms revealed an excellent reversibility in the redox cycles. The deposited polymer films also showed reversible color change between oxidized and neutral states.

In Chapter 2, three different conjugated polymers having interesting properties and/or useful applications were synthesized and end-capped with norbornene using the hydroarylation reaction. These norbornene end-capped CPs became macroinitiators using Grubbs' catalysts, and they were used to prepare block copolymers by polymerizing ROMP monomers. Prepared block copolymers were rubbery like outer elastomers while having similar optical properties to their center CPs.

In Chapter 3, three different iptycene-poly(phenylene ethynylene)s, which were known to form well-aligned and chain-extended structures in nematic liquid crystals (LCs), were synthesized and end-capped with the compound capable of strong hydrogen bonding. Then, LC-polymer gels were prepared to see their effect on the vertically aligned nematic liquid crystal display's switching speed, particularly relaxation time. Prepared LC mixtures had similar phase transition temperature to pure LC. Unfortunately, the polymers could not improve the LC's switching speed in the vertically aligned mode probably because these polymers could not form a stable physical gel state within the LC test cell.

Thesis Supervisor: Timothy M. Swager  
Title: Department Head, Professor of Chemistry

## Table of Contents

Abstract .....	4
Table of Contents .....	5
List of Figures .....	6
List of Tables .....	9
List of Schemes .....	10
<b>Chapter 1: Conductive Block Copolymers Integrated into Polynorbornene-Derived Scaffolds .....</b>	<b>11</b>
Introduction .....	12
Results and Discussion .....	18
Conclusions .....	40
Experimental Section .....	41
References .....	51
<b>Chapter 2: Block Copolymers from Norbornene End Functionalized Conjugated Polymers Using ROMP .....</b>	<b>54</b>
Introduction .....	55
Results and Discussion .....	62
Conclusions .....	77
Experimental Section .....	78
References .....	86
<b>Chapter 3: Liquid Crystalline Gels Using Iptycene-PPEs Through Hydrogen Bonding .....</b>	<b>90</b>
Introduction .....	91
Results and Discussion .....	99
Conclusions .....	108
Experimental Section .....	109
References .....	114
Curriculum Vitae .....	117
Acknowledgements .....	119
Appendix 1: NMR spectra for Chapter 1 .....	121
Appendix 2: NMR spectra for Chapter 2 .....	145
Appendix 3: NMR spectra for Chapter 3 .....	158

## List of Figures

### Chapter 1

<b>Figure 1-1.</b>	Families of conducting polymers. ....	12
<b>Figure 1-2.</b>	Oxidative polymerization mechanism of thiophene. ....	13
<b>Figure 1-3.</b>	Electronic band diagram for CPs showing (a) neutral state, (b) polaron states, (c) bipolaron states and (d) bipolaron bands. ....	14
<b>Figure 1-4.</b>	A general mechanism of ROMP. ....	16
<b>Figure 1-5.</b>	Grubbs' catalysts. ....	20
<b>Figure 1-6.</b>	Structures of homopolymers. ....	20
<b>Figure 1-7.</b>	<sup>1</sup> H-NMR spectra in CDCl <sub>3</sub> of poly( <b>12</b> ) polymerized with <b>15</b> (top) and <b>13</b> (bottom). ....	22
<b>Figure 1-8.</b>	GPC traces of poly( <b>12</b> ) and resulting block copolymer <b>BCP4</b> . ....	24
<b>Figure 1-9.</b>	<sup>1</sup> H-NMR spectra in CDCl <sub>3</sub> of poly( <b>9</b> ) (top left), hydrogenated poly( <b>9</b> ) (bottom left), poly( <b>12</b> ) (top right) and hydrogenated poly( <b>12</b> ) (bottom right). ....	26
<b>Figure 1-10.</b>	Freestanding films of block copolymers and their hydrogenated polymers. ....	27
<b>Figure 1-11.</b>	DSC curves of (a) block copolymers and (b) their hydrogenated block copolymers. ....	28
<b>Figure 1-12.</b>	The generic electrochemical cell for cyclic voltammetry (W, working electrode; R, reference electrode; C, counter electrode). ....	30
<b>Figure 1-13.</b>	Electropolymerizations of monomers <b>4</b> (a), <b>5</b> (b) and <b>6</b> (c), and block copolymers <b>BCP1</b> (d), <b>BCP2</b> (e) and <b>BCP3</b> (f) on Pt button electrodes in CH <sub>3</sub> CN (for monomers <b>4</b> – <b>6</b> ) or CH <sub>2</sub> Cl <sub>2</sub> (for polymers <b>BCP1</b> – <b>BCP3</b> ) solutions containing 0.1 M TBAPF <sub>6</sub> . Dotted lines represent the first scans and all CVs obtained at scan rate of 100 mV/s. ....	31
<b>Figure 1-14.</b>	CVs of electrodeposited films of monomers <b>4</b> (a), <b>5</b> (b) and <b>6</b> (c), and homopolymers poly( <b>4</b> ) (d), poly( <b>5</b> ) (e) and poly( <b>6</b> ) (f) on Pt button electrodes in CH <sub>3</sub> CN (for monomers <b>4</b> – <b>6</b> ) or CH <sub>2</sub> Cl <sub>2</sub> (for homopolymers poly( <b>4</b> ) – poly( <b>6</b> )) solutions containing 0.1 M TBAPF <sub>6</sub> . Polymer film CVs were obtained at 25 – 200 mV/s. ....	32
<b>Figure 1-15.</b>	CVs of electrodeposited films of block copolymers <b>BCP1</b> (a), <b>BCP2</b> (b) and <b>BCP3</b> (c), and hydrogenated block copolymers <b>BCP1</b> (d), <b>BCP2</b> (e) and <b>BCP3</b> (f) on Pt button electrodes in 0.1 M TBAPF <sub>6</sub> of CH <sub>2</sub> Cl <sub>2</sub> solution. Polymer film CVs were obtained at 25 – 200 mV/s. ....	35

<b>Figure 1-16.</b>	CVs of electrodeposited films of block copolymers <b>BCP4</b> (a), <b>BCP5</b> (b) and <b>BCP6</b> (c), and hydrogenated block copolymers <b>BCP4</b> (d), <b>BCP5</b> (e) and <b>BCP6</b> (f) on Pt button electrodes in 0.1 M TBAPF <sub>6</sub> of CH <sub>2</sub> Cl <sub>2</sub> solution. Polymer film CVs were obtained at 25 – 200 mV/s. ....	36
<b>Figure 1-17.</b>	Reversible color change (forest green to black) of deposited polymer film ( <b>BCP1</b> ) on a gold electrode during redox cycle and CV of the corresponding polymer film. ....	37
<b>Figure 1-18.</b>	UV–vis absorption spectra of <b>5</b> (top), <b>BCP2</b> (middle) and hydrogenated <b>BCP5</b> (bottom) on ITO-coated glass electrodes in CH <sub>2</sub> Cl <sub>2</sub> solution containing 0.1 M TBAPF <sub>6</sub> between 0.0 V and 0.9 V (vs Ag/Ag <sup>+</sup> ). ....	38
 <b>Chapter 2</b>		
<b>Figure 2-1.</b>	Representative base structures of conjugated polymers synthesized by organometallic coupling reactions. ....	55
<b>Figure 2-2.</b>	Two examples of ABA-type triblock copolymers containing CPs. ....	56
<b>Figure 2-3.</b>	Three selected conjugated polymers prepared by three different cross-coupling reactions; <b>P1</b> from the Stille reaction, <b>P2</b> from the Sonogashira reaction and <b>P3</b> from the Suzuki reaction. ....	59
<b>Figure 2-4.</b>	Grubbs' catalysts. ....	63
<b>Figure 2-5.</b>	A gel state of (a) polymerized <b>4</b> and (b) polymerized <b>6</b> in the vials. (The faint colors originated from residual catalysts.) ....	64
<b>Figure 2-6.</b>	Image of <b>P4</b> in solution and its fluorescent image. ....	66
<b>Figure 2-7.</b>	Absorption and fluorescence spectra of <b>P4</b> ( <i>M<sub>n</sub></i> = 14,900) measured (a) in THF solution and (b) in a spin-cast thin film. ....	66
<b>Figure 2-8.</b>	(a) A gel state of <b>P5</b> after ROMP, (b) its fluorescent image and (c) a gel state of <b>P6</b> after ROMP. (The faint colors originated from residual catalysts.) ....	70
<b>Figure 2-9.</b>	GPC traces of a block copolymer, PNB- <b>P4</b> -PNB, with refractive index detection (---) and UV/vis detection (—) (450 nm). ....	73
<b>Figure 2-10.</b>	ROMP monomers examined for block copolymerization. ....	73
<b>Figure 2-11.</b>	GPC traces of a block copolymer, poly(10)- <b>P4</b> -poly(10), with refractive index detection (---) and UV/vis detection (—) (450 nm). ....	75
 <b>Chapter 3</b>		
<b>Figure 3-1.</b>	Schematic illustration of phase transition behavior and the molecular order of LCs and their different structural representation. ....	91

<b>Figure 3-2.</b>	Setup and basic principle of the VA switching mode. ....	92
<b>Figure 3-3.</b>	Representative LCs with negative dielectric anisotropy ( $\Delta \epsilon$ ) and medium birefringence ( $\Delta n$ ). ....	93
<b>Figure 3-4.</b>	(a) Definition of “internal free volume” and (b) “minimization of free volume” alignment of iptycene in nematic LCs. ....	95
<b>Figure 3-5.</b>	(a) The PPE structure having the highest anisotropic ordering in nematic LCs and (b) the dimerization of the Upy functional group via quadruple hydrogen bonding (keto tautomer). ....	96
<b>Figure 3-6.</b>	Gelated <b>P1</b> in $\text{CHCl}_3$ (4.0 mg of <b>P1</b> in 0.2 ml $\text{CHCl}_3$ ) and dried polymer film. ....	101
<b>Figure 3-7.</b>	Preparation of LC-polymer gel. ....	102
<b>Figure 3-8.</b>	The LC test cell filled with MLC-6884 (a) light transmission state (0 V) (b) light scattering state (10 V). ....	104
<b>Figure 3-9.</b>	(a) Fluorescent image of a LC test cell filled with <b>P1</b> in MLC-6884 under illumination with 365 nm light and (b) schematic illustration of the LC test cell. ....	105
<b>Figure 3-10.</b>	The electro-optic response of MLC-6884 when a square wave driving voltage (1 kHz AC, 2.25 V) was applied for approximately 5 seconds. (The noise in the voltage was caused by the data acquisition device due to the high frequency of the square wave. The small peak after 5s was induced by switching the power off.) ....	106
<b>Figure 3-11.</b>	Wire attached LC test cell. ....	110
<b>Figure 3-12.</b>	Experimental setup for switching tests. ....	110

## List of Tables

### Chapter 1

<b>Table 1-1.</b>	GPC results of homopolymerizations .....	21
<b>Table 1-2.</b>	GPC results of block copolymerizations .....	24
<b>Table 1-3.</b>	$T_g$ s of block copolymers .....	27
<b>Table 1-4.</b>	Experimental band gaps (eV) of conjugated polymers from monomers and block copolymers.....	39
<b>Table 1-5.</b>	Reported band gaps (eV) of poly[1,4-bis(2-heterocycle)- <i>p</i> -phenylenes] .....	39

### Chapter 2

<b>Table 2-1.</b>	Molecular weight of norbornene end-capped CPs .....	69
<b>Table 2-2.</b>	Molecular weight of CPs and their macroinitiators .....	71
<b>Table 2-3.</b>	GPC results of homopolymerizations .....	74
<b>Table 2-4.</b>	Molecular weight of block copolymers .....	76

### Chapter 3

<b>Table 3-1.</b>	Physical properties of MLC-6884 .....	98
<b>Table 3-2.</b>	GPC results of polymerizations .....	101
<b>Table 3-3.</b>	$T_{iso}$ of LC mixtures .....	103
<b>Table 3-4.</b>	$\tau_{decay}$ of LC mixtures .....	107

## List of Schemes

### Chapter 1

<b>Scheme 1-1.</b> .....	17
<b>Scheme 1-2.</b> .....	18
<b>Scheme 1-3.</b> .....	19
<b>Scheme 1-4.</b> .....	23
<b>Scheme 1-5.</b> .....	25
<b>Scheme 1-6.</b> .....	29

### Chapter 2

<b>Scheme 2-1.</b> .....	57
<b>Scheme 2-2.</b> .....	58
<b>Scheme 2-3.</b> .....	62
<b>Scheme 2-4.</b> .....	64
<b>Scheme 2-5.</b> .....	65
<b>Scheme 2-6.</b> .....	67
<b>Scheme 2-7.</b> .....	68

### Chapter 3

<b>Scheme 3-1.</b> .....	100
--------------------------	-----



**CHAPTER 1**

**Conductive Block Copolymers Integrated into  
Polynorbornene-Derived Scaffolds**

Adapted from

Kang, H.; Bronstein, H. E.; Swager, T. M. *Macromolecules* **2008**, *41*, 5540-5547.

## Introduction

Since the discovery of conductivity in polymers in 1961 by Hatano and coworkers and conductivity enhancement of doped polyacetylene in 1977 by Shirakawa, MacDiarmid and Heeger, conducting polymers (CPs) continue to receive broad attention due to expanding applications possibilities resulting from their electronic and optical properties.<sup>1</sup> This new class of polymers has been devised with the remarkable ability to conduct electrical current unlike the insulating properties of most polymers (plastics). The ability of CPs to display both the mechanical properties of a polymer and the electrical properties of a conductor has ensured their potential for technological applications. However, the applicability of polyacetylene, the first CP, is very limited because of difficulty in processing and the rapid decrease in conductivity upon exposure to air. Therefore, CPs based on poly(*p*-phenylene), polypyrrole and polythiophene backbones have been studied the most since they are chemically and electronically stable in both the oxidized and neutral states (Figure 1-1).<sup>2</sup>

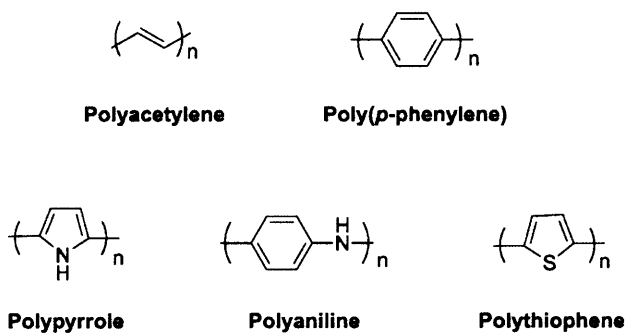


**Figure 1-1.** Families of conducting polymers.

CPs are generally synthesized via chemical or electrochemical polymerizations that

proceed by a step growth mechanism, that is shown in Figure 1-2 using thiophene as an example. The heterocycle ring is oxidized to form a radical cation, which then reacts with a second radical cation to form a dimer by elimination of two protons. This dimer, more easily oxidized than the monomer, then reacts further to give higher oligomers, until the oligomers become insoluble and precipitate onto the electrode surface or substrate as a polymer.

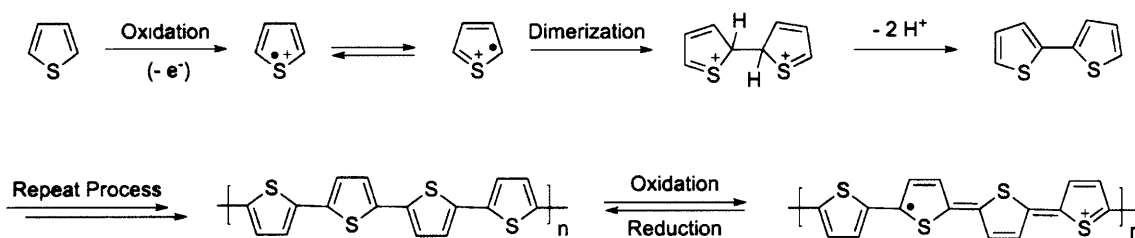


**Figure 1-2.** Oxidative polymerization mechanism of thiophene.

All conductive polymers have one thing in common: they contain extended  $\pi$ -conjugated systems. The electrical properties of materials are determined by their electronic structures. In band theory, the highest energy band formed at 0 K from a set of full orbitals is termed the valence band (VB), and the lowest energy band formed from orbitals at 0 K that have not been filled is termed the conductance band (CB). The spacing between these two bands is called the band gap. If very little energy is required to excite electrons to higher energy levels then partially occupied bands are present and the material is conductive. Alternatively, if there is no gap then the material can have metallic properties. If the band gap is too large for electrons to be excited across the gap at room temperature, the material is

an insulator. In a semiconductor, the band gap is small enough (arbitrarily defined as  $< 3$  eV) for electrons to be energetically excited from one band to another, thereby enabling current to flow upon application of an appropriate stimulus.

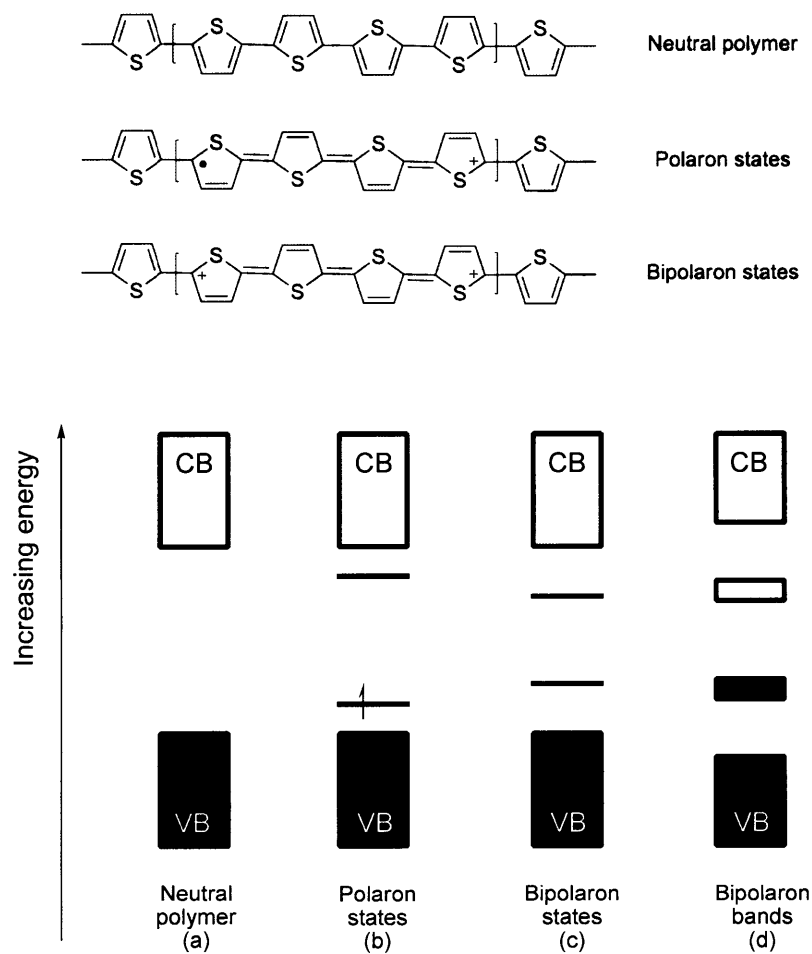


**Figure 1-3.** Electronic band diagram for CPs showing (a) neutral state, (b) polaron states, (c) bipolaron states and (d) bipolaron bands (adapted from ref 3).

CPs conduct current without having a partially empty (or partially filled) band.

Figure 1-3 illustrates the electronic band diagram for CPs at various oxidation stages. The

neutral CP is a semiconductor and its electronic band model is characterized by an empty band gap (Figure 1-3(a)). When an electron is removed from the polymer chain by oxidation, a radical cation is produced which partially delocalizes over a small number of monomer units and causing changes in the local band lengths.<sup>3</sup> This delocalized radical cation is termed a polaron, derived from the fact that it polarizes its surroundings in order to stabilize itself. This polarization results in two localized electronic levels within the band gap (Figure 1-3(b)). If another electron is removed from the polymer by further oxidation, it can either come from a separate site, in which case a second polaron is created, or the lone electron in the polaron can be removed to create a bipolaron (Figure 1-3(c)). When the polymer contains a high density of bipolarons, wherein these delocalized species interact then a band of states is formed (Figure 1-3(d)).

Although electrochemical syntheses of CPs are convenient methods, there are several limitations to this approach such as low yields, low processability and complex morphologies.<sup>4,5</sup> One approach to overcome these limitations is the use of precursor polymers having pendant electroactive moieties.<sup>5,6</sup> In previous investigations, processable precursor polymers obtained from ring-opening metathesis polymerization (ROMP),<sup>7</sup> which can provide controlled molecular weights, produced high quality of CPs after oxidative cross-linking. Most recently, the Sotzing group has developed a solid-state oxidative cross-linking (SOC) technique in which a precursor polymer containing pendant terthiophene prepared by ROMP was electropolymerized in the solid swollen state.<sup>4</sup> An advantage of the SOC technique is to afford more highly conjugated CPs than conventional electrochemical polymerization, and this technique was applied to the fabrication of plastic nanoscale electronic devices using scanning probe-based lithography.<sup>4(c)</sup>

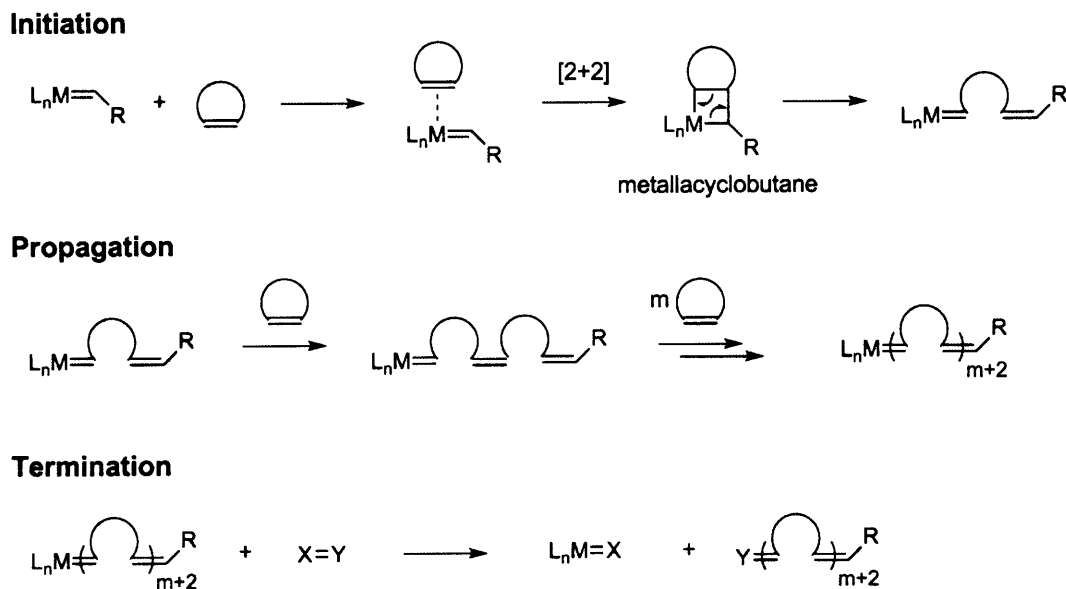


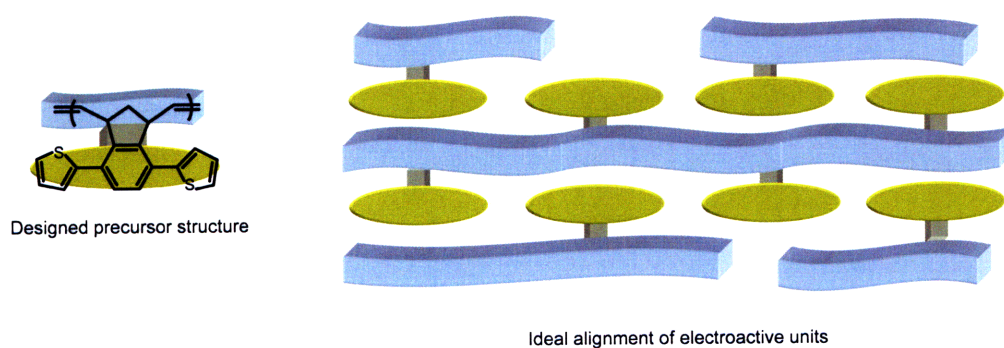
**Figure 1-4.** A general mechanism of ROMP (adapted from ref 8(c)).

ROMP has been shown to be an efficient method to control a polymer's molecular structure, size and bulk properties since its discovery in the 1960s.<sup>8</sup> Currently, well-defined ruthenium-based catalysts are the most popular for ROMP because of their tolerance toward oxygen, moistures, and a variety of functionalities in addition to high activities.<sup>9</sup> Functionalized norbornene derivatives are excellent monomers in the preparation of a wide range of polymeric structures via ROMP. They are active monomers for living ROMP due to the strained nature of the norbornene ring. Besides, functionalized norbornene derivatives are readily prepared via Diels-Alder reaction of a diene, most generally furan or cyclopentadiene, and a dienophile possessing a desired functional group.<sup>10</sup> The reaction mechanism of ROMP involves the [2+2] cycloaddition of metal-alkylidene species with a

cyclic olefin to form a metallacyclobutane intermediate, which subsequently undergoes ring opening to regenerate the metal-alkylidene species (Figure 1-4).<sup>8(c),10</sup> The reaction is driven forward by the release of ring strain in the cyclic olefin.

The tendency of the block copolymer blocks to phase-separate can result in self-assembly of these electronic polymers into a variety of nanoscale structures.<sup>11</sup> Well-defined nanostructures of conducting polymers are especially attractive because controlled structures are needed to optimize numerous applications. Toward this end, we have designed new precursor monomers with a two point fused phenylene ring to force co-alignment of CP backbone with the initial backbone produced by ROMP (Scheme 1-1).

**Scheme 1-1.**



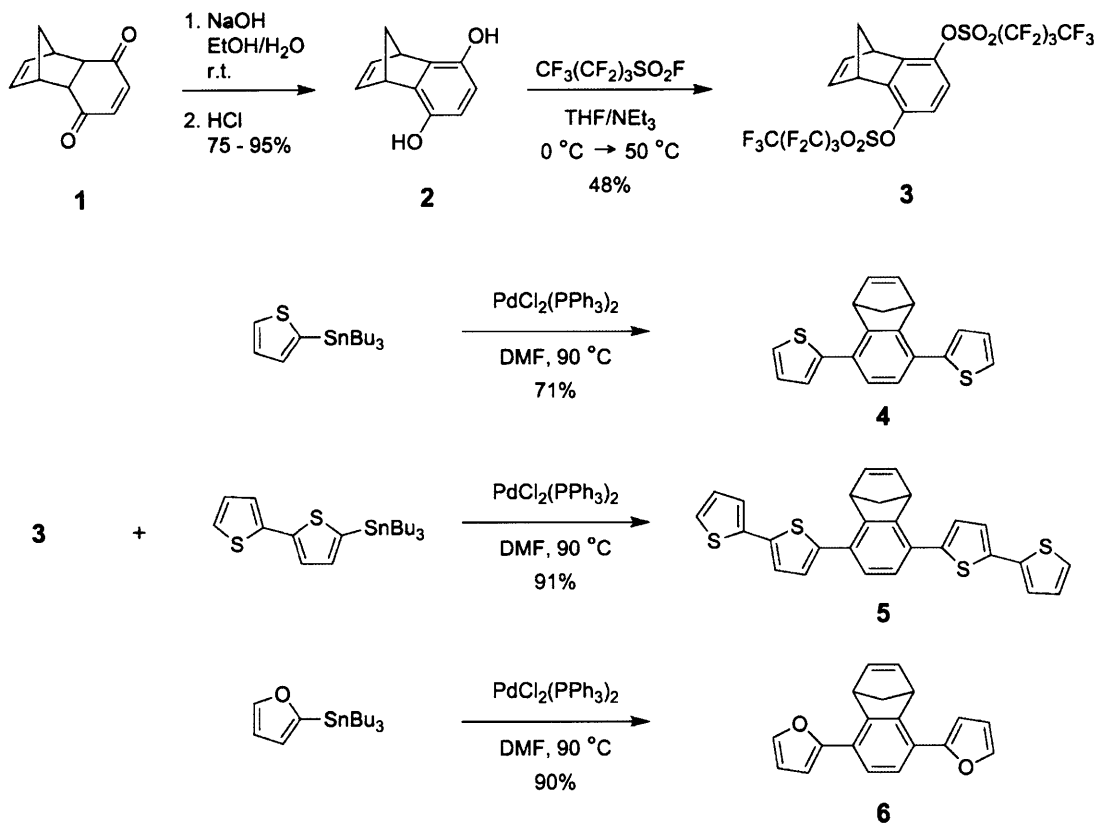
In this chapter, we report conductive block copolymers synthesized from three different norbornene derivatives having phenylene–thiophene, phenylene–bithiophene and phenylene–furan structures. The polynorbornene backbone is a choice structure because of its flexibility, low glass transition temperature, inertness to electrochemical side reactions,<sup>12</sup> and ease of preparation via living ROMP.<sup>13</sup>

## Results and Discussion

### Monomer Synthesis

A series of norbornene derivatives having thiophene (**4**), bithiophene (**5**) and furan (**6**) moieties were synthesized as monomers for electroactive block copolymers (Scheme 1-2). A Diels-Alder reaction between 1,3-cyclopentadiene and 1,4-benzoquinone afforded compound **1**. Without purification, **1** was tautomerized to diol **2**, which was subsequently converted into **3** using perfluoro-1-butananesulfonyl fluoride.<sup>14</sup> Compounds **4**, **5** and **6** were obtained from the Stille coupling reaction between aryl dinonaflate **3** and suitably stannylated heterocyclic precursors, and purified by both column chromatography and recrystallization.

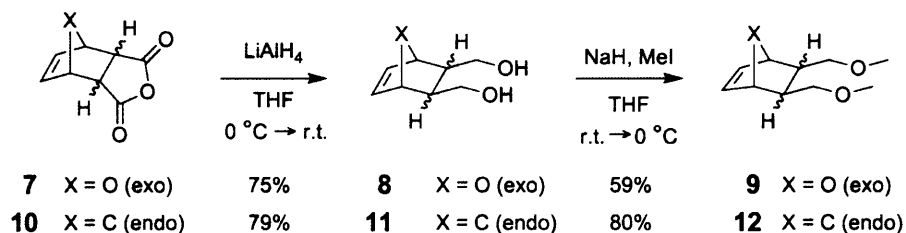
Scheme 1-2.





We followed the literature syntheses of monomers **9**<sup>15</sup> and **12**<sup>16</sup> as described in Scheme 1-3. Diels-Alder reactions of furan or 1,3-cyclopentadiene and maleic anhydride afforded **7** (exo major) or **10** (endo major), respectively. These adducts were reduced with lithium aluminum hydride to afford diol **8** and **11**. A double Williamson ether synthesis in the presence of excess sodium hydride followed by treatment with methyl iodide resulted in the diether monomers **9** and **12** as viscous oils after vacuum distillation. All of the monomers were characterized by <sup>1</sup>H NMR and <sup>13</sup>C NMR spectroscopy and mass spectrometry.

Scheme 1-3.



### Homopolymerizations

Homopolymers of each monomer were synthesized to examine reactivity with ROMP catalysts before the synthesis of block copolymers. Homopolymerization reactions of monomers (**4**, **5**, **6**, **9** and **12**) with Grubbs' catalyst, **13**, **14** and **15** (Figure 1-5) were examined in CH<sub>2</sub>Cl<sub>2</sub> at room temperature, and the polymers poly(**4**), poly(**5**), poly(**6**), poly(**9**) and poly(**12**) (Figure 1-6) were isolated by precipitation into methanol or hexane. We found that catalyst **13** polymerized *exo*-7-oxanorbornene derivative **9** quantitatively within 1 h, but **13** polymerized *endo*-norbornene derivative **12** more slowly (70% yield for a 6 h reaction).

Previous studies have shown that *exo* isomers react faster than the corresponding *endo* isomers for the ROMP of norbornene derivatives due to steric interactions between the penultimate repeat unit of propagating polymer chains and the *endo* substituents of the approaching monomer.<sup>17</sup>

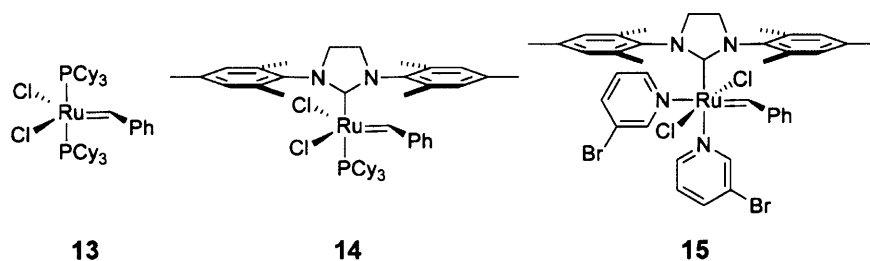


**Figure 1-5.** Grubbs' catalysts.

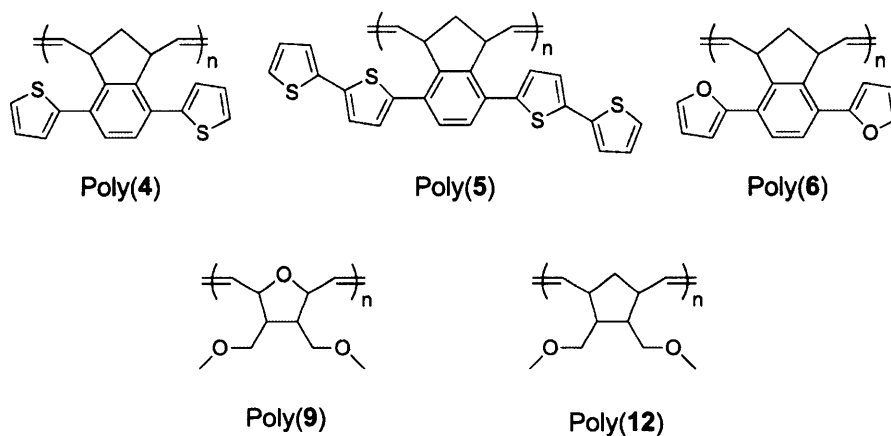


**Figure 1-6.** Structures of homopolymers.

We also found that monomers having sulfur (**4** and **5**) were slow to polymerize and

could not be driven to completion with **13** possibly because the catalyst was deactivated by coordination to the sulfur center.<sup>18</sup> In the case of **5**, only oligomers ( $M_n = 2,100$ , PDI = 1.07) were obtained, apparently due to its poor solubility and sluggish polymerization. It is known that catalyst **14** displays higher activity than catalyst **13** toward olefinic substrates<sup>19</sup> and is tolerant of the substrates containing sulfur atoms.<sup>18</sup> Consistent behavior was observed with our monomers, and higher molecular weight polymers (an insoluble polymer from monomer **5**) with broader PDIs were obtained using **14**. Grubbs has reported a next generation catalyst **15** which has superior initiation properties over **14** for the metathesis of simple olefins and is easily synthesized in one step from **14**.<sup>20</sup> We also polymerized all monomers with this catalyst. The monomers having heterocyclic ring (**4**, **5** and **6**) precipitated during polymerization, while poly(**9**) and poly(**12**) were synthesized in a controlled polymerization with living characteristics within 1 h by **15**. Table 1-1 summarizes the GPC results of the homopolymerizations.

**Table 1-1.** GPC results of homopolymerizations

monomer	catalyst	time (h)	yield (%)	[M]/[Cat.]	$M_n$	PDI
<b>4</b>	<b>13</b>	24	25	180	12,700	1.10
<b>6</b>	<b>13</b>	24	80	345	67,800	1.18
<b>9</b>	<b>13</b>	2	90	200	53,400	1.04
<b>9</b>	<b>15</b>	1	98	375	60,100	1.11
<b>12</b>	<b>13</b>	6	70	245	33,400	1.18
<b>12</b>	<b>15</b>	2	97	180	38,100	1.05

Poly(**12**) polymerized with different catalysts had different configurations of double

bonds (Figure 1-7). Consistent with the  $^1\text{H}$  NMR spectral data previously reported,<sup>13,21</sup> a 75:25 ratio of trans to cis olefins was revealed by integration of the signals for H(2) for the poly(12) polymerized from 13 (Figure 1-7, bottom). However, a 33:67 ratio of trans to cis olefins was observed for poly(12) polymerized from 15 (Figure 1-7, top). The stereochemistry of poly(9) was insensitive to the catalyst used and the ratio was approximately a 50:50 ratio of trans to cis olefins.

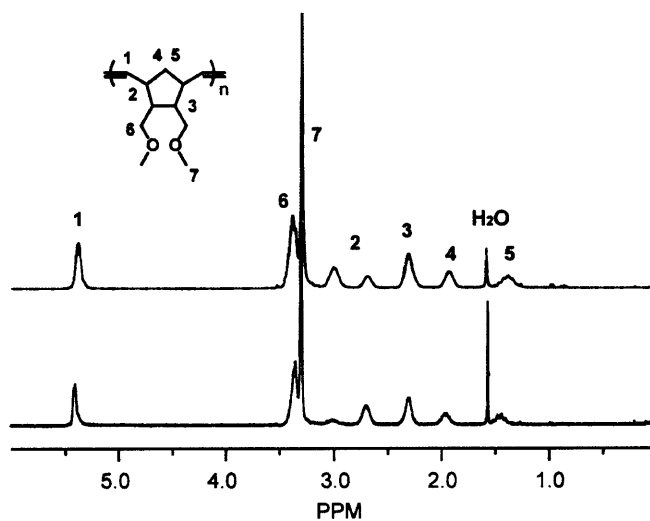


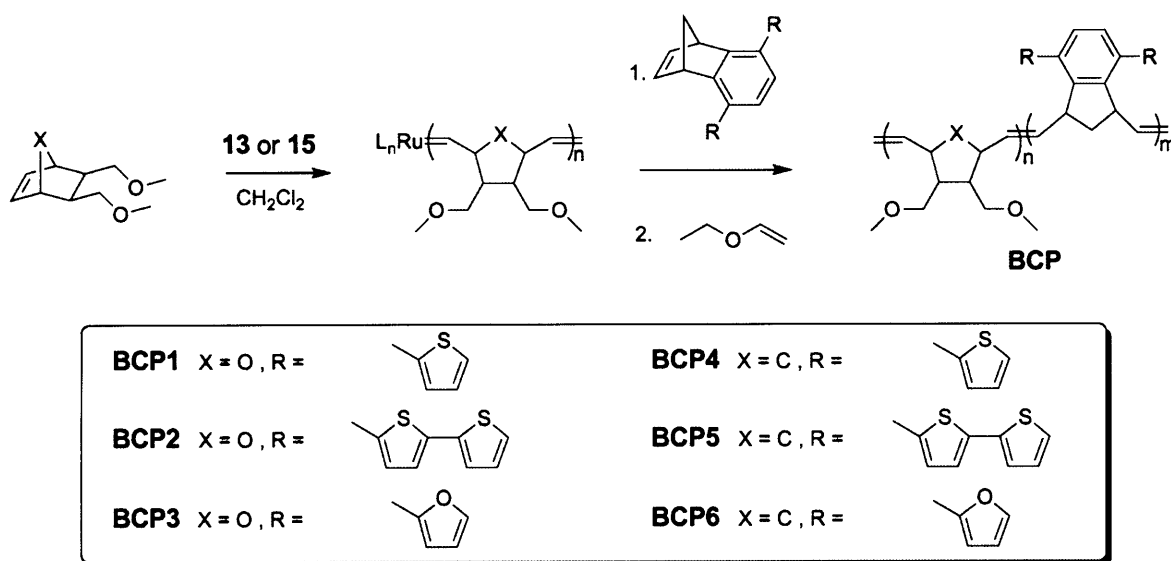
**Figure 1-7.**  $^1\text{H}$  NMR spectra in  $\text{CDCl}_3$  of poly(12) polymerized with 15 (top) and 13 (bottom).

### Block Copolymerizations

Based on the homopolymerization of monomers, the synthesis of block copolymers was accomplished by adding monomers 4 – 6 to the growing polymer chain of poly(9) that was initiated by catalyst 13 (Scheme 1-4). Catalyst 13 afforded soluble copolymers with narrow PDIs. The polymerization of 9 was allowed to proceed for 2 h at room temperature,

and then solutions of **4**, **5** or **6** were added. A small amount of sample was taken from the initial polymerization just before the addition of second monomer for GPC analysis. After stirring for another 22 h, the reaction mixture was quenched with ethyl vinyl ether and precipitated into hexane to afford copolymers as pale yellow (**BCP1**), yellow (**BCP2**) or white (**BCP3**) solids.

Scheme 1-4.



The synthesis of block copolymers based on **12** and **4** – **6** were also performed in the same manner. Catalyst **15** was used for the synthesis of these block copolymers because **13** was ineffective for the polymerization of **12**. However, **BCP4** synthesized by **15** displayed apparent high molecular weights with low solubility. Therefore, we used **13** to synthesize soluble forms of **BCP4**. Figure 1-8 is a GPC trace of **BCP4**, which shows the increase of molecular weight after addition of monomer **4** to the growing polymer chain of poly(**12**)

keeping PDI narrow.

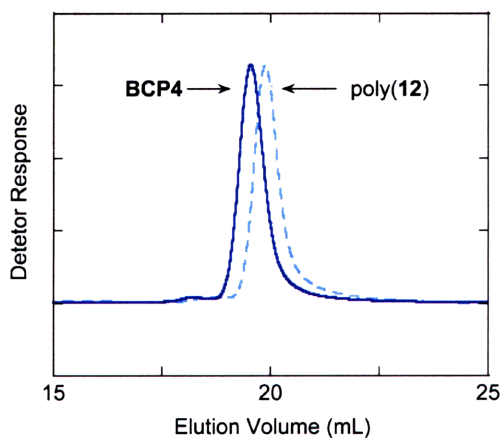


**Figure 1-8.** GPC traces of poly(12) and resulting block copolymer **BCP4**.

**Table 1-2.** GPC results of block copolymerizations

polymer	M <sub>1</sub>	M <sub>2</sub>	Cat.	[M <sub>1</sub> ]/[M <sub>2</sub> ]/[Cat.]	M <sub>n</sub>	PDI	n/m
<b>BCP1</b>	<b>9</b>	<b>4</b>	<b>13</b>	210/50/1	58,600	1.02	290/15
<b>BCP2</b>	<b>9</b>	<b>5</b>	<b>13</b>	220/20/1	53,700	1.03	270/10
<b>BCP3</b>	<b>9</b>	<b>6</b>	<b>13</b>	220/110/1	69,200	1.10	300/50
<b>BCP4</b>	<b>12</b>	<b>4</b>	<b>13</b>	220/60/1	59,300	1.05	270/35
<b>BCP5</b>	<b>12</b>	<b>5</b>	<b>15</b>	210/10/1	47,800	1.06	240/10
<b>BCP6</b>	<b>12</b>	<b>6</b>	<b>15</b>	190/50/1	53,800	1.08	240/35

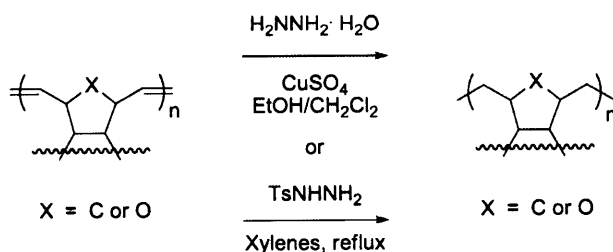
Table 1-2 summarizes the GPC results of the block copolymers. The relative ratios of each copolymer block were determined by GPC or <sup>1</sup>H NMR spectroscopy. As the ratio of monomer **9** or **12** increased, the copolymer became qualitatively more elastic. The elastomeric properties of poly(**9**) and poly(**12**) provides for qualitatively improved mechanical

properties and reduced brittleness. Although the polymerization of the second block was not completely living, the PDIs of the resulting polymers were narrow.

### Hydrogenation of Polymers

The as-synthesized block copolymers are not indefinitely stable in air. The polymers, when stored under ambient conditions, became insoluble after weeks while the polymers stored under nitrogen atmosphere were still soluble. It is likely that the unsaturated C=C double bonds and tertiary C–H bonds, which are both allylic and benzylic, are responsible for the oxidation and degradation of polymers.<sup>22</sup> **BCP1 – BCP3** that have tetrahydrofuran groups are also prone to oxidation due to additional activation of tertiary allylic C–H bonds by the oxygen. The double bonds could be also affected when the polymers are chemically or electrochemically oxidized. We therefore decided to remove the double bonds by hydrogenation to solve these problems.

**Scheme 1-5.**



Hydrogenation of the polymer backbone was carried out using hydrazine and copper sulfate in the mixture of ethanol and  $\text{CH}_2\text{Cl}_2$  with slow bubbling of air through the mixture as

shown in Scheme 1-5.<sup>23</sup> Refluxing in xylenes with tosyl hydrazide<sup>24</sup> was also an effective hydrogenation method for our block copolymers and gave similar results (Scheme 1-5). The olefin protons completely disappeared after hydrogenation when analyzed by <sup>1</sup>H NMR spectroscopy (Figure 1-9). The films made of hydrogenated polymers were less sticky to the glass and more flexible than the original polymers. Figure 1-10 shows the freestanding films of block copolymers.

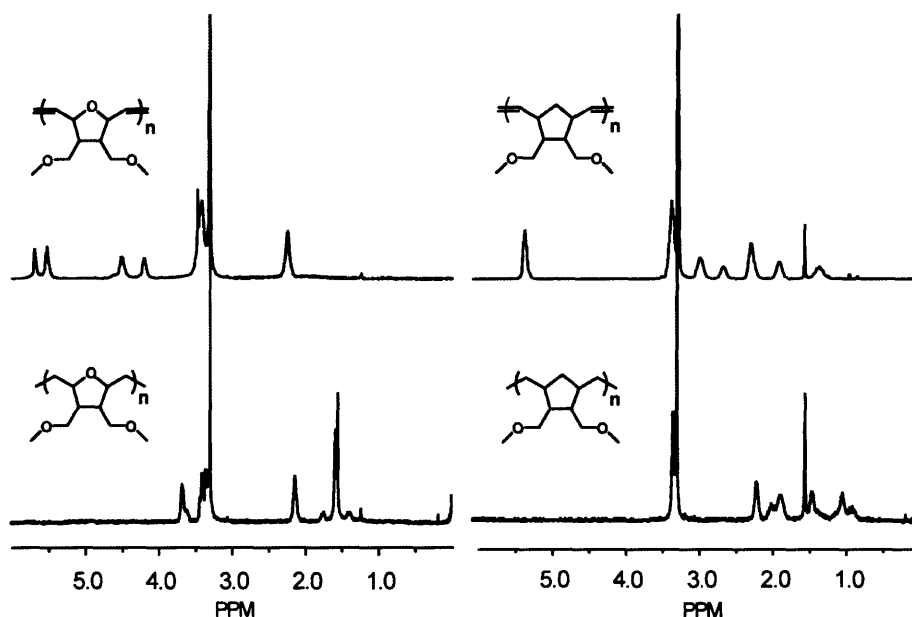


**Figure 1-9.** <sup>1</sup>H NMR spectra in CDCl<sub>3</sub> of poly(9) (top left), hydrogenated poly(9) (bottom left), poly(12) (top right) and hydrogenated poly(12) (bottom right).

Hydrogenation was also found to lower the  $T_g$ 's of polymers due to increased freedom of rotation in the backbone (Table 1-3 and Figure 1-11). **BCP4** experiences about 15 °C decrease in  $T_g$  as compared with **BCP5** and **BCP6**. As mentioned before, poly(12) in **BCP4**



had different stereochemical composition since it was polymerized with **13**.  $T_g$  of **BCP4** polymerized with **15** was 73.6 °C. We should mention that observed  $T_g$ s are mainly for the first blocks (poly(**9**) or poly(**12**)) of block copolymers. Homopolymers, poly(**4**) and poly(**6**), have  $T_g$ s of 250.0 °C and 245.0 °C, respectively. However, we could not observe other  $T_g$ s for the block copolymers even when heated up to 350 °C.

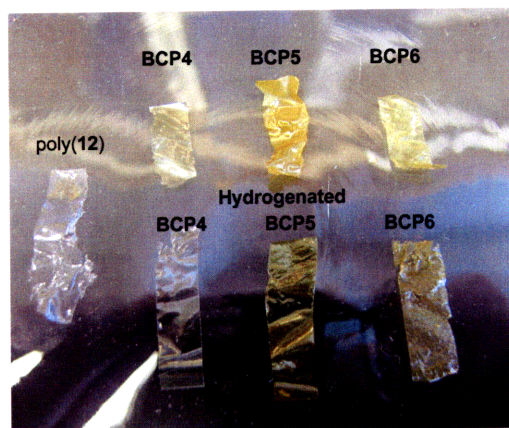


**Figure 1-10.** Freestanding films of block copolymers and their hydrogenated polymers.

**Table 1-3.**  $T_g$ s of block copolymers

polymer	$T_g$ (°C) before hydrogenation	$T_g$ (°C) after hydrogenation
<b>BCP1</b>	26.5	5.4
<b>BCP2</b>	22.2	2.3
<b>BCP3</b>	21.3	4.8
<b>BCP4</b>	50.2	42.2
<b>BCP5</b>	66.4	44.6
<b>BCP6</b>	64.2	42.1

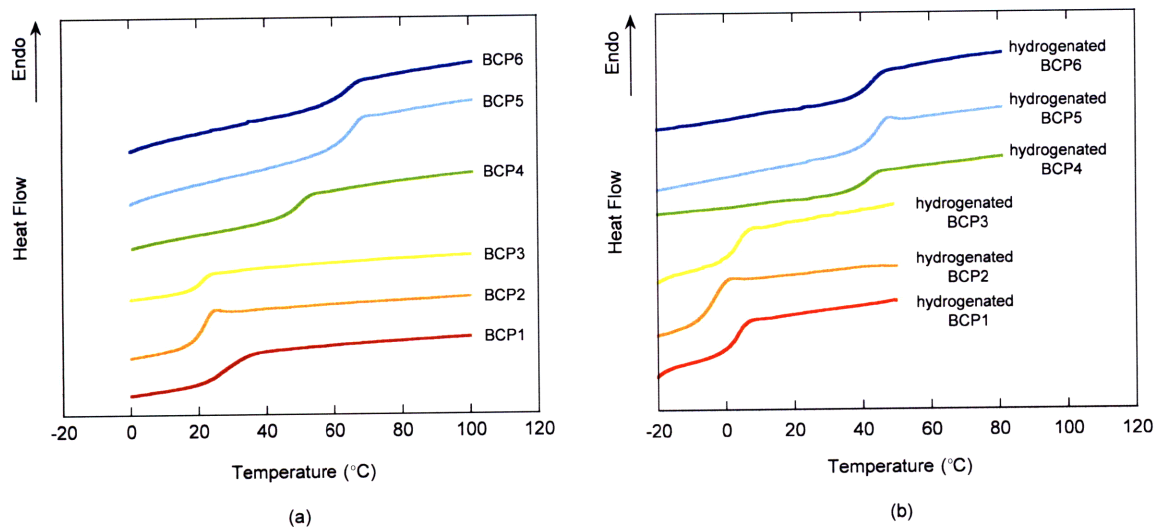
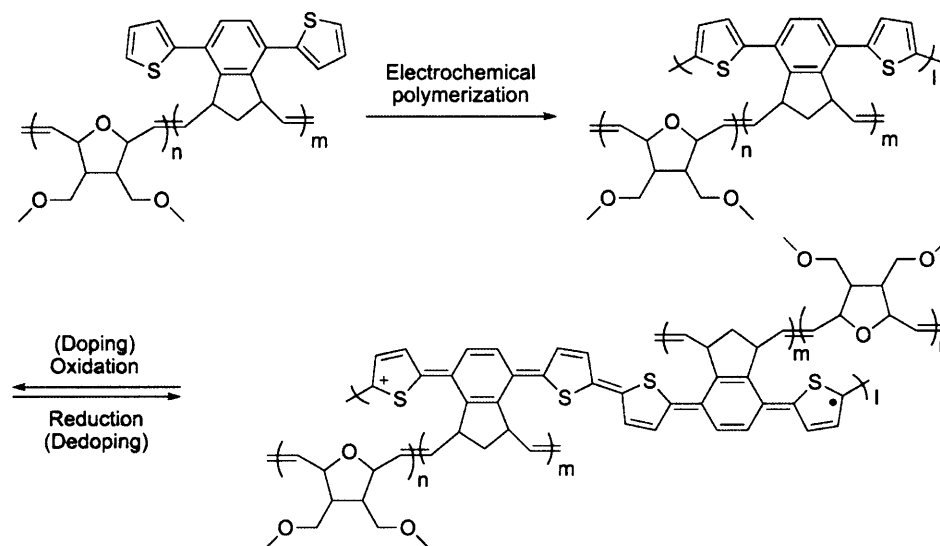


**Figure 1-11.** DSC curves of (a) block copolymers and (b) their hydrogenated polymers.

## Electrochemistry

All electropolymerizations to create interpenetrating polymer networks were performed by electrodeposition of compounds on Pt button electrodes under swept potential conditions (Scheme 1-6). In the first step of electropolymerization, neutral monomers are oxidized to radical cations at the electrode. Then the monomers dimerize (mainly at the  $\alpha$ -position) and protons are eliminated, forming a neutral species. Since the dimer with its greater conjugation is more easily oxidized than the monomer, it is immediately reoxidized to the cation, which can further couple with other cations to extend the chain. The process of oxidative coupling and proton elimination continues until insoluble oligomers form and are deposited on the electrode surface.

Scheme 1-6.



The generic three-electrode cell for electrochemical study is shown in Figure 1-12. First, electropolymerizations of three electroactive monomers (**4** – **6**) were performed in  $\text{CH}_3\text{CN}$  solutions containing ca. 5 mM of each monomer and 0.1 M of  $\text{TBAPF}_6$  as an electrolyte. Figures 1-13(a) – (c) depict the anodic polymerization of monomers **4** – **6**. The irreversible oxidative peaks in the first scans (dotted lines in Figure 1-13) are attributed to the oxidation of heterocyclic units. The anodic peaks corresponding to the oxidation of the conducting polymers typically appeared after the second cycle. The increase in current after each potential scan indicates polymer film growth on the working electrode. The monomer possessing a bithiophene moiety, **5**, oxidized at the lowest potential (0.60 V). The oxidation onset value for the monomer having thiophene, **4**, was higher than that of the monomer having furan, **6** (0.80 and 0.62 V, respectively). This is likely due to the larger

size of sulfur compared to oxygen, resulting in greater steric interactions and a nonplanar conformation for the phenyl–thienyl linkages.<sup>25</sup>

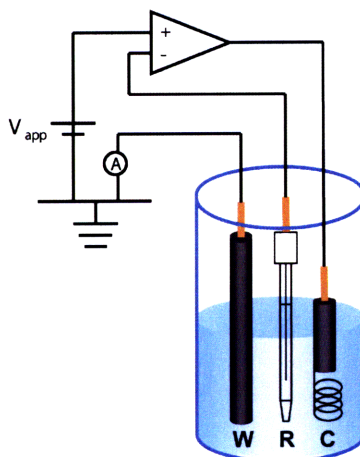


**Figure 1-12.** The generic electrochemical cell for cyclic voltammetry.  
(W, working electrode; R, reference electrode; C, counter electrode)

Electropolymerizations of homopolymers (poly(**4**) – poly(**6**)) and block copolymers (**BCP1**–**BCP6** and their hydrogenated polymers) were also carried out. Figures 1-13(d) – (f) depict representative anodic polymerizations of block copolymers (**BCP1** – **BCP3**) on Pt button electrodes. Because of solubility problems, electropolymerization of polymers were performed in  $\text{CH}_2\text{Cl}_2$  solutions containing ca.  $4 \mu\text{M}$  of electroactive unit ( $2 - 3 \text{ mg/mL}$  of each polymer) and  $0.1 \text{ M}$  of  $\text{TBAPF}_6$  as an electrolyte. Cyclic voltammograms (CVs) for homopolymers' electropolymerization showed similar peaks to those observed for block copolymers.

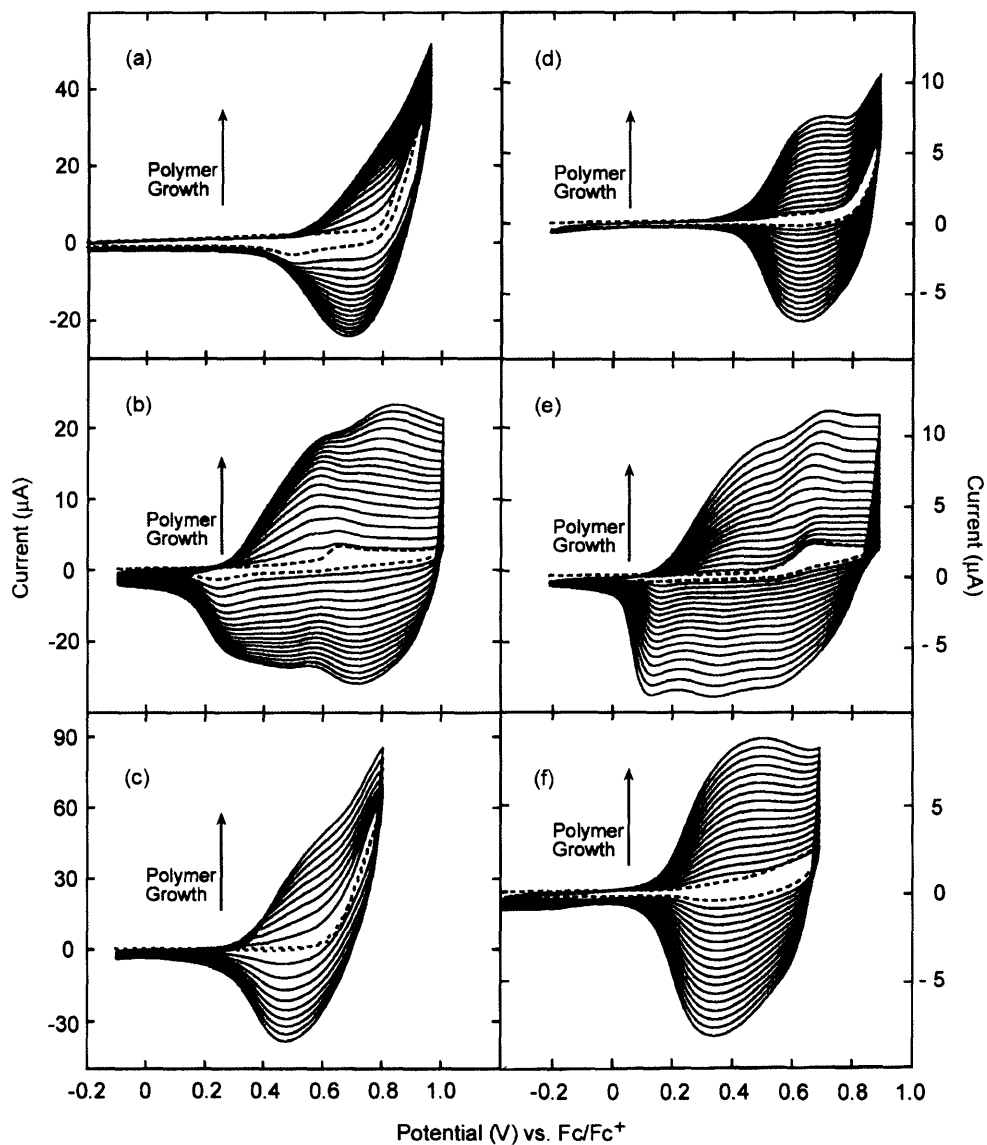


**Figure 1-13.** Electropolymerizations of monomers **4** (a), **5** (b) and **6** (c), and block copolymers **BCP1** (d), **BCP2** (e) and **BCP3** (f) on Pt button electrodes in  $\text{CH}_3\text{CN}$  (for monomers **4** – **6**) or  $\text{CH}_2\text{Cl}_2$  (for polymers **BCP1** – **BCP3**) solutions containing 0.1 M TBAPF<sub>6</sub>. Dotted lines represent the first scans, and all CVs were obtained at scan rate of 100 mV/s.

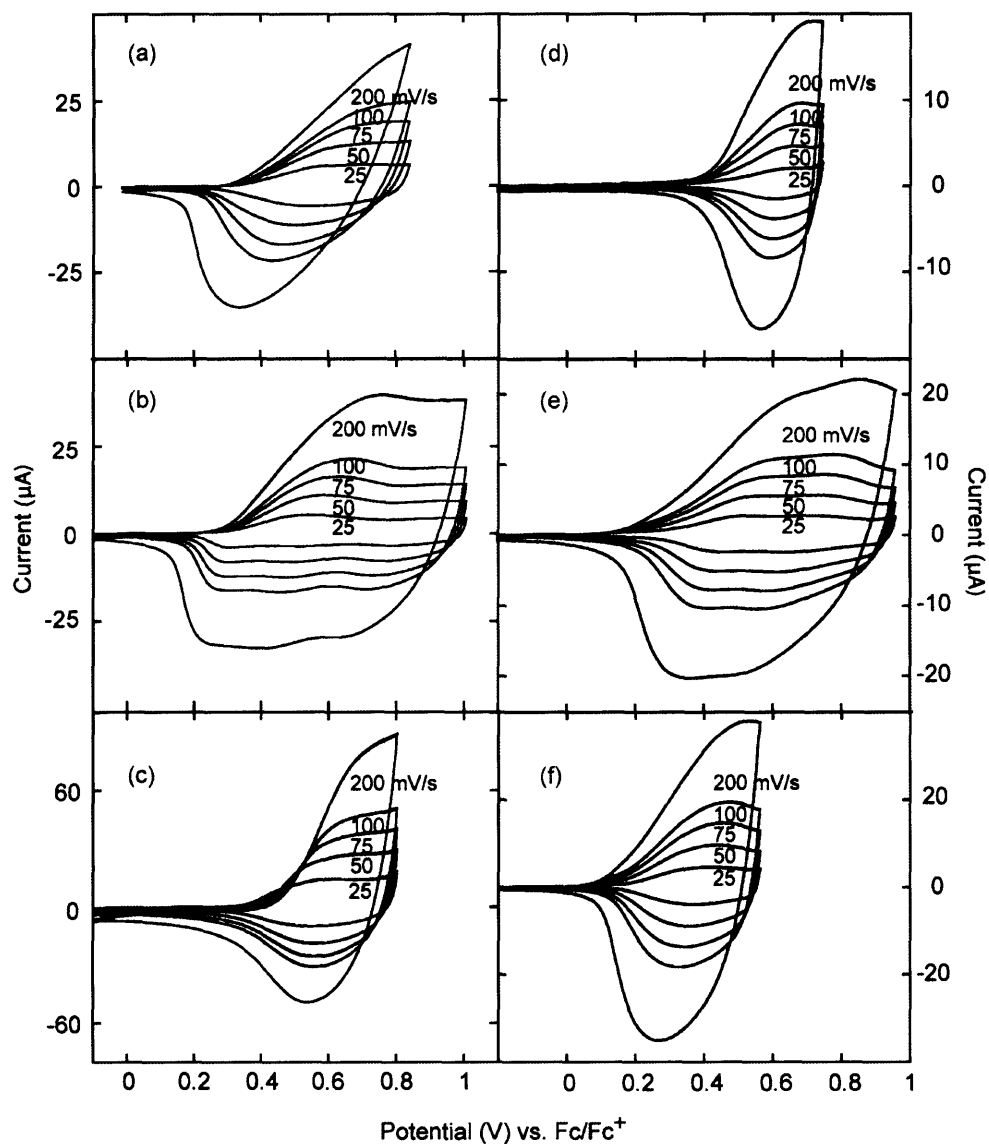


**Figure 1-14.** CVs of electrodeposited films of monomers **4** (a), **5** (b) and **6** (c), and homopolymers poly(**4**) (d), poly(**5**) (e) and poly(**6**) (f) on Pt button electrodes in CH<sub>3</sub>CN (for monomers **4** – **6**) or CH<sub>2</sub>Cl<sub>2</sub> (for homopolymers poly(**4**) – poly(**6**)) solutions containing 0.1 M TBAPF<sub>6</sub>. Polymer film CVs were obtained at 25 – 200 mV/s.

The oxidation potentials obtained for the block copolymers are nominally different

from those obtained for the monomers in part because of a difference in the solvent used for both experiments (Figures 1–13 and 1–14). Specifically, the half-wave potential for  $\text{Fc}/\text{Fc}^+$  in  $\text{CH}_2\text{Cl}_2$  is ca. 0.15 V higher than that in  $\text{CH}_3\text{CN}$ ; the potential values obtained in  $\text{CH}_3\text{CN}$  are higher than those obtained in  $\text{CH}_2\text{Cl}_2$  when  $\text{Fc}/\text{Fc}^+$  is used as the internal reference.

Both interchain and intrachain cross-linking are likely in the precursor polymers, even though we cannot quantitatively determine the extent of each. The peak current increases indicate a constant growth of the polymer films with repeated scans and demonstrate that these copolymers have sufficient conductivities to serve as a working electrode even though the conducting blocks are much shorter than non-conducting blocks. If the polymer was insulating or polymerization only proceeded at the electrode surface, there would be a decrease in the rate of film growth.<sup>4</sup> However, attempts to obtain *in situ* conductivities were unsuccessful due to poor adhesion of polymer films on interdigitated microelectrodes.

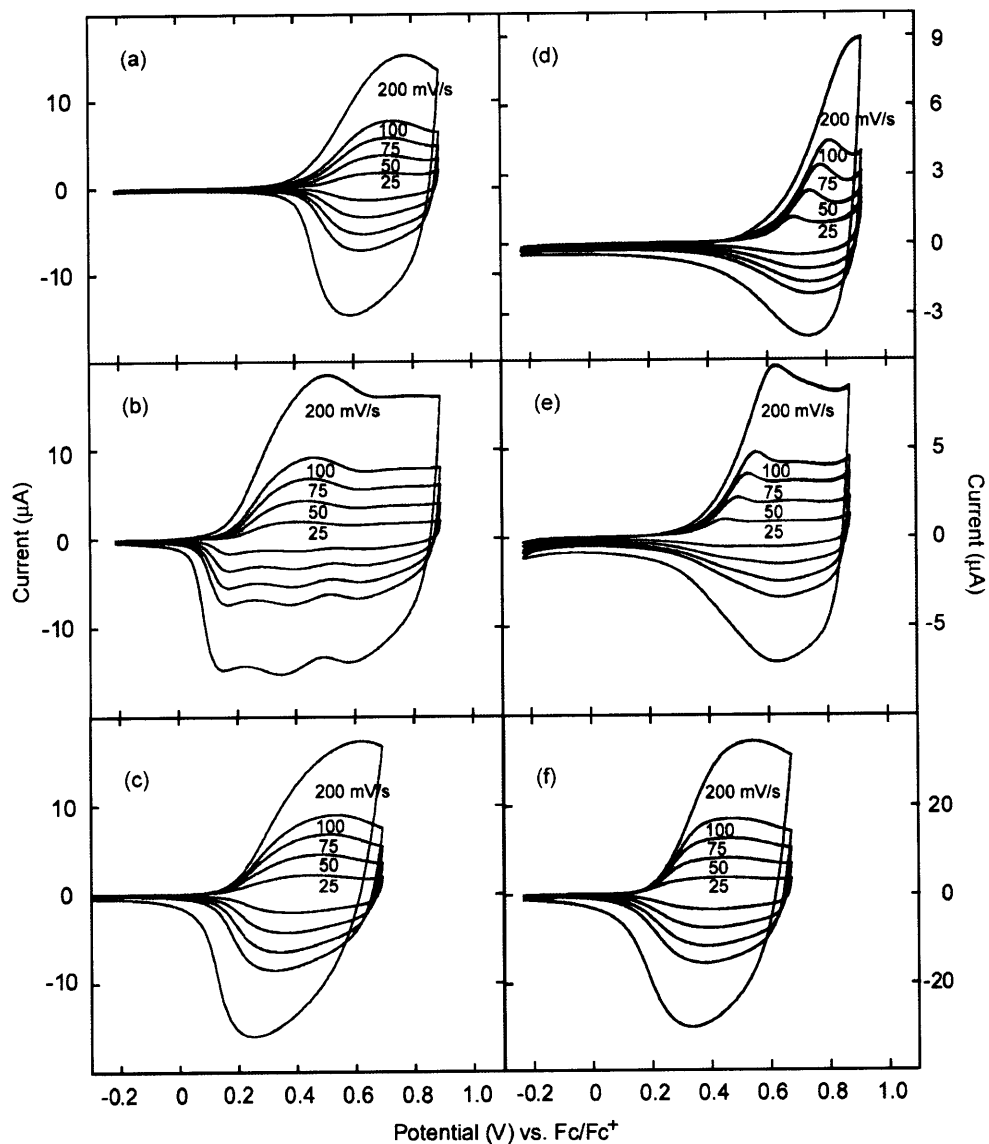
After electropolymerization, the electrode coated with a polymer was washed with  $\text{CH}_3\text{CN}$  or  $\text{CH}_2\text{Cl}_2$  and placed into a polymer-free solution of 0.1 M  $\text{TBAPF}_6$  in order to examine the electrochemical processes of the electrodeposited polymer. Figure 1-14 depicts the CVs of resulting electrodeposited CPs from the monomers and homopolymers. Figure 1-15 compares the CVs of the block copolymers and their hydrogenated polymers of **BCP1** – **BCP3**. The linear increase of the peak current with respect to the scan rate establishes that the observed redox processes arise from surface-deposited materials. The CVs for the electropolymerized films, especially polymers having bithiophene moieties, exhibit reversible redox waves over a broad range of potentials, findings consistent with the highly delocalized nature of  $\pi$ -extended systems. Glenis *et al.*

reported that with the electrolyte,  $\text{PF}_6^-$  polyfuran could not be electropolymerized because of strong association of this dopant with the oxidized polymers, which results in irreversible chemical reactions.<sup>26</sup> However, monomer **6** and polymers (poly(**6**), **BCP3** and **BCP6**) which have a furan moiety were found to electropolymerize in the presence of  $\text{TBAPF}_6$ , and the CVs of the resulting electrodeposited polymer films displayed stable electroactivities.

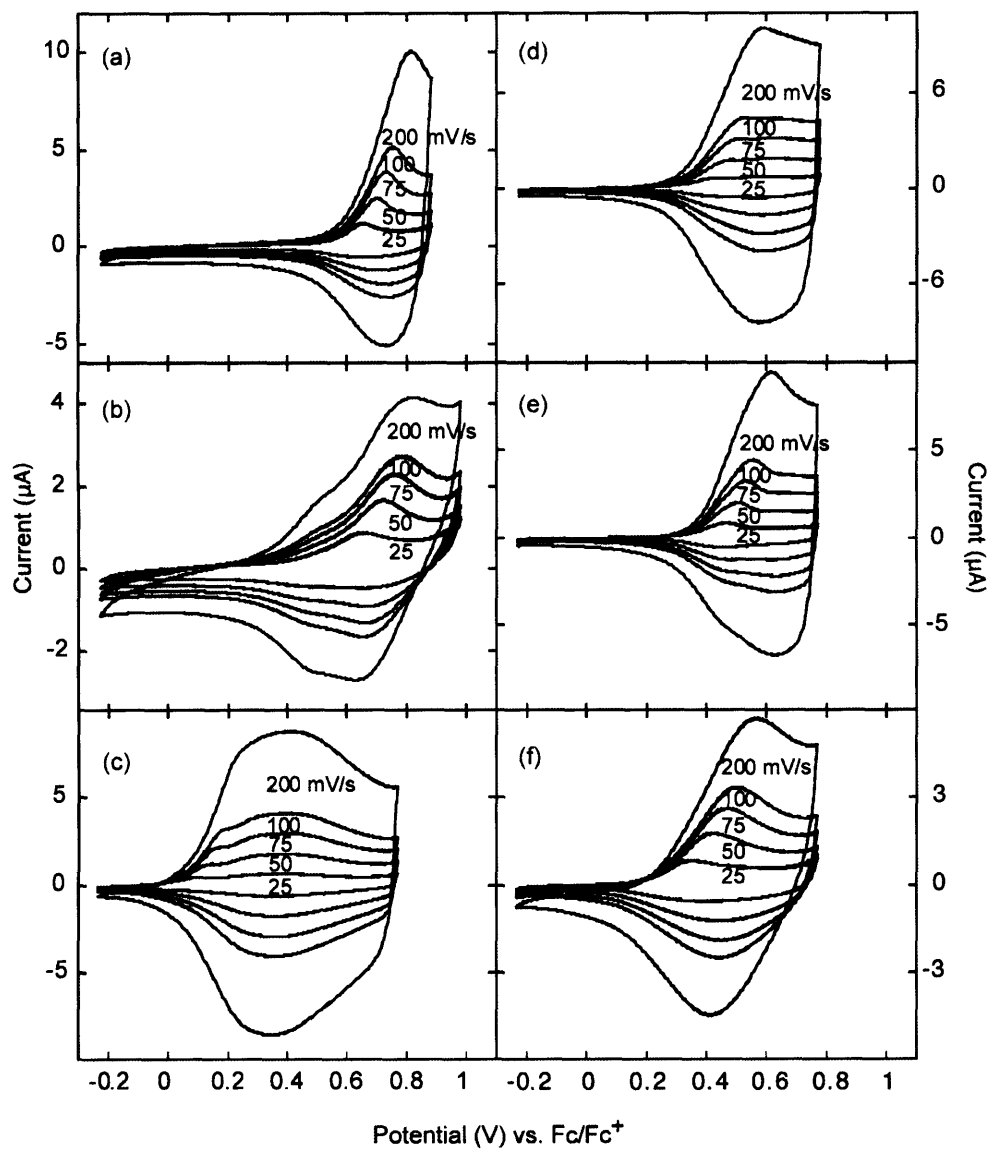
We had expected that hydrogenation of double bonds in the polymer backbone would not alter the electrochemical properties of original polymers since electroactive moieties were not affected by hydrogenation. Hydrogenated block copolymers retained the stable electroactivity; however, they display slightly higher oxidation onset values and narrower peak widths compared with their original polymers (Figure 1-15). The CV of hydrogenated **BCP1** changed the most since it had the highest oxidation potential which may produce trapped sites inaccessible to counterion transport.<sup>25</sup> The general effects of hydrogenation on the electrochemical behavior are likely the result of (a) an increase in the nonpolar nature of the materials, which does not favor a highly charged doped state, and (b) increased steric bulk in the polymer backbone, which may limit the ability of oxidized pendant thienyl and furyl groups to couple.

**BCP5** and **BCP6**, which were polymerized using **15**, displayed poorer electrochemical characteristics (Figure 1-16). Most noteworthy is **BCP4** synthesized using **15**, which did not show any electroactivity, possibly because of decreased counterion mobility in the higher molecular weight and potentially cross-linked structure. **BCP4** polymerized using **13** exhibits similar electrochemistry to hydrogenated **BCP1**. On the other hand, hydrogenated **BCP5** and **BCP6** showed similar CVs to hydrogenated **BCP2** and **BCP3**, respectively.





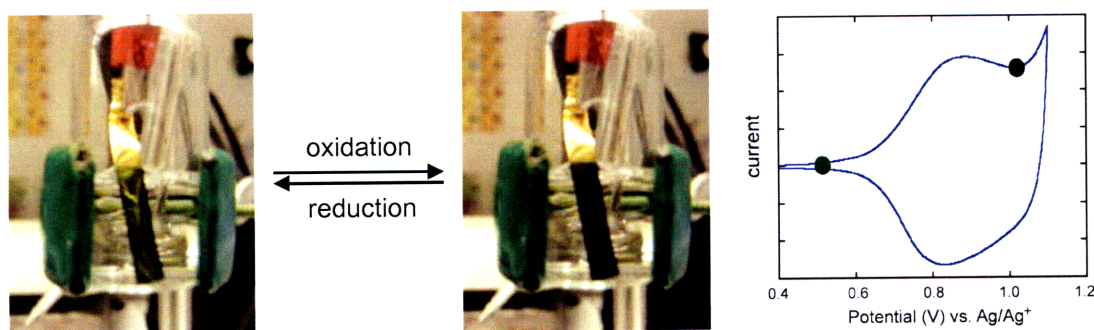
**Figure 1-15.** CVs of electrodeposited films of block copolymers **BCP1** (a), **BCP2** (b) and **BCP3** (c), and hydrogenated block copolymers **BCP1** (d), **BCP2** (e) and **BCP3** (f) on Pt button electrodes in 0.1 M TBAPF<sub>6</sub> of CH<sub>2</sub>Cl<sub>2</sub> solution. Polymer film CVs were obtained at 25 – 200 mV/s.



**Figure 1-16.** CVs of electrodeposited films of block copolymers **BCP4** (a), **BCP5** (b) and **BCP6** (c), and hydrogenated block copolymers **BCP4** (d), **BCP5** (e) and **BCP6** (f) on Pt button electrodes in 0.1 M TBAPF<sub>6</sub> of CH<sub>2</sub>Cl<sub>2</sub> solution. Polymer film CVs were obtained at 25 – 200 mV/s.

## Spectroelectrochemistry

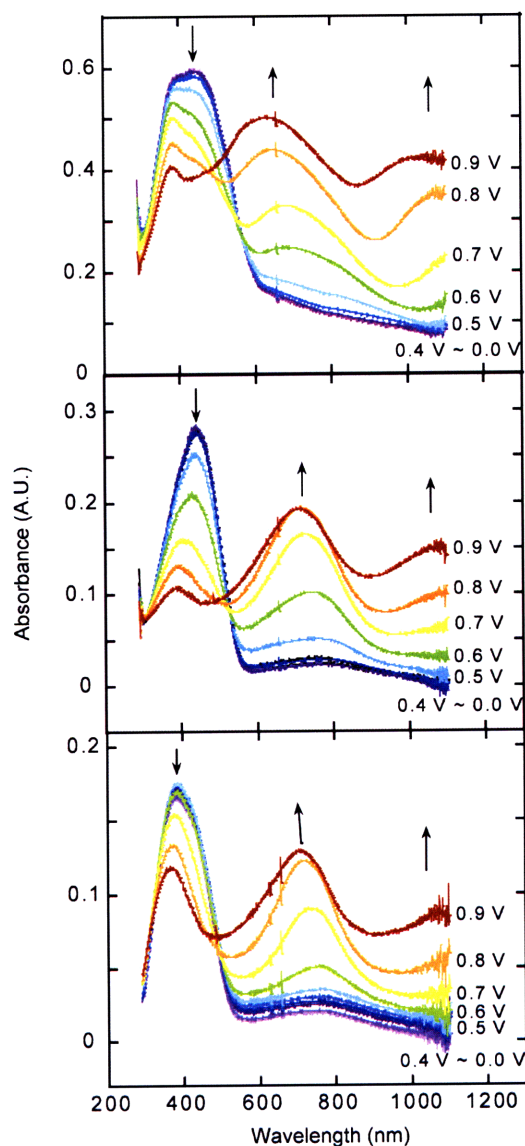
Reversible, uniform color changes were observed during redox cycles of the electrodeposited conducting polymer films (Figure 1-17). Figure 1-18 shows representative *in situ* measurements of the UV-vis absorption of electropolymerized polymers having bithiophene moieties deposited onto ITO-coated glass electrodes. Each of the polymers in the series exhibits similar behavior.



**Figure 1-17.** Reversible color change (forest green to black) of deposited polymer film (**BCP1**) on a gold electrode during redox cycle and CV of the corresponding polymer film.

At first, there is no long wavelength absorbance in the spectrum with absorption onset at 620 nm for **5** and 550 nm for block copolymers **BCP2** and hydrogenated **BCP5**. The onset of the optical absorptions corresponds to  $\pi$  to  $\pi^*$  transitions that give the approximate band gaps of the conducting polymers. The determined band gaps of monomers and block copolymers are shown in Table 1-4. These values match the trend with observed oxidation onset potentials of electropolymerization; polymers having thiophene moieties have the largest band gaps (2.6 – 2.7 eV) and polymers having bithiophene moieties have the smallest

band gaps (2.3 eV). These band gaps are similar to the previously reported band gaps of poly[1,4-bis(2-heterocycle)-*p*-phenylenes], which are shown in Table 1-5.<sup>25</sup>

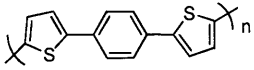
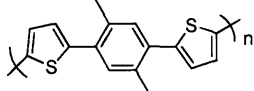
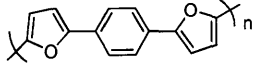
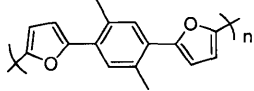


**Figure 1-18.** UV-vis absorption spectra of **5** (top), **BCP2** (middle) and hydrogenated **BCP5** (bottom) on ITO-coated glass electrodes in  $\text{CH}_2\text{Cl}_2$  solution containing 0.1 M  $\text{TBAPF}_6$  between 0.0 V and 0.9 V (vs  $\text{Ag}/\text{Ag}^+$ ).

**Table 1-4.** Experimental band gaps (eV) of CPs from monomers and block copolymers

compound	band gap (eV)	compound	band gap (eV)	compound	band gap (eV)
<b>4</b>	2.5	<b>5</b>	2.0	<b>6</b>	2.1
<b>BCP1</b>	2.6	<b>BCP2</b>	2.3	<b>BCP3</b>	2.4
<b>BCP4</b>	2.6	<b>BCP5</b>	2.3	<b>BCP6</b>	2.4
hydrogenated <b>BCP4</b>	2.7	hydrogenated <b>BCP5</b>	2.3	hydrogenated <b>BCP6</b>	2.4

**Table 1-5.** Reported band gaps (eV) of poly[1,4-bis(2-heterocycle)-*p*-phenylenes]<sup>25</sup>

polymer	band gap (eV)
	2.3
	2.6
	2.3
	2.4

The applied potential was increased at 0.1 V intervals, and a spectrum was recorded at each potential up to 0.9 V (vs Ag/Ag<sup>+</sup>). New, lower energy absorbance peaks become apparent with applied potential above 0.5 V (vs Ag/Ag<sup>+</sup>). The absorbance for the  $\pi$  to  $\pi^*$  transitions, with maximum around 400 nm, continues to decrease while the absorbances at

lower energies continue to increase upon further oxidation. Since the midgap states are created at the expense of the highest energy states, the  $\pi$  to  $\pi^*$  transition is shifted to slightly higher energy. A peak at near 1100 nm is commonly attributed to a transition from the valence band to intermediate bipolaron states for intrinsically conducting polymers. As expected, hydrogenation did not affect the electronic band structures. On the basis of these results and the electrochemical behavior, it is clear that oxidation of the block copolymer produces a network of conducting polymer chains.

## Conclusions

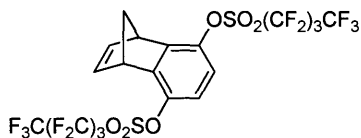
We have utilized ROMP to synthesize novel precursor block copolymers having heterocyclic moieties to form conducting polymers. These block copolymers, which have electroactive blocks, showed stable electroactivity after subsequent electropolymerization. Hydrogenation of polymer backbones increased the polymers' stability without dramatically reducing electrochemical properties. These types of materials can be used to prepare nanostructures and may further applied in the formation of actuators and electrochromic devices.

## Experimental Section

**Materials.**  $\text{CH}_2\text{Cl}_2$  and THF were purified by passage through solvent purification columns containing activated alumina. *N,N*-Dimethylformamide (DMF) was distilled from  $\text{MgSO}_4$  and stored over 4 Å molecular sieves. Tetrabutylammonium hexafluorophosphate ( $\text{TBAPF}_6$ ) was recrystallized from ethanol. 5-Tributylstannyl-2,2'-bithiophene<sup>27</sup> and *exo*-5,6-dimethoxymethyl-7-oxabicyclo[2.2.1]hept-2-ene (**9**)<sup>15</sup> were prepared according to the literature procedure. All other reagents were used without further purification unless otherwise noted.

**Instrumentation.** NMR spectra were recorded on Varian Unity 300 MHz, Varian Mercury 300 MHz or Varian Inova 500 MHz spectrometer. Chemical shifts were reported in ppm and referenced to residual NMR solvent peaks ( $\text{CDCl}_3$ :  $\delta$  7.27 ppm for  $^1\text{H}$ ,  $\delta$  77.23 ppm for  $^{13}\text{C}$ ,  $\text{CD}_2\text{Cl}_2$ :  $\delta$  5.32 ppm for  $^1\text{H}$ ,  $\delta$  54.00 ppm for  $^{13}\text{C}$ ). Mass spectra (MS) were obtained at the MIT Department of Chemical Instrumentation Facility (DCIF) using Bruker Daltonics APEX II 3T FT-ICR-MS. Melting points were measured on a Mel-Temp II apparatus (Laboratory Devices INC) and were not corrected. Number-average molecular weight ( $M_n$ ) and polydispersity index (PDI) of polymers were obtained on a HP series 1100 gel permeation chromatography (GPC) system in THF and calibrated with polystyrene standards. Glass transition temperature ( $T_g$ ) was determined using a TA Instruments Q100 differential scanning calorimetry (DSC) at scan rate of 10 °C/min under nitrogen atmosphere. Electrochemical studies were performed using an Autolab PGSTAT 20 potentiostat (Eco Chemie) in a three-electrode cell consisting of a Pt button (1.6 mm diameter), or indium tin oxide (ITO)-coated

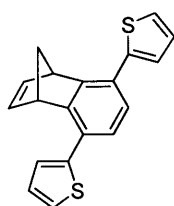
glass (100  $\Omega$  sheet resistance) working electrode, a Pt wire counter electrode and a Ag wire reference electrode in contact with 0.01 M AgNO<sub>3</sub>/0.1 M TBAPF<sub>6</sub> in anhydrous solvent. The ferrocene/ferrocenium (Fc/Fc<sup>+</sup>) redox couple was used as an internal reference. Spectroelectrochemistry was performed under ambient laboratory conditions on polymer films electrodeposited onto ITO-coated glass electrodes using Agilent 8453 UV-vis spectrophotometer.



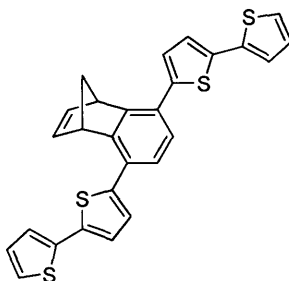
**1,4-Dihydro-1,4-methanonaphthalene-5,8-dione (1).** 1,4,4a,8a-Tetrahydro-1,4-methanonaphthalene-5,8-dione (**1**) (10.46 g, 60 mmol) was added to a solution of NaOH (5 g, 125 mmol) in ethanol (120 mL) and water (120 mL). The mixture was stirred at room temperature for 15 min, and then 5% HCl solution was added to acidify the solution. The mixture was extracted with ether and the organic portions were combined, washed with brine, dried over MgSO<sub>4</sub>, and filtered. The crude mixture was obtained as a black powder (10.34 g). Crude compound **2** (7.15 g, 41 mmol) was dissolved in dry THF (160 mL), and the solution was cooled in an ice bath under argon atmosphere. Trimethylamine (11 mL, 80 mmol) and perfluoro-1-butanesulfonyl fluoride (18.0 mL, 100 mmol) were added into the solution. The reaction mixture was brought to room temperature and stirred for 7 h. The solution was diluted with CH<sub>2</sub>Cl<sub>2</sub> and washed with 5% HCl solution and brine. After drying over MgSO<sub>4</sub>, the solution was filtered and the solvent was removed. The solid powder was loaded onto a short silica gel column and flushed with 10% CH<sub>2</sub>Cl<sub>2</sub> in hexane, giving pure



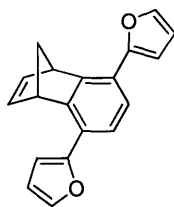
compound **3** (14.6 g, 48%) as a clear oil.  $^1\text{H}$  NMR (300 MHz,  $\text{CDCl}_3$ ):  $\delta$  6.93 (s, 2H), 6.88 (t, 2H,  $J = 1.8$  Hz), 4.29 – 4.26 (m, 2H), 2.40 (dt, 1H,  $J = 7.8$  Hz,  $J = 1.6$  Hz), 2.34 (dt, 1H,  $J = 7.8$  Hz,  $J = 1.7$  Hz).  $^{13}\text{C}$  NMR (75 MHz,  $\text{CDCl}_3$ ):  $\delta$  148.12, 142.78, 120.16, 69.32, 49.03.  $^{19}\text{F}$  NMR (188 MHz,  $\text{CDCl}_3$ ):  $\delta$  -81.07, -109.56, -121.26, -126.28. HR-MS (ESI): calcd for  $\text{C}_{19}\text{H}_8\text{F}_{18}\text{O}_6\text{S}_2$   $[\text{M} + \text{Na}]^+$ , 760.937; found 760.938.



**5,8-Di(2-thienyl)-1,4-dihydro-1,4-methanonaphthalene (4).** Compound **3** (9.687 g, 13.1 mmol) and 2-(tributylstannyl)thiophene (10 mL, 31.5 mmol) were dissolved in DMF (80 mL) under argon atmosphere.  $\text{PdCl}_2(\text{PPh}_3)_2$  (II) (462 mg, 0.66 mmol) was then added, and the reaction mixture was heated at 90 °C. After stirring for 12 h, the mixture was cooled to room temperature, diluted with ether, and washed with water and brine. After drying over  $\text{MgSO}_4$ , the solution was filtered, and the solvent was distilled off under reduced pressure. Column chromatography of the crude material on silica gel (5%  $\text{CH}_2\text{Cl}_2$  in hexane) provided the product as a white solid (2.87 g, 71%). The final purification was achieved by recrystallization from  $\text{CH}_2\text{Cl}_2$ /hexane; mp 120–121 °C.  $^1\text{H}$  NMR (300 MHz,  $\text{CDCl}_3$ ):  $\delta$  7.36 (dd, 2H,  $J = 5.1$  Hz,  $J = 1.1$  Hz), 7.22 (dd, 2H,  $J = 3.5$  Hz,  $J = 1.1$  Hz), 7.16 (s, 2H), 7.14 (dd, 2H,  $J = 3.6$  Hz,  $J = 5.1$  Hz), 6.98 (t, 2H,  $J = 1.8$  Hz), 4.44 – 4.43 (m, 2H), 2.31 – 2.25 (m, 2H).  $^{13}\text{C}$  NMR (75 MHz,  $\text{CDCl}_3$ ):  $\delta$  150.04, 143.27, 142.75, 128.12, 127.79, 125.35, 125.32, 125.22, 69.16, 49.92. HR-MS (EI): calcd for  $\text{C}_{19}\text{H}_{14}\text{S}_2$   $[\text{M}]^+$ , 306.053; found 306.054.

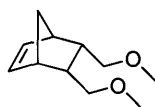


**5,8-Di(2-dithienyl)-1,4-dihydro-1,4-methanonaphthalene (5).** This compound was synthesized by the same procedure as described for compound **4** using the following quantities of reagents: compound **3** (3.025 g, 4.1 mmol), 5-(tributylstannyl)-2,2'-bithiophene (4.84 g, 10.6 mmol), PdCl<sub>2</sub>(PPh<sub>3</sub>)<sub>2</sub> (II) (141 mg, 0.20 mmol) and DMF (30 mL). Purification by column chromatography (silica gel, 5% CH<sub>2</sub>Cl<sub>2</sub> in hexane) provided the product as a yellow solid (1.76 g, 91%). The final purification was achieved by recrystallization from CH<sub>2</sub>Cl<sub>2</sub>/ethanol; mp 183 °C. <sup>1</sup>H NMR (300 MHz, CDCl<sub>3</sub>): δ 7.27 (dd, 2H, *J* = 5.1 Hz, *J* = 1.2 Hz), 7.25 (dd, 2H, *J* = 3.6 Hz, *J* = 1.2 Hz), 7.22 (d, 2H, *J* = 3.8 Hz), 7.17 (s, 2H), 7.16 (d, 2H, *J* = 3.8 Hz), 7.07 (dd, 2H, *J* = 3.7 Hz, *J* = 5.1 Hz), 7.01 (t, 2H, *J* = 1.8 Hz), 4.50 – 4.48 (m, 2H), 2.32 (dt, 1H, *J* = 7.3 Hz, *J* = 1.7 Hz), 2.26 (dt, 1H, *J* = 7.3 Hz, *J* = 1.5 Hz). <sup>13</sup>C NMR (75 MHz, CDCl<sub>3</sub>): δ 150.07, 143.24, 141.59, 137.55, 137.33, 128.10, 127.89, 126.09, 124.93, 124.63, 124.48, 123.87, 69.19, 49.98. HR-MS (EI): calcd for C<sub>27</sub>H<sub>18</sub>S<sub>4</sub> [M]<sup>+</sup>, 470.029; found 470.028.



**5,8-Di(2-furyl)-1,4-dihydro-1,4-methanonaphthalene (6).** This compound was

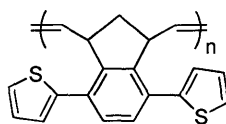
synthesized by the same procedure as described for compound **4** using the following quantities of reagents: compound **3** (5.953 g, 8.06 mmol), 2-(tributylstannyl)furan (6.1 mL, 19.4 mmol), PdCl<sub>2</sub>(PPh<sub>3</sub>)<sub>2</sub> (II) (286 mg, 0.41 mmol) and DMF (50 mL). Purification by column chromatography (silica gel, 5% CH<sub>2</sub>Cl<sub>2</sub> in hexane) provided the product as a white solid (2.15 g, 90%). The final purification was achieved by recrystallization from ethanol; mp 118 °C. <sup>1</sup>H NMR (300 MHz, CDCl<sub>3</sub>): δ 7.52 (dd, 2H, *J* = 1.8 Hz, *J* = 0.8 Hz), 7.26 (s, 2H), 6.92 (t, 2H, *J* = 1.8 Hz), 6.63 (dd, 2H, *J* = 3.4 Hz, *J* = 0.8 Hz), 6.51 (dd, 2H, *J* = 3.4 Hz, *J* = 1.8 Hz), 4.57 – 4.55 (m, 2H), 2.31 (dt, *J* = 7.3 Hz, *J* = 1.7 Hz), 2.25 (dt, *J* = 7.3 Hz, *J* = 1.6 Hz). <sup>13</sup>C NMR (75 MHz, CDCl<sub>3</sub>): 153.89, 148.87, 143.25, 142.03, 124.22, 122.18, 111.67, 106.79, 68.47, 49.66. HR-MS (EI): calcd for C<sub>19</sub>H<sub>14</sub>O<sub>2</sub> [M]<sup>+</sup>, 274.099; found 274.099.



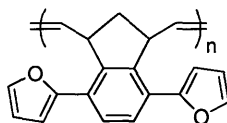
**endo-5,6-bis(methoxymethyl)bicyclo[2.2.1]hept-2-ene (12).** This compound was synthesized using a method adapted from the preparation of compound **9**.<sup>15</sup> A solution of *endo*-bicyclo[2.2.1]hept-ene-2,3-dicarboxylic acid anhydride (**10**) (25 g, 152 mmol) in THF (120 mL) was added slowly to a suspension of LiAlH<sub>4</sub> (7.21 g, 190 mmol) in THF (200 mL) under argon atmosphere at 0 °C. Then the reaction mixture was stirred at room temperature for 18 h. After the same work-up procedure that was used for the preparation of compound **9**,<sup>15</sup> the crude product (**11**) was obtained as a white solid (18.55 g, 79%). Diol **11** (19.70 g, 127 mmol) in THF (130 mL) was added slowly to NaH suspension (16.5 g, 60% in mineral oil, 413 mmol) in THF (200 mL) under argon atmosphere, and the mixture was stirred for 1 h. Methyl iodide (30 mL, 481 mmol) was added slowly. The reaction mixture was stirred for 1

h at room temperature and another 3 h at 40 °C and then cooled to room temperature. After neutralization, it was extracted with diethyl ether and washed with water. The solution was dried over MgSO<sub>4</sub> and filtered, and the solvent was removed. The crude product was vacuum distilled from sodium to give a clear oil (18.65 g, 80%). <sup>1</sup>H NMR (300 MHz, CDCl<sub>3</sub>): δ 6.10 (t, 2H, *J* = 1.8 Hz), 3.60 (s, 6H), 3.18 – 2.94 (m, 4H), 2.88 (m, 2H), 2.47 – 2.37 (m, 2H), 1.44 (dt, 1H, *J* = 8.3 Hz, *J* = 1.8 Hz), 1.28 (d, 1H, *J* = 8.3 Hz). <sup>13</sup>C NMR (75 MHz, CDCl<sub>3</sub>): 135.37, 72.97, 58.80, 49.18, 45.62, 41.50. HR-MS (ESI): calcd for C<sub>11</sub>H<sub>18</sub>O<sub>2</sub> [M + Na]<sup>+</sup>, 205.120; found 205.120.

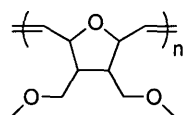
**General Procedure for Homopolymerizations.** Under nitrogen atmosphere in a glove box, a solution of the monomer (**4**, **5**, **6**, **9**, or **12**) in CH<sub>2</sub>Cl<sub>2</sub> (0.1 g/mL concentration) was added in one portion to the vigorously stirred solution including the desired amount of catalyst (**13**, **14** or **15**) in CH<sub>2</sub>Cl<sub>2</sub>. The reaction mixture was vigorously stirred at room temperature for various periods of time before quenching with ethyl vinyl ether. The reaction mixture was poured into methanol or hexane to precipitate the polymer, which was dried *in vacuo*.



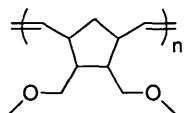
**Poly(4).** This polymer was obtained as a white solid (25%) for 24 h reaction using catalyst **13**. <sup>1</sup>H NMR (500 MHz, CD<sub>2</sub>Cl<sub>2</sub>): δ 7.16, 6.90 (br, 8H), 4.94 (br, 2H), 4.45, 3.97 (br, 2H), 2.40, 1.55 (br, 2H). <sup>13</sup>C NMR (125 MHz, CD<sub>2</sub>Cl<sub>2</sub>): 142.54, 131.79, 129.48, 128.50, 127.71, 126.56, 125.60, 46.97, 43.49.



**Poly(6).** This polymer was obtained as a white solid (80%) for 24 h reaction using catalyst **13**.  $^1\text{H}$  NMR (500 MHz,  $\text{CD}_2\text{Cl}_2$ ):  $\delta$  7.44, 6.28 (br, 8H), 5.29 (br, 2H), 4.58, 3.94 (br, 2H), 2.57, 1.62 (br, 2H).  $^{13}\text{C}$  NMR (125 MHz,  $\text{CD}_2\text{Cl}_2$ ): 152.90, 142.62, 142.12, 133.45, 127.30, 125.34, 112.09, 109.11, 47.41, 43.20.



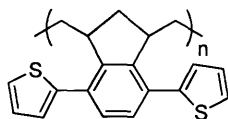
**Poly(9).** This polymer was obtained as a clear tacky solid (90%) for 2 h reaction using catalyst **13**.  $^1\text{H}$  NMR (500 MHz,  $\text{CDCl}_3$ ):  $\delta$  5.72, 5.55 (br, m, 2H), 4.53, 4.22 (br, m, 2H), 3.48 (br, m, 4H), 3.33 (s, 6H), 2.26 (br, 2H).  $^{13}\text{C}$  NMR (125 MHz,  $\text{CD}_2\text{Cl}_2$ ): 133.78, 82.17, 77.43, 77.09, 71.23, 70.98, 70.63, 70.41, 59.12, 48.38, 47.95, 47.60, 47.29. The yield was 98% for 1 h reaction using catalyst **15**.



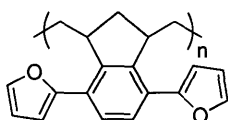
**Poly(12).** The polymer was obtained as a white solid (70%) for 6 h reaction using catalyst **13**.  $^1\text{H}$  NMR (500 MHz,  $\text{CDCl}_3$ ):  $\delta$  5.38 (br, 2H), 3.38 (br, t, 4H), 3.29 (s, 6H), 3.00, 2.69 (br, m, 2H), 2.31 (br, 2H), 1.93, 1.38 (br, m, 2H).  $^{13}\text{C}$  NMR (125 MHz,  $\text{CDCl}_3$ ): 131.96, 71.57, 71.35, 71.22, 58.73, 45.82, 44.19, 40.76, 39.60, 38.90. The yield was 97% for 2 h reaction using catalyst **15**.

**General Procedure for Block Copolymerizations.** Under nitrogen atmosphere in a glove box, a solution of the first monomer (**9** or **12**) in  $\text{CH}_2\text{Cl}_2$  (0.1 g/mL concentration) was added in one portion to the vigorously stirred solution including desired amount of the catalyst (**13** or **15**) in  $\text{CH}_2\text{Cl}_2$ . The reaction mixture was stirred at room temperature for 2 h (6 h for monomer **12** when catalyst **13** was used) before adding solution of second monomer (**4**, **5** or **6**) in  $\text{CH}_2\text{Cl}_2$  (0.1 g/mL concentration). A small sample was taken just before the second monomer solution addition for GPC analysis. The copolymerization was allowed to stir another 22 h and quenched by addition of a drop of ethyl vinyl ether. The reaction mixture was poured into methanol or hexane to precipitate the copolymer, which was dried *in vacuo*. The polymerization yields varied from 65% to 96%. All protons and carbons of each block in copolymers corresponded to those of the appropriate homopolymers in  $^1\text{H}$  NMR and  $^{13}\text{C}$  NMR spectra.

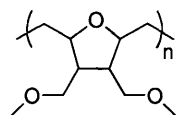
**General Procedure for Hydrogenation of Polymers.** In a typical experiment, a polymer (50 mg) was dissolved in  $\text{CH}_2\text{Cl}_2$  (1 mL), and then ethanol (10 mL),  $\text{CuSO}_4$  (0.02 g, 0.08 mmol) and hydrazine (0.1 mL, 3.2 mmol) were added to the reaction flask. Air was slowly bubbled through overnight at room temperature and then filtered. After ethanol was removed, the mixture was extracted with  $\text{CH}_2\text{Cl}_2$  and the organic portions were combined, washed with brine, and dried over magnesium sulfate. Evaporation of the solvent under reduced pressure afforded a tacky polymer. A literature procedure using tosyl hydrazide<sup>24</sup> was also used for hydrogenation of polymers. Since the aliphatic protons of both blocks of the copolymers had overlapping chemical shifts, it was difficult to isolate and assign the peaks.



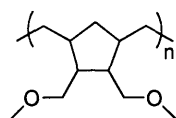
**Hydrogenated Poly(4).**  $^1\text{H}$  NMR (500 MHz,  $\text{CDCl}_3$ ):  $\delta$  7.24, 6.99 (br, 8H), 3.36 (br, 2H), 1.81 (br, 1H), 1.44 (br, 3H), 1.00 (br, 2H).  $^{13}\text{C}$  NMR (125 MHz,  $\text{CD}_2\text{Cl}_2$ ): 146.19, 142.84, 131.00, 129.92, 127.50, 125.56, 125.36, 44.44, 42.47, 35.64, 33.84.



**Hydrogenated Poly(6).**  $^1\text{H}$  NMR (500 MHz,  $\text{CDCl}_3$ ):  $\delta$  7.34, 6.35 (br, 8H), 3.39 (br, 2H), 2.14, 1.58 (br, 6H).  $^{13}\text{C}$  NMR (125 MHz,  $\text{CD}_2\text{Cl}_2$ ): 153.56, 144.50, 141.90, 126.31, 125.30, 111.73, 107.55, 44.54, 42.65, 36.14, 33.48.



**Hydrogenated Poly(9).**  $^1\text{H}$  NMR (300 MHz,  $\text{CDCl}_3$ ):  $\delta$  3.70 (br, m, 2H), 3.43 (br, m, 4H), 3.32 (br, s, 6H), 2.16 (br, 2H), 1.60 (br, 4H).  $^{13}\text{C}$  NMR (125 MHz,  $\text{CDCl}_3$ ): 81.10, 80.98, 80.81, 71.47, 58.95, 46.44, 45.99, 32.00.



**Hydrogenated Poly(12).**  $^1\text{H}$  NMR (300 MHz,  $\text{CDCl}_3$ ):  $\delta$  3.36 (br, m, 4H), 3.31 (br, s, 6H), 2.23 (br, m, 2H), 2.03 (br, m, 1H), 1.90 (br, 2H), 1.48 (br, m, 2H), 1.06 (br, 1H), 0.93 (br, m,

2H).  $^{13}\text{C}$  NMR (125 MHz,  $\text{CDCl}_3$ ): 71.36, 58.83, 44.60, 40.96, 38.61, 30.49.



**References**

1. (a) Hatano, M.; Kambara, S.; Okamoto, S. *J. Polym. Sci.* **1961**, *51*, S26–S29. (b) Shirakawa, H.; Louis, E. J.; MacDiarmid, A. G.; Chiang, C. K.; Heeger, A. J. *J. Chem. Soc., Chem. Commun.* **1977**, 578–580. (c) *Handbook of Conducting Polymers*, 2nd ed.; Skotheim, T. A., Elsenbaumer, R. L., Reynolds, J. R., Eds.; Marcel Dekker: New York, 1998. (d) *Handbook of Organic Conductive Molecules and Polymers*; Nalwa, H. S., Ed.; Wiley: New York, 1997.
2. (a) Roncali, J. *Chem. Rev.* **1997**, *97*, 173–205. (b) Kraft, A.; Grimsdale, A. C.; Holmes, A. B. *Angew. Chem., Int. Ed.* **1998**, *37*, 402–428. (c) *Handbook of Oligo- and Polythiophenes*; Fichou, D., Ed.; Wiley-VCH: New York, 1999. (d) Roncali, J. *J. Mater. Chem.* **1999**, *9*, 1875–1893. (e) Kanazawa, K. K.; Diaz, A. F.; Geiss, R. H.; Gill, W. D.; Kwock, J. F.; Logan, A.; Rabolt, J. F.; Street, G. B. *J. Chem. Soc., Chem. Commun.* **1979**, 854–855.
3. (a) Saunders, B. R.; Fleming, R. J.; Murry, K. S. *Chem. Mater.* **1995**, *7*, 1082–1094. (b) Čabala, R.; Škarda, J.; Potje-Kamloth, K. *Phys. Chem. Chem. Phys.* **2000**, *2*, 3283–3291. (c) *Polymer Sensors and Actuators*; Osada, Y., De Rossi, D. E., Eds.; Springer: Berlin, Germany, 2000.
4. (a) Jang, S.; Sotzing, G. A. *Macromolecules* **2002**, *35*, 7293–7300. (b) Jang, S.; Sotzing, G. A.; Marquez, M. *Macromolecules* **2004**, *37*, 4351–4359. (c) Jang, S.; Marquez, M.; Sotzing, G. A. *J. Am. Chem. Soc.* **2004**, *126*, 9476–9477.
5. Xia, C.; Fan, X.; Park, M.; Advincula, R. C. *Langmuir* **2001**, *17*, 7893–7898.
6. Xia, C.; Advincula, R. C. *Chem. Mater.* **2001**, *13*, 1682–1691.
7. Watson, K. J.; Wolfe, P. S.; Nguyen, S. T.; Zhu, J.; Mirkin, C. A. *Macromolecules* **2000**,

- 33, 4628–4633.
8. (a) Buchmeiser, M. R. *Chem. Rev.* **2000**, *100*, 1565–1604. (b) Frenzel, U.; Nuyken, O. *J. Polym. Sci., Part A: Polym. Chem.* **2002**, *40*, 2895–2916. (c) Bielawska, C. W.; Grubbs, R. H. *Prog. Polym. Sci.* **2007**, *32*, 1–29.
9. Trnka T. M.; Grubbs, R. H. *Acc. Chem. Res.* **2001**, *34*, 18–29.
10. Ivin, K. J.; Mol, J. C. *Olefin Metathesis and Metathesis Polymerization*; Academic Press: San Diego, 1997.
11. Förster, S.; Plantenberg, T. *Angew. Chem., Int. Ed.* **2002**, *41*, 688–714.
12. Albagli, D.; Bazan, G.; Wrighton, M. S.; Schrock, R. R. *J. Am. Chem. Soc.* **1992**, *114*, 4150–4158.
13. Gilliom, L. R.; Grubbs, R. H. *J. Am. Chem. Soc.* **1986**, *108*, 733–742.
14. Stang, P. J.; Hanack, L.; Subramanian, R. *Synthesis* **1982**, 85–126.
15. Manka, J. T.; Douglass, A. G.; Kaszynski, P.; Friedli, A. C. *J. Org. Chem.* **2000**, *65*, 5202–5206.
16. Lynn, D. M.; Kanaoka, S.; Grubbs, R. H. *J. Am. Chem. Soc.* **1996**, *118*, 784–790.
17. (a) Seehof, N.; Grutke, S.; Risse, W. *Macromolecules* **1993**, *26*, 695–700. (b) Rule, J. D.; Moore, J. S. *Macromolecules* **2002**, *35*, 7878–7882. (c) Pollino, J. M.; Stubbs, L. P.; Weck, M. *Macromolecules* **2003**, *36*, 2230–2234.
18. (a) Carlisle, J.; Fox, D. J.; Warren, S. *Chem. Commun.* **2003**, 2696–2697. (b) Spagnol, G.; Heck, M.; Nolan, S. P.; Mioskowski, C. *Org. Lett.* **2002**, *4*, 1767–1770.
19. Sanford, M. S.; Love, J. A.; Grubbs, R. H. *J. Am. Chem. Soc.* **2001**, *123*, 6543–6554.
20. Love, J. A.; Morgan, J. P.; Trnka, T. M.; Grubbs, R. H. *Angew. Chem., Int. Ed.* **2002**, *41*, 4035–4037.

21. Nomura, K.; Sagara, A.; Imanishi, Y. *Macromolecules* **2002**, *35*, 1583–1590.
22. Delaude, L.; Demonceau, A.; Noels, A. F. *Macromolecules* **1999**, *32*, 2091–2103.
23. Brown, H. C.; Bakshi, R. K.; Singaram, B. *J. Am. Chem. Soc.* **1988**, *110*, 1529–1534.
24. Scherman, O. A.; Kim, H. M.; Grubbs, R. H. *Macromolecules* **2002**, *35*, 5366–5371.
25. Child, A. D.; Sankaran, B.; Larmat, F.; Reynolds J. R. *Macromolecules* **1995**, *28*, 6571–6578.
26. Glenis, S.; Benz, M.; LeGoff, E.; Schindler, J. L.; Kannewurf, R.; Kanatzidis, M. G. *J. Am. Chem. Soc.* **1993**, *115*, 12519–12525.
27. Zhu, S. S.; Swager, T. M. *J. Am. Chem. Soc.* **1997**, *119*, 12568–12577.

## **CHAPTER 2**

# **Block Copolymers from Norbornene End Functionalized Conjugated Polymers Using ROMP**

## Introduction

Since the discovery of the conductivity in oxidized polyacetylene, efforts have focused on synthesizing conducting polymers (CPs) with improved processability, and finding new applications for the unique conjugated electronic structure of CPs as mentioned in the previous chapter.<sup>1</sup> Recently, cross-coupling reactions catalyzed by transition metals have been frequently used to synthesize conjugated polymers having various structural modifications.<sup>2</sup> For example, the Suzuki reaction is explored to synthesize poly(*p*-phenylene)s (PPPs), the Heck reaction is successfully utilized to synthesize poly(phenylenevinylene)s (PPVs), the Sonogashira reaction is preferred for the synthesis of poly(phenyleneethynylene)s (PPEs), and the Stille reaction is applied to synthesize poly(phenylenethiophene)s (PPTs) (Figure 2-1). The main advantage of these reactions is that they only require mild conditions and can tolerate many functional groups and therefore, can build regio- and stereoregular conjugated structures with a wide range of functional groups.

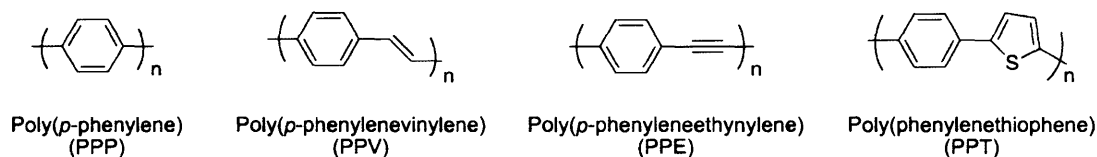


**Figure 2-1.** Representative base structures of conjugated polymers synthesized by organometallic coupling reactions.

Combining the fascinating self-assembly properties of block copolymers with the

active electronic and/or optical function of CPs is an attractive approach to prepare materials with desired properties and applications by the formation of a rich variety of nanoscopic organizations.<sup>3</sup> François et al. have discovered the formation of a regular (honeycomb) morphology from polystyrene (PS) diblock copolymer with PPP<sup>4(a)-(c)</sup> and polythiophene (PT).<sup>4(d)-(e)</sup> Hadziioannou et al. also reported a honeycomb morphology for block copolymers of PS and PPV.<sup>5</sup> The synthesis of block copolymers consisting of poly(ethylene oxide) or polydimethylsilane as a coil segment with a rod segments such as PPE, PPP, and polyfluorene and study of their morphologies were carried out by Müllen et al.<sup>6</sup> McCullough et al. described the synthesis and self-assembly of well-defined block copolymers based on regioregular poly(3-alkylthiophene)s with PS, polymethacrylate, polyurethane, and polyisoprene by converting PT into macroinitiators using living radical polymerization techniques.<sup>7</sup>

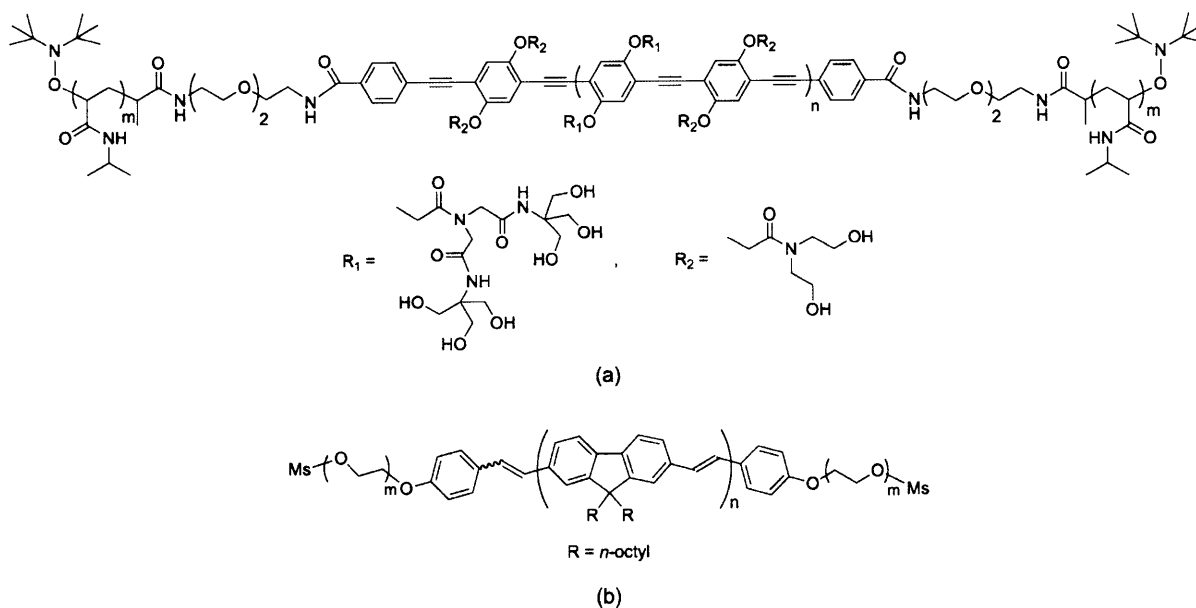
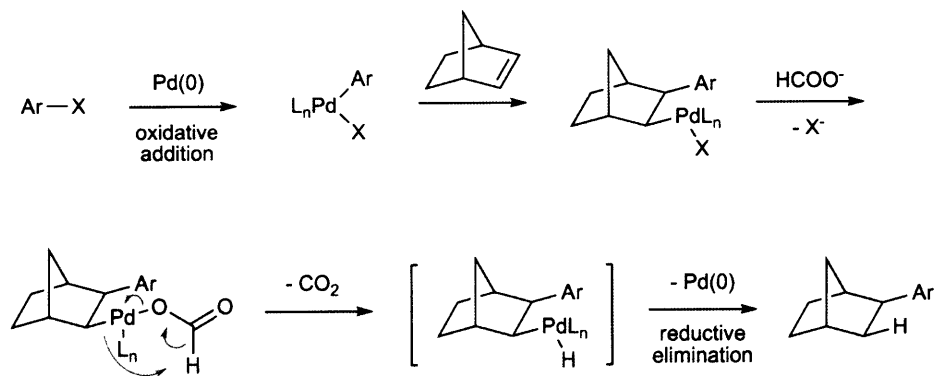


**Figure 2-2.** Two examples of ABA-type triblock copolymers containing CPs.

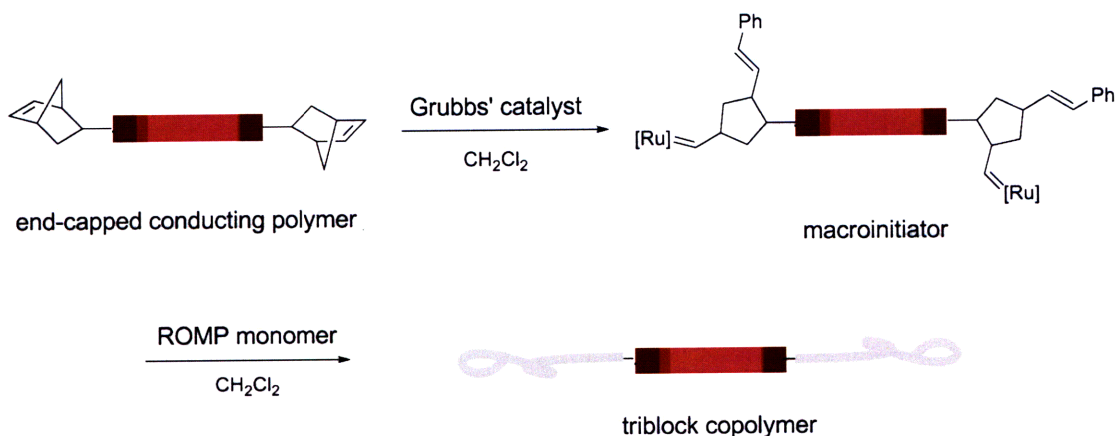
Block copolymers, especially ABA copolymers with a soft segment A and a hard block B, overcome a CP's intractable and infusible properties while preserving its nature. The highly soluble blocks effectively drag the hard segment in the center block into solution.<sup>8(a)</sup> Generally, a synthesis of an ABA-type triblock copolymer with a monofunctional initiator requires two changes of monomers and thus three different polymerization steps.<sup>8</sup> However, it can be also synthesized with difunctional initiators<sup>9</sup> or macroinitiators<sup>7(a),10</sup> by preparing the middle block B first and changing monomers only once (two step polymerization). Our group presented a thermally responsive fluorescent block copolymer of a nonionic water-soluble PPE and poly(*N*-isopropylacrylamide), which precipitated from aqueous solution upon heating, resulting in the isolation of the PPE for facile fluorescence measurements (Figure 2-2(a)).<sup>10(c)</sup> Recently, Nomura and coworkers reported the synthesis of ABA-type amphiphilic triblock copolymers containing poly(fluorenevinylene) by grafting poly(ethylene glycol) via functionalization of poly(fluorenevinylene) chain ends (Figure 2-2(b)).<sup>10(d)</sup>

Scheme 2-1.



The hydroarylation reaction of norbornene or norbornadiene is a useful methodology to synthesize aryl norbornanes or aryl norbornenes from various aryl halides using formic acid as a reducing agent and a palladium catalyst.<sup>11</sup> A proposed mechanism of this reaction is shown in Scheme 2-1.<sup>12</sup> Aryl palladium complexes can react with C=C double bonds to produce vinylic substitution products through a syn-addition and a syn- $\beta$ -elimination (the Heck reaction). The syn- $\beta$ -elimination is impossible when cyclic, strained olefins, like norbornenes, are used as substrates because they lack a H cis to the PdX group. Therefore, the final addition product is generated through decarboxylation and reductive elimination after a formate anion reacts with the intermediate to generate a [RPdLnH] species as shown in Scheme 2-1. Most substituted olefinic systems do not undergo hydroarylation reactions.

Scheme 2-2.



Norbornene end-functionalized CPs can be easily prepared using the hydroarylation reaction when aryl halides at the end of each CP chain react with norbornadiene after the



cross-coupling reaction to prepare the CPs. These macromolecules are monomer candidates for ring-opening metathesis polymerization (ROMP).<sup>13</sup> ROMP provides a method for producing low polydispersity block copolymers using functionalized norbornenes without protecting group chemistry. This is a distinct advantage over other living polymerization techniques, such as anionic polymerization and controlled free radical polymerization. Block copolymers can be synthesized by addition of active ROMP monomers to the solution of these norbornene end-functionalized CPs if they can be initiated by catalysts (Scheme 2-2). This is a novel method to link polymer blocks, and can be applied for the synthesis of new block copolymer structures for various applications, such as CP nanoparticles. The CP nanoparticles are promising candidates for fluorescence labeling and sensing applications because of the small diameters, exceptional optoelectronic properties and high fluorescence quantum yield, and efficient fluorescence quenching by metal nanoparticles.<sup>14</sup>

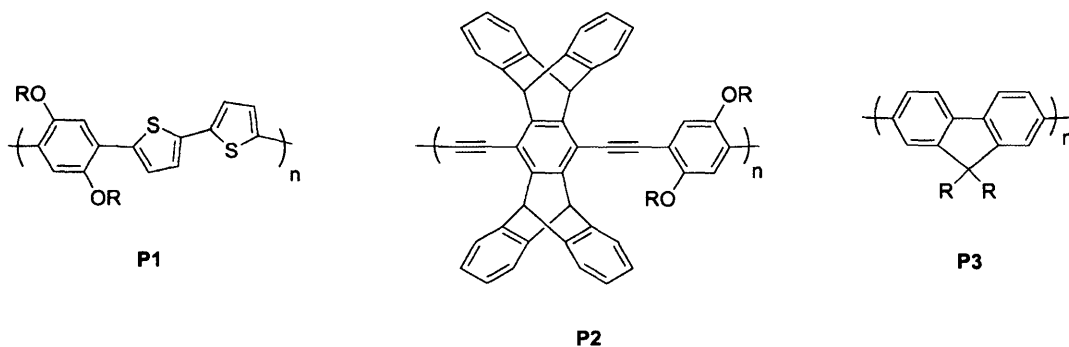


**Figure 2-3.** Three selected conjugated polymers prepared by three different cross-coupling reactions; **P1** from the Stille reaction, **P2** from the Sonogashira reaction and **P3** from the Suzuki reaction.

We present in this chapter our preliminary achievements in the synthesis of block copolymers from the norbornene end-functionalized CPs. The copolymers were synthesized in a straightforward manner via ROMP with functionalized norbornene derivatives and Grubbs' catalysts. Three different structures having interesting properties and/or useful applications were selected as CPs in the center of block copolymers (Figure 2-3). Each of these CPs was synthesized using three different palladium-catalyzed cross-coupling reactions.

**P1** is a benzene and bithiophene alternating copolymer and can be obtained by the Stille cross-coupling reaction, which offers flexibility in the selection of both the monomers and the reaction conditions.<sup>2</sup> This CP belongs to an interesting class of electroactive polymers, and has been further developed as photorefractive polymers with pendant nonlinear optical chromophores or liquid crystalline polymers or chiral polymer conductors using various alkyl side chains.<sup>15</sup>

A pentyptycene-derived PPE, **P2** is produced by the Sonogashira cross-coupling reaction. This highly fluorescent and spectroscopically stable polymer, developed in our group along with other iptycene derivatives, can detect explosives such as 2,4,6-trinitrotoluene (TNT) and 2,4-dinitrotoluene (DNT) using an ultra sensitive fluorescent quenching response.<sup>16</sup> The presence of an extremely bulky structure prevents aggregation in the solid state, and therefore, reduces interchain electron/orbital coupling and self-quenching. The highly porous internal structure of the loosely packed polymer also facilitates passive diffusion of the analyte molecules, resulting in a faster signal response.

Polyfluorene, **P3** and its copolymers can emit color across the entire visible range, possess high thermal stability, and can be easily functionalized at the methylene bridge for fine tuning of emissive properties.<sup>17</sup> These characteristics make polyfluorene homo- and co-

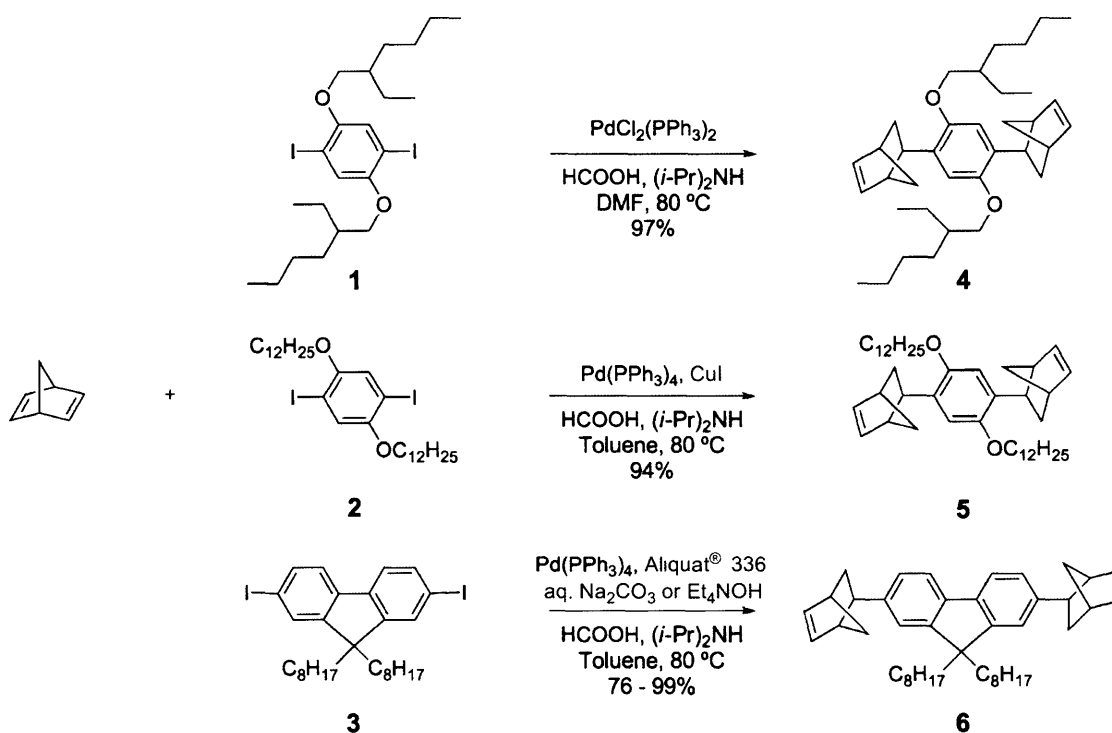
polymers attractive for luminescent materials in polymer light-emitting diodes. Many polyfluorene derivatives have been prepared by the nickel-mediated Yamamoto polymerization.<sup>17(a),18</sup> However, the Suzuki reaction based on the palladium-catalyzed reaction (sometimes in the presence of a phase transfer agent, aliquat<sup>®</sup> 336) is more widely used now since it is able to provide polymers with high structural variety, owing to the compatibility of the reaction conditions with a wide range of functional groups.<sup>19</sup>

## Results and Discussion

### Model Reaction

First, the hydroarylation reactions of norbornadiene with three aryl dihalide monomers (**1**, **2** and **3**) were examined. Since the hydroarylation reaction would be conducted in situ upon completion of a cross-coupling polymerization, we wanted to ensure that the polymerization conditions would not interfere with the hydroarylation reaction, and therefore reagents for each cross-coupling reaction were also used in addition to formic acid and diisopropylamine (Scheme 2-3).

Scheme 2-3.



Aryl norbornenes **4**, **5** and **6** were successfully synthesized from the three corresponding monomers, and purified by either column chromatography (**4** and **6**) or recrystallization (**5**). A protodehalogenated derivative of the starting dihalide was considered as a side product via a direct reduction of the carbon-halogen bond. All of these compounds (**4** – **6**) were characterized by  $^1\text{H}$  NMR and  $^{13}\text{C}$  NMR spectroscopy and mass spectrometry.

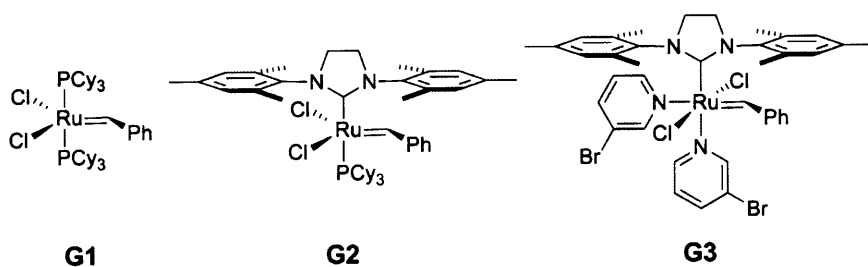


**Figure 2-4.** Grubbs' catalysts.

These compounds (**4**, **5** and **6**) were subjected to ROMP using Grubbs' catalyst since they contain norbornene groups, which is an active ROMP monomer. The chemical structures of the Grubbs' catalysts are shown in Figure 2-4. All bis-norbornene aryl compounds (**4**, **5** and **6**) formed gels when they were polymerized in  $\text{CH}_2\text{Cl}_2$  with the 2nd generation Grubbs' catalyst (**G2**) due to cross-linking (Scheme 2-4 and Figure 2-5). The gels precipitated and formed rubbery balls if  $\text{CH}_3\text{CN}$  was added into solutions. However, they became insoluble, brittle films upon drying. We did not further investigate these compounds for ROMP, but they were expected to be interesting ROMP monomers. For example, 1,4-bis-norbornene-benzene, synthesized using the same hydroarylation method,

was used as a cross-linker to prepare ROMPgel supported reagents.<sup>20</sup>

**Scheme 2-4.**

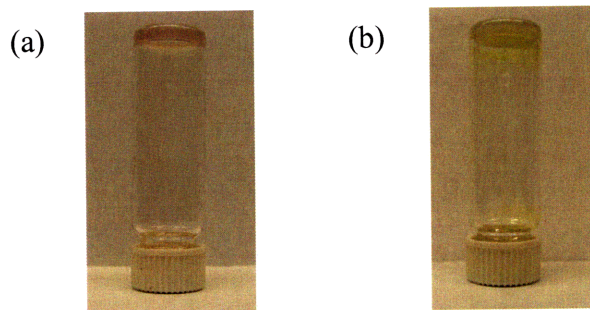
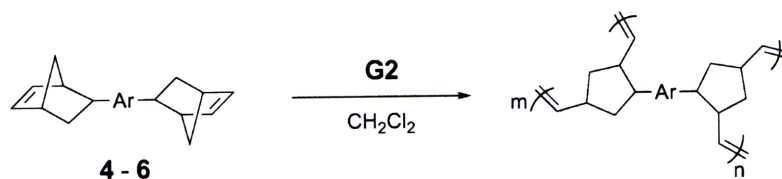


**Figure 2-5.** A gel state of (a) polymerized **4** and (b) polymerized **6**. (The faint colors originated from residual catalysts.)

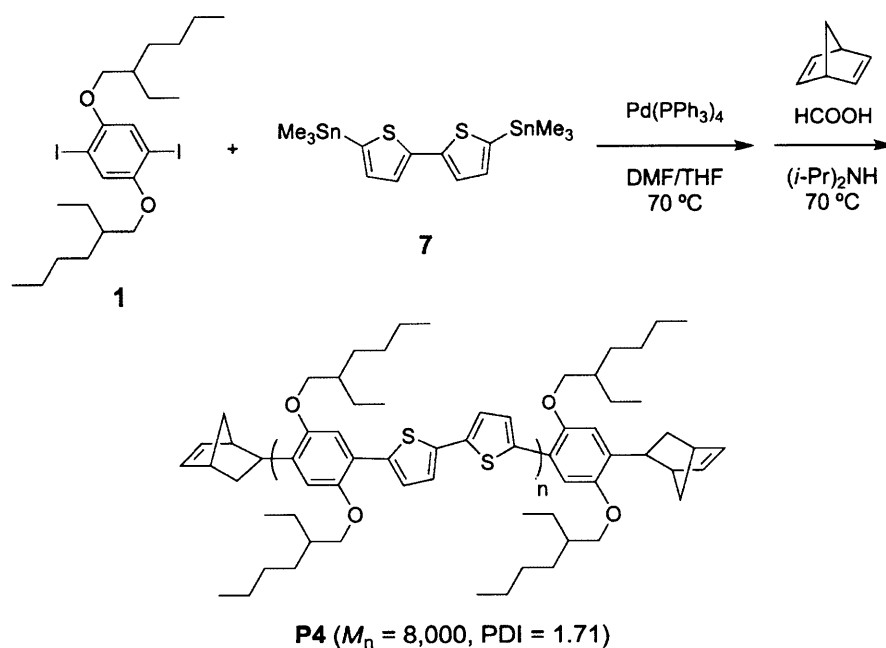
### End-Functionalized CP Synthesis

After the hydroarylation reactions of norbornadiene with aryl dihalides were confirmed to proceed under each cross-coupling reaction condition, three different CPs were synthesized by three different cross-coupling reactions and then, end-functionalized with norbornene by the hydroarylation reaction.<sup>21</sup>

A dialkoxyl-substituted benzene and bithiophene alternating copolymer **P4** was obtained as a dark red solid by the Stille coupling reaction between a small excess of dialkoxyl

diiodobenzene **1** and stannylated bithiophene **7**, and end-capped with norbornene as shown in Scheme 2-5. Growing polymer chains were observed to precipitate out of the reaction during polymerization when DMF was used as solvent due to limited solubility ( $M_n$  of **P4** was observed to be 9,600 and PDI was 2.77). Polymerization in DMF/THF mixtures, THF or toluene also gave polymers with similar molecular weights ( $M_n = 6,800 - 9,400$ ).

Scheme 2-5.



**P4** is a highly fluorescent polymer as shown in Figure 2-6. The absorption and emission spectra of polymer **P4** in THF and spin-cast films are shown in Figure 2-7. The absorption and emission of **P4** are red-shifted by ca. 25 nm compared to the alkoxy-substituted PPT (Figure 2-1) due to the additional  $\pi$ -conjugated thiophene unit.<sup>15(c)</sup> **P4** also

has longer absorption and emission maxima than **P1** ( $R = n$ -hexyloxy in Figure 2-3,  $\lambda_{\text{max}}(\text{abs}) = 450 \text{ nm}$  and  $\lambda_{\text{max}}(\text{em}) = 520 \text{ nm}$  in  $\text{CHCl}_3$  solution), which was synthesized through the Suzuki coupling reaction.<sup>22</sup> This result is likely due to **P4**'s enhanced solubility giving a higher  $M_n$  material than the previous reports.



**Figure 2-6.** Image of **P4** in solution and its fluorescent image.

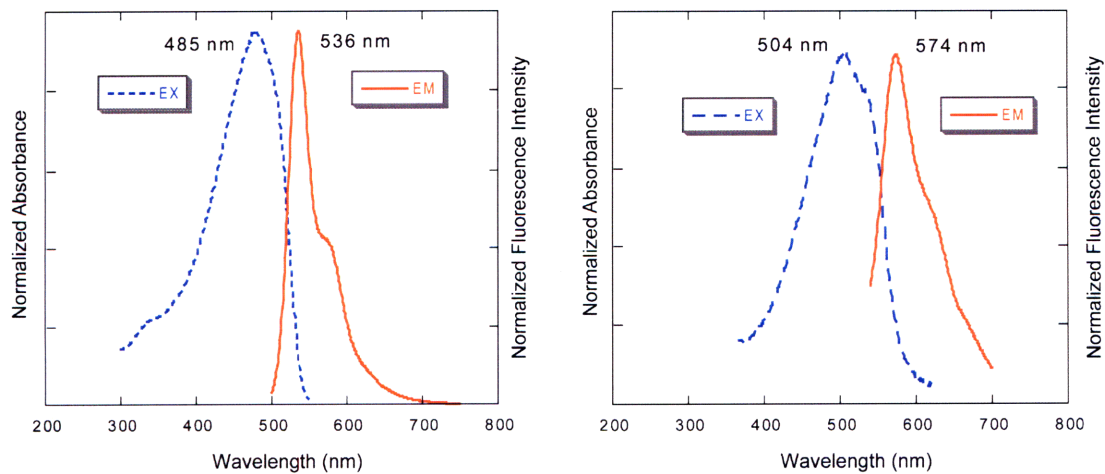
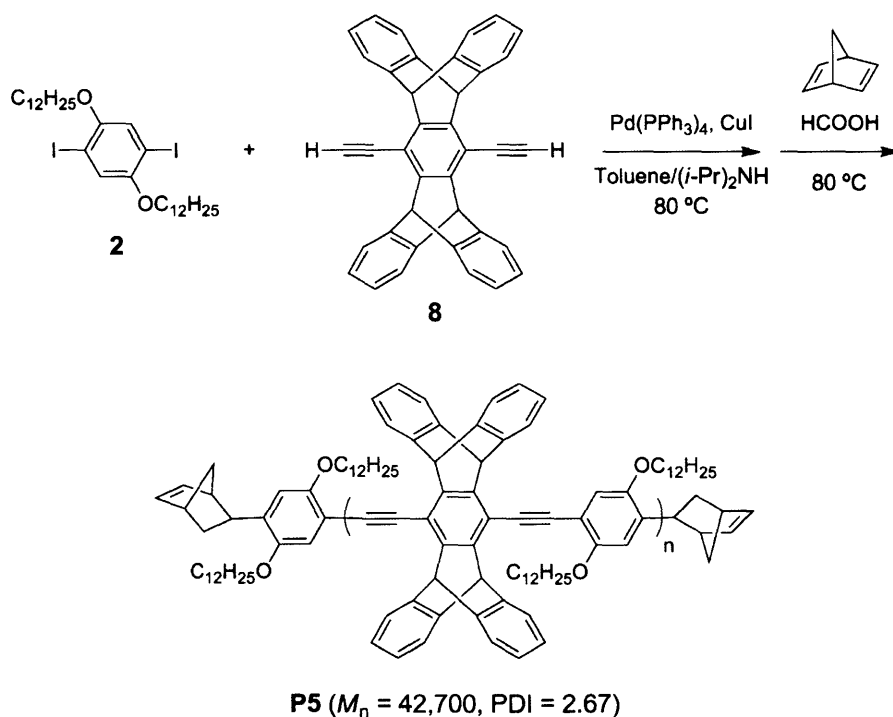


**Figure 2-7.** Absorption and fluorescence spectra of **P4** ( $M_n = 14,900$ ) measured (a) in THF solution and (b) in a spin-cast thin film.



A small excess of dialkoxy diiodobenzene **2** was polymerized with pentyptycene diacetylene **8** under the Sonogashira coupling condition and end-functionalized with norbornene to afford **P5** as a yellow solid (Scheme 2-6).<sup>16</sup> The optical properties of this polymer have been reported before.<sup>16,23</sup>

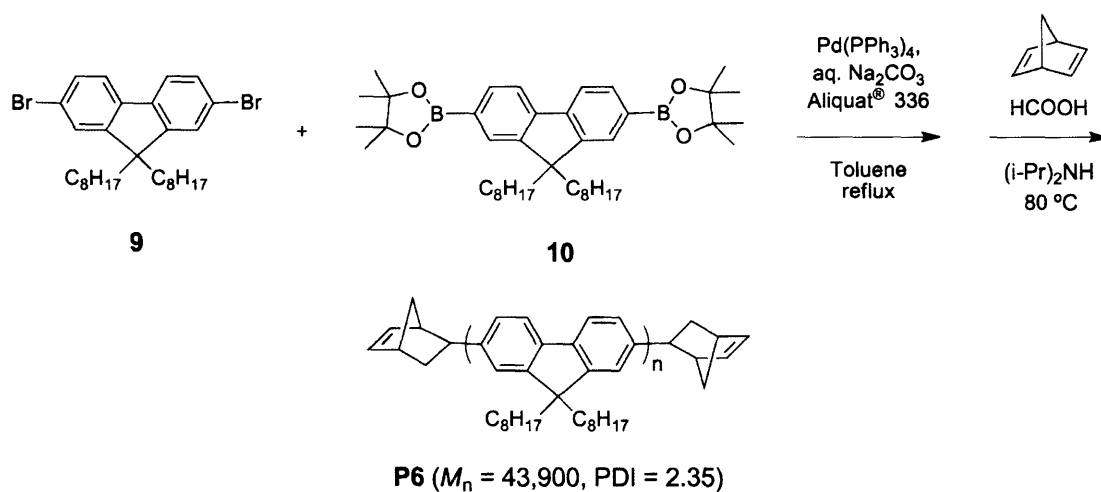
Scheme 2-6.



Norbornene end-capped polyfluorene, **P6** was synthesized through an AB-type monomer route via palladium-catalyzed Suzuki coupling reaction. We examined several reaction conditions<sup>19,24</sup> by changing bases (aq.  $\text{Na}_2\text{CO}_3$ ,  $\text{K}_2\text{CO}_3$  or  $\text{Et}_4\text{NOH}$ ), aryl diboron compounds (diboronic acid or diboronic ester) or aryl dihalides (dibromide or diiodide), and

the molecular weight range obtained for **P6** was between 4,200 and 43,900. The highest molecular weight was obtained when pinacol borate ester **10** was coupled with the dibromo derivative **9** using  $\text{Pd}(\text{PPh}_3)_4$  and  $\text{Na}_2\text{CO}_3$  in the presence of a phase transfer agent (Aliquat<sup>®</sup> 336) (Scheme 2-7). The optical and electrical properties of this polyfluorene have been well studied and our results are in accord with the published results.<sup>24,25</sup>

Scheme 2-7.



The norbornene end group of each CP could be identified by  $^1\text{H}$  NMR spectroscopy (see Appendix 2). Table 2-1 summarizes the molecular weight of the norbornene end-capped CPs based on both GPC and  $^1\text{H}$  NMR. The molecular weights obtained by GPC, using a PS calibration standard, usually overestimate the molecular weight of these polymers because of the rigid rod nature of CPs. Considering this fact, the actual molecular weights of CPs (**P4** – **P6**) are expected to be lower than the  $M_n$  (GPC) values. Polymer molecular weights based on NMR were calculated by taking the ratio between the integrals of the

signals for aromatic protons of the polymer and the signals for the double bond of the end group, multiplying this number by two (because of the presence of two end groups), and then multiplying by the molecular weight of the repeat unit.

**Table 2-1.** Molecular weight of norbornene end-capped CPs

polymer	$M_n$ (GPC)	PDI (GPC)	$M_n$ (NMR)	$M_n$ ratio (GPC/NMR)
<b>P4</b>	6,900	1.48	9,100	0.76
<b>P4</b>	20,200	1.56	31,000	0.652
<b>P5</b>	22,900	3.33	22,500	1.02
<b>P5</b>	49,100	1.80	51,700	0.950
<b>P6</b>	13,600	2.43	13,600	1.00
<b>P6</b>	49,000	1.52	54,700	0.896

Incomplete end-capping will increase the integration ratio of polymer to the end group, and so lead to a high apparent  $M_n$  (NMR). If the calculated  $M_n$  (NMR) values are higher than the  $M_n$  (GPC) values, we can assume that the  $M_n$  (NMR) values have been artificially “inflated” due to incomplete end capping, and therefore the part of polymer chains were not functionalized with norbornene group. The end capping of **P4** was less efficient than **P5** and **P6** since the discrepancy between the  $M_n$  (GPC) and  $M_n$  (NMR) values for **P4** is much greater than those for **P5** and **P6**. Moreover, for the same kind of polymer, high  $M_n$  samples showed a greater discrepancy between  $M_n$  (GPC) and  $M_n$  (NMR), thus implying that the end-capping reaction is less efficient for high molecular weight polymer samples.

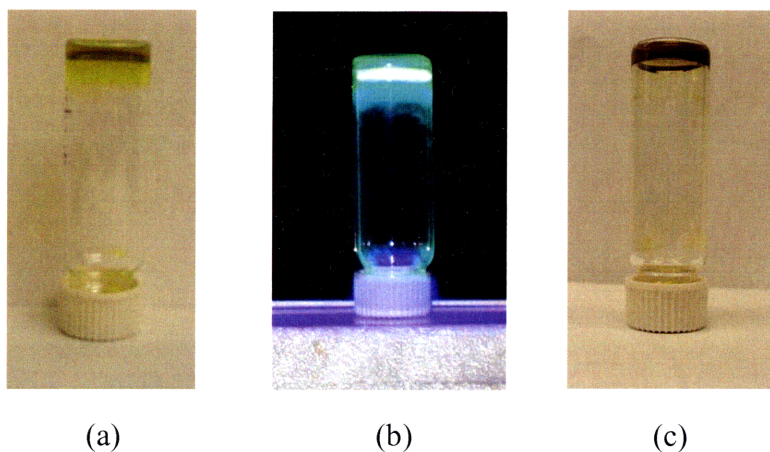


**Figure 2-8.** (a) A gel state of **P5** after ROMP, (b) its fluorescent image and (c) a gel state of **P6** after ROMP. (The faint colors originated from residual catalysts.)

Before synthesizing block copolymers from CPs (**P4**, **P5** and **P6**), the ROMPs of these polymers in  $\text{CH}_2\text{Cl}_2$  were tested with the Grubbs' catalyst, **G2**. Since **P4** was only sparingly soluble in  $\text{CH}_2\text{Cl}_2$  (ca. 4 mg/1 mL), the polymerization solution was too dilute to form a gel, and only became viscous within 20 min. The isolated material was insoluble in common organic solvents. On the other hand, **P5** and **P6** formed gels upon addition of **G2** (Figure 2-8). This gelation also serves as the proof that the CPs were end-functionalized with norbornene groups, which can be polymerized by ROMP catalysts. The polymers without norbornene end groups did not change the viscosity of the solution after addition of the Grubbs' catalyst.

**Table 2-2.** Molecular weight of CPs and their macroinitiators

polymer	reaction atmosphere	catalyst	[Cat.]/[P]	polymer's		macroinitiator's	
				$M_n$	PDI	$M_n$	PDI
<b>P4</b>	air	<b>G1</b>	3.0	20,200	1.56	42,200	2.76
<b>P4</b>	air	<b>G2</b>	5.0	9,600	1.38	24,800	2.34
<b>P4</b>	air	<b>G2</b>	2.5	20,200	1.56	44,800	8.70
<b>P4</b>	air	<b>G2</b>	5.0	20,200	1.56	33,100	2.78
<b>P4</b>	air	<b>G3</b>	3.0	9,600	1.38	19,800	1.70
<b>P4</b>	air	<b>G3</b>	5.0	9,600	1.38	17,500	1.54
<b>P4</b>	air	<b>G3</b>	5.0	20,200	1.56	26,200	1.96
<b>P4</b>	N <sub>2</sub>	<b>G1</b>	6.0	9,600	1.38	26,600	2.04
<b>P4</b>	N <sub>2</sub>	<b>G2</b>	7.0	9,600	1.38	40,600	4.58
<b>P4</b>	N <sub>2</sub>	<b>G3</b>	10.0	9,600	1.38	23,600	1.78
<b>P5</b>	air	<b>G1</b>	2.2	60,700	3.72	78,800	4.60
<b>P5</b>	air	<b>G2</b>	5.0	22,900	3.33	136,200	5.62
<b>P5</b>	air	<b>G2</b>	5.0	49,100	1.80	93,900	6.06
<b>P5</b>	air	<b>G2</b>	5.0	60,700	3.72	109,700	6.51
<b>P5</b>	air	<b>G2</b>	4.0	137,900	2.76	145,600	3.30
<b>P5</b>	N <sub>2</sub>	<b>G1</b>	4.2	60,700	3.72	102,600	3.31
<b>P5</b>	N <sub>2</sub>	<b>G2</b>	2.5	22,900	3.33	74,300	3.18
<b>P5</b>	N <sub>2</sub>	<b>G3</b>	10.0	49,100	1.80	130,900	2.46
<b>P6</b>	air	<b>G2</b>	2.5	4,300	2.74	29,000	1.69
<b>P6</b>	air	<b>G2</b>	2.5	14,600	2.54	50,100	5.89
<b>P6</b>	air	<b>G2</b>	2.5	36,700	3.79	126,000	6.52
<b>P6</b>	air	<b>G2</b>	2.5	117,300	2.04	233,800	6.71
<b>P6</b>	air	<b>G3</b>	5.0	49,000	1.52	129,100	8.33
<b>P6</b>	air	<b>G3</b>	5.0	117,300	2.04	222,300	4.79
<b>P6</b>	N <sub>2</sub>	<b>G1</b>	10.0	32,000	1.57	156,500	3.25
<b>P6</b>	N <sub>2</sub>	<b>G2</b>	10.0	49,000	1.52	107,400	10.1
<b>P6</b>	N <sub>2</sub>	<b>G3</b>	10.0	49,000	1.52	121,600	13.8

### Block Copolymer Synthesis

The macroinitiator from each CP (**P4** – **P6**) was prepared by addition of Grubbs' catalysts to the solutions of CPs in CH<sub>2</sub>Cl<sub>2</sub>, and purified by precipitation into hexanes (Scheme 2-2). Table 2-2 summarizes the GPC results of the synthesized macroinitiators. We found that the catalysts not only initiated but also propagated a norbornene group at the end of CP chains even when excess amount of catalysts were used (up to 10 equivalents to the CP). The  $M_n$  values of the prepared macroinitiators were mostly 2 to 3 times higher than their initial CPs, and their PDIs became broader since the macroinitiators had mixtures of coupled and non-coupled CPs. Generally, the higher the  $M_n$  of CPs, the lower the coupling rate between polymer chains. This is probably due to relatively low mobility and end-functionalization ratio of higher  $M_n$  CPs as mentioned before. The reactions were carried out both under air and inert atmospheres, but all macroinitiators were exposed to air during the purification procedure.

First, the polymerization of a norbornene, which is the most active ROMP monomer, with these macroinitiators was examined. The macroinitiators had low solubilities compared to their source CPs since molecular weights were increased. Therefore, sonication was necessary to dissolve most of macroinitiators in CH<sub>2</sub>Cl<sub>2</sub>. The macroinitiators formed from **G2** and **G3** could synthesize polynorbornene (PNB), which were confirmed by <sup>1</sup>H NMR spectroscopy (see Appendix 2) and GPC. The similarity in the GPC traces obtained from a refractive index detector and a UV/vis detector monitoring at 450 nm indicates that the block copolymer formed contains CP blocks since PNB does not absorb visible light (Figure 2-9). The macroinitiators formed from less reactive catalyst, **G1** could not synthesize block copolymers.

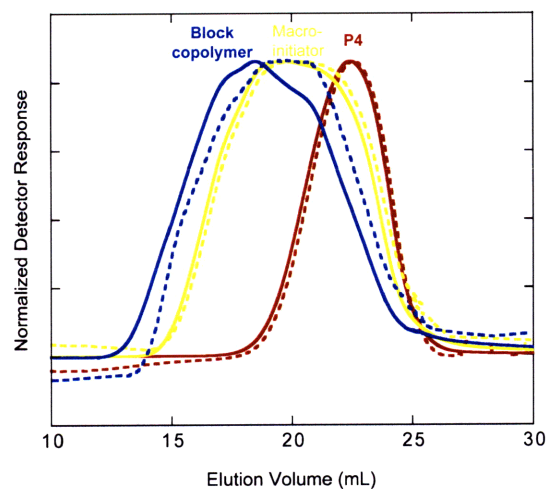


**Figure 2-9.** GPC traces of a block copolymer, PNB-**P4**-PNB, with refractive index detection (---) and UV/vis detection (—) (450 nm).

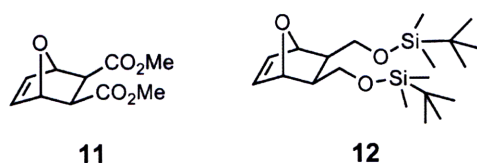


**Figure 2-10.** ROMP monomers examined for block copolymerization.

After we confirmed that these macroinitiators could polymerize norbornene, we used other monomers **11**<sup>26</sup> and **12**<sup>27</sup> for the preparation of block copolymers (Figure 2-10). These monomers are active ROMP monomers and also have synthetic handles that are easy to transform into other functional groups, especially hydrophilic groups. The

homopolymerizations of monomers **11** and **12** were examined with the Grubbs' catalysts in CH<sub>2</sub>Cl<sub>2</sub> at room temperature before being subjected to block copolymerization. For both monomers, homopolymers with relatively narrow PDIs were obtained using **G1** and **G3**, but high molecular weight polymers with broader PDIs were obtained using **G2**. Table 2-3 summarizes the GPC results of the homopolymerizations.

**Table 2-3.** GPC results of homopolymerizations

Monomer	catalyst	[M]/[Cat.]	$M_n$	PDI	DP	yield (%)
<b>11</b>	<b>G1</b>	175	48,000	1.09	230	84
<b>11</b>	<b>G2</b>	230	749,900	1.59	3,530	99
<b>11</b>	<b>G3</b>	220	67,000	1.23	320	87
<b>12</b>	<b>G1</b>	200	54,500	1.20	140	92
<b>12</b>	<b>G2</b>	200	1,003,500	1.63	2,610	98
<b>12</b>	<b>G3</b>	280	111,600	1.03	290	97

The polymerization of **11** or **12** using the macroinitiators was carried out to afford the block copolymer. A solution of **11** or **12** in CH<sub>2</sub>Cl<sub>2</sub> was added to a solution of the macroinitiator in CH<sub>2</sub>Cl<sub>2</sub>, and the reaction mixture was stirred for 20 h. After adding ethyl vinyl ether in order to terminate the ROMP reaction, the block copolymer was obtained by precipitation into acetone or hexane and subsequent reprecipitation. Unreacted macroinitiators could be separated by reprecipitation. Obtained block copolymers were confirmed by <sup>1</sup>H NMR spectroscopy (see Appendix 2) and GPC (Figure 2-11).



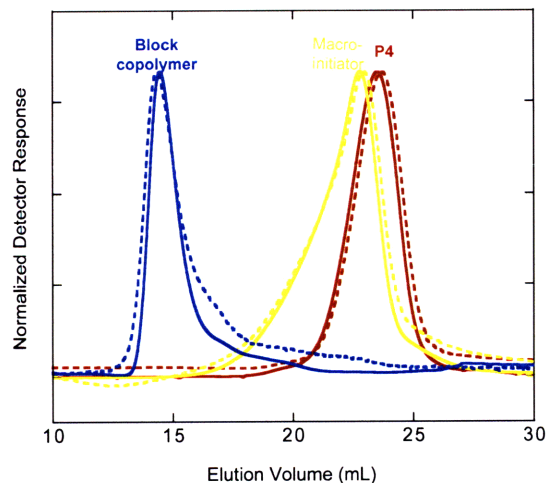


**Figure 2-11.** GPC traces of a block copolymer, poly(**11**)-**P4**-poly(**11**), with refractive index detection (---) and UV/vis detection (—) (450 nm).

Monomer **11** could be polymerized with all macroinitiators in high yields (64 – 99%). However, monomer **12** was only polymerized by the macroinitiator from **P4** in low yield (3.8%) and the block copolymer showed only slight increase in  $M_n$  from its macroinitiator even though its reactivity was similar to **11** in homopolymerizations. Table 2-4 summarizes the molecular weights of the obtained block copolymers. Although Grubbs' catalysts are known to be air stable, the polymerizations under an inert atmosphere produced higher  $M_n$  in higher yields than reactions under air. Also the macroinitiators synthesized under an inert atmosphere polymerized ROMP monomers better. It is hypothesized that the catalyst concentration decreased due to oxidization by oxygen in solution and moisture and, therefore, low turnover numbers were obtained during the metathesis of olefins.

**Table 2-4.** Molecular weight of block copolymers

CP	catalyst	macroinitiator's		monomer	block copolymer's	
		$M_n$	PDI		$M_n$	PDI
<b>P4</b>	<b>G2</b>	40,600	4.58	<b>11</b>	581,400	3.86
<b>P4</b>	<b>G3</b>	23,600	1.78	<b>11</b>	701,200	5.10
<b>P4</b>	<b>G3</b>	23,600	1.78	<b>12</b>	26,900	4.02
<b>P5</b>	<b>G2</b>	69,000	6.33	<b>11</b>	93,700	7.80
<b>P5</b>	<b>G2</b>	42,600	6.83	<b>11</b>	620,600	22.4
<b>P5</b>	<b>G3</b>	130,900	2.46	<b>11</b>	511,200	6.30
<b>P6</b>	<b>G2</b>	29,000	1.69	<b>11</b>	528,300	2.52
<b>P6</b>	<b>G2</b>	74,900	2.09	<b>11</b>	86,300	2.91
<b>P6</b>	<b>G3</b>	121,600	13.8	<b>11</b>	177,300	7.82

Since poly(**11**) and poly(**12**) are transparent, the block copolymers preserve their CPs' color (red for **P4** and yellow for **P5** and **P6**) while they have rubbery property. The absorption and emission spectra of these materials are similar to those of center CPs. The outer elastomers (PNB or poly(**11**)) do not seem to significantly affect the CPs' electronic structures. The similarity in the fluorescence is likely due to energy migration from the terminal portions of the CP that are more affected by the outer block to the center of the CP. Therefore, the emission corresponding to the lower energy gap in the center of the CP dominates the spectrum.<sup>10(c)</sup> Applying these materials to prepare CP nanoparticles is under investigation.

## Conclusions

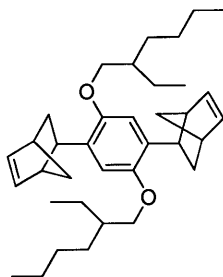
We have utilized the hydroarylation reaction and ROMP to synthesize novel block copolymers having CPs in the center. Three different norbornene end-functionalized CPs were synthesized as macroinitiators using three different palladium-catalyzed cross-coupling reactions and the hydroarylation reaction, which polymerized ROMP monomers subsequently. Prepared block copolymers were rubbery like outer elastomers while having similar optical properties to their center CPs. These types of materials can be used to prepare CP nanoparticles and applied to fluorescence labeling and detection of target biological molecules. The research for precise synthesis and application is under investigation in our group.

## Experimental Section

**Materials.** Toluene, CH<sub>2</sub>Cl<sub>2</sub> and THF were purified by passage through solvent purification columns containing activated alumina. *N,N*-Dimethylformamide (DMF) was distilled from MgSO<sub>4</sub> and stored over 4Å molecular sieves. Diisopropylamine was distilled from CaH<sub>2</sub>. Bicyclo[2.2.1]hepta-2,5-diene (norbornadiene) was distilled from alumina. Bicyclo[2.2.1]hept-2-ene (norbornene) was distilled from sodium. 1,4-bis((2-ethylhexyl)oxy)-2,5-diiodobenzene (**1**)<sup>28</sup>, 1,4-bis(*n*-dodecyloxy)-2,5-diiodobenzene (**2**)<sup>29</sup>, 5,5'-trimethylstannyl-2,2'-bithiophene (**7**)<sup>30</sup>, 2,7-bis(4,4,5,5-tetramethyl-1,3,2-dioxaborolan-2-yl)-9,9-dioctylfluorene (**10**)<sup>24(c)</sup>, 2,3-*exo*-dicarboxylic acid dimethyl ester-7-oxabicyclo[2.2.1]hept-5-ene (**11**)<sup>26</sup> and 2,3-*exo*-bis(*tert*-butyldimethylsilyloxymethyl)-7-oxabicyclo[2.2.1]hept-5-ene (**12**)<sup>27</sup> were prepared according to the literature procedure. All other reagents were used without further purification unless otherwise noted.

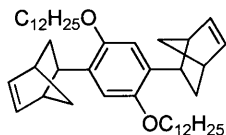
**Instrumentation.** NMR spectra were recorded on Varian Mercury 300 MHz or Varian Inova 500 MHz spectrometer. Chemical shifts were reported in ppm and referenced to residual NMR solvent peaks (CDCl<sub>3</sub>: δ 7.27 ppm for <sup>1</sup>H, δ 77.23 ppm for <sup>13</sup>C). Mass spectra (MS) were obtained at the MIT Department of Chemical Instrumentation Facility (DCIF) using Bruker Daltonics APEX II 3T FT-ICR-MS. Melting points were measured on a Mel-Temp II apparatus (Laboratory Devices INC) and were not corrected. Number average molecular weight (*M<sub>n</sub>*) and polydispersity index (PDI) of polymers were obtained on a HP series 1100 gel permeation chromatography (GPC) system in THF and calibrated with polystyrene standards. Ultraviolet-visible absorption spectra were measured with an Agilent 8453 diode array spectrophotometer. Fluorescence spectra were measured on a SPEX

Fluorolog- $\tau$ 3 fluorometer (model FL-321, 450 W Xenon lamp).

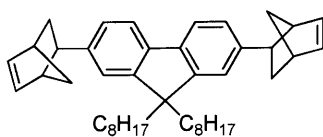


**1,4-Bis(bicyclo[2.2.1]hept-5-en-2-yl)-2,5-bis((2-ethylhexyl)oxy)benzene (4).** Compound 1 (0.50 g, 0.85 mmol) and PdCl<sub>2</sub>(PPh<sub>3</sub>)<sub>2</sub> (II) (12.6 mg, 17.9  $\mu$ mol) were placed in a Schlenk flask with a stir bar. The flask was evacuated and backfilled with argon three times before addition of bicyclo[2.2.1]hepta-2,5-diene (0.40 mL, 3.93 mmol), DMF (4.0 mL) and diisopropylamine (1.0 mL). This reaction flask was subjected to three cycles of freeze-pump-thaw. Formic acid (0.20 mL, 5.30 mmol) was added slowly, and the reaction mixture was heated at 80 °C for overnight. Then, the mixture was cooled to room temperature, diluted with CH<sub>2</sub>Cl<sub>2</sub> and washed with water and brine several times. After drying over MgSO<sub>4</sub>, the solution was filtered, and the solvent was distilled off under reduced pressure. Column chromatography of the crude material on silica gel (CH<sub>2</sub>Cl<sub>2</sub>:hexane (3:10)) provided the product as a viscous oil (0.431 g, 97%). <sup>1</sup>H NMR (500 MHz, CDCl<sub>3</sub>):  $\delta$  6.79 (s, 2H), 6.26 (dd, 2H,  $J$  = 5.61 Hz,  $J$  = 3.05 Hz), 6.19 (dd, 2H,  $J$  = 5.61 Hz,  $J$  = 2.88 Hz), 3.85 (m, 4H), 2.97 (s, 2H), 2.93 (m, 2H), 2.90 (s, 2H), 1.71 (m, 2H), 1.63 (m, 4H), 1.59 (d, 4H,  $J$  = 7.85), 1.56 – 1.41 (m, 8H), 1.37 – 1.31 (m, 8H), 0.97 – 0.91 (m, 12H). <sup>13</sup>C NMR (125 MHz, CDCl<sub>3</sub>):  $\delta$  151.08, 137.53, 137.40, 132.26, 110.10, 70.44, 47.12, 46.27, 42.47, 40.09, 37.21, 33.14, 31.00, 29.43, 24.35, 23.32, 14.35, 11.56. HR-MS (ESI): calcd for C<sub>36</sub>H<sub>54</sub>O<sub>2</sub> [M+Na]<sup>+</sup>,

541.402; found 541.399.

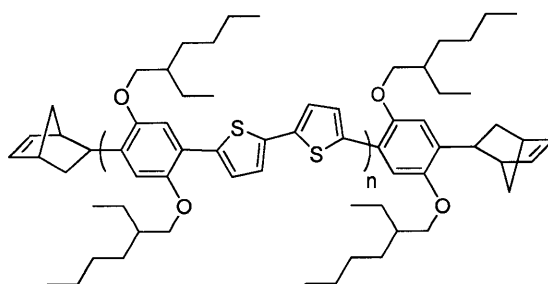


**1,4-Bis(bicyclo[2.2.1]hept-5-en-2-yl)-2,5-bis(n-dodecyloxy)benzene (5).** This compound was synthesized by the same procedure as described for compound **4** using following quantities of reagents: compound **2** (1.0 g, 1.43 mmol), bicyclo[2.2.1]hepta-2,5-diene (1.5 mL, 14.7 mmol), Pd(PPh<sub>3</sub>)<sub>4</sub> (0) (40.0 mg, 35 μmol), CuI (20.0 mg, 0.10 mmol), formic acid (0.70 mL, 18.5 mmol), diisopropylamine (2.5 mL) and toluene (10.0 mL). Purification by column chromatography provided the product as a white solid (0.849 g, 93%). The final purification was achieved by recrystallization from acetone; mp 64°C. <sup>1</sup>H NMR (500 MHz, CDCl<sub>3</sub>): δ 6.77 (s, 2H), 6.25 (dd, 2H, *J* = 5.64 Hz, *J* = 3.08 Hz), 6.17 (dd, 2H, *J* = 5.64 Hz, *J* = 2.75 Hz), 3.92 (t, 4H, *J* = 6.3 Hz), 2.95 (s, 2H), 2.92 – 2.89 (m, 4H), 1.76 (m, 4H), 1.64 (m, 2H), 1.57 (m, 4H), 1.50 – 1.43 (m, 6H), 1.36 – 1.26 (m, 32H), 0.89 (t, 6H, *J* = 6.94 Hz). <sup>13</sup>C NMR (125 MHz, CDCl<sub>3</sub>): δ 151.26, 137.51, 137.41, 132.63, 110.71, 69.03, 46.89, 46.31, 42.49, 37.16, 33.52, 32.15, 29.91, 29.89, 29.88, 29.85, 29.81, 29.62, 29.58, 26.43, 22.92, 14.36. HR-MS (ESI): calcd for C<sub>44</sub>H<sub>70</sub>O<sub>2</sub> [M+H]<sup>+</sup>, 631.545; found 631.545.



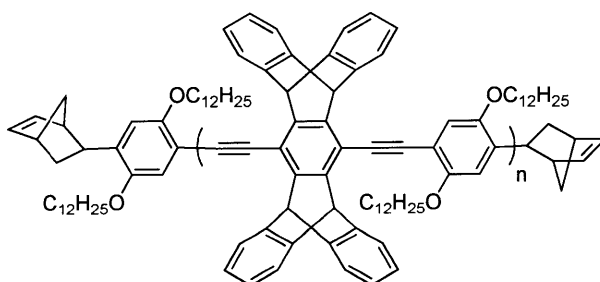
**1,4-Bis(bicyclo[2.2.1]hept-5-en-2-yl)-9,9-dioctylfluorene (6).** This compound was synthesized by the same procedure as described for compound **4** using following quantities of

reagents: compound **3** (0.022 g, 0.034 mmol), bicyclo[2.2.1]hepta-2,5-diene (0.02 mL, 0.20 mmol), Pd(PPh<sub>3</sub>)<sub>4</sub> (0) (1.0 mg, 0.86 μmol), aliquat<sup>®</sup> 336 (0.01 mL), tetraethylammonium hydroxide solution 20% in water (0.10 mL), formic acid (0.01 mL, 0.26 mmol), diisopropylamine (0.20 mL) and toluene (1.0 mL). Column chromatography of the crude material on silica gel (10% CH<sub>2</sub>Cl<sub>2</sub> in hexane) provided the product as a viscous oil (0.016 g, 82%). <sup>1</sup>H NMR (500 MHz, CDCl<sub>3</sub>): δ 7.57 (d, 2H, *J* = 7.63 Hz), 7.23 – 7.21 (m, 4H), 6.30 (dd, 2H, *J* = 5.64 Hz, *J* = 3.05 Hz), 6.20 (dd, 2H, *J* = 5.64 Hz, *J* = 2.90 Hz), 3.00 (s, 2H), 2.94 (s, 2H), 2.81 (m, 2H), 1.96 – 1.91 (m, 4H), 1.80 (m, 2H), 1.68 (m, 2H), 1.64 (d, 2H, *J* = 8.39 Hz), 1.46 (m, 2H), 1.23 – 1.07 (m, 20H), 0.83 (t, 6H, *J* = 7.17 Hz), 0.67 (m, 4H). <sup>13</sup>C NMR (125 MHz, CDCl<sub>3</sub>): δ 151.07, 144.84, 138.90, 137.58, 126.16, 122.24, 119.16, 54.97, 48.82, 45.98, 44.19, 44.19, 42.57, 40.41, 34.05, 32.00, 30.13, 29.37, 29.30, 23.91, 22.84, 14.30. HR-MS (ESI): C<sub>43</sub>H<sub>58</sub> [M]<sup>+</sup>, 574.453; found 574.452.



**P4.** Compound **1** (1.28 g, 2.19 mmol), compound **7** (1.03 g, 2.08 mmol) and Pd(PPh<sub>3</sub>)<sub>4</sub> (0) (0.088 g, 76 μmol) were placed in a Schlenk with a stir bar. The flask was evacuated and backfilled with argon three times before addition of DMF (20 mL) and THF (20 mL). This reaction flask was subjected to three cycles of freeze-pump-thaw, and the reaction mixture was heated at 70 °C. After stirring for 24 h, THF (10 mL), diisopropylamine (0.60 mL),

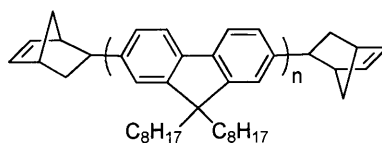
bicyclo[2.2.1]hepta-2,5-diene (0.40 mL, 3.9 mmol) and formic acid (0.20 mL, 5.2 mmol) were added successively. The mixture was stirred for another 24 h, cooled to room temperature, diluted with  $\text{CHCl}_3$ , and washed with saturated ammonium chloride solution and water. After drying over  $\text{MgSO}_4$ , the solution was filtered and the filtrate was passed through a short column of silica gel with  $\text{CHCl}_3$ . The solvent was removed, and the residue was redissolved in a small volume of  $\text{CH}_2\text{Cl}_2$  and precipitated into stirred acetone. The precipitate was separated, washed with acetone and dried *in vacuo*. This afforded 1.01 g of **P4** as a red solid.  $^1\text{H}$  NMR (500 MHz,  $\text{CDCl}_3$ ):  $\delta$  7.53 (br, d, 2H,  $J = 3.58$  Hz), 7.29 (br, s, 2H), 7.24 (br, d, 2H,  $J = 2.78$  Hz), 6.28, 6.22 (br, m, end group), 4.06 (br, d, 4H,  $J = 5.19$  Hz), 3.00, 2.94 (br, end group), 1.94 (br, m, 2H), 1.72 – 1.49 (br, m, 8H), 1.41 (br, m, 8H), 1.04 – 0.94 (br, m, 12H).  $^{13}\text{C}$  NMR (125 MHz,  $\text{CDCl}_3$ ):  $\delta$  149.60, 138.28, 237.81, 126.30, 123.35, 122.79, 111.96, 72.12, 39.95, 31.01, 24.36, 23.36, 14.40, 11.55.



**P5.** This polymer was synthesized by the similar procedure as described for **P4** at 80 °C using the following quantities of reagent: compound **2** (0.176 g, 0.25 mmol), compound **8** (0.117 g, 0.24 mmol),  $\text{Pd}(\text{PPh}_3)_4$  (0) (11 mg, 9.5  $\mu\text{mol}$ ),  $\text{CuI}$  (7.2 mg, 38  $\mu\text{mol}$ ), toluene (3.0 mL), diisopropylamine (0.80 mL), bicyclo[2.2.1]hepta-2,5-diene (0.20 mL, 2.0 mmol) and formic acid (0.10 mL, 2.6 mmol). This afforded 0.188 g of **P5** as a yellow solid.  $^1\text{H}$  NMR



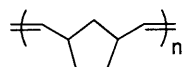
(500 MHz,  $\text{CDCl}_3$ ):  $\delta$  7.50 (br, 8H), 7.44 (br, 2H), 7.03 (br, 8H), 6.34, 6.26 (br, m, end group), 6.10 (br, 4H), 4.46 (br, 4H), 3.05, 3.03 (br, end group), 2.23 (br, 4H), 1.73 (br, 4H), 1.46 (br, 4H), 1.26 – 1.17 (br, 28H), 0.86 (br, 6H).  $^{13}\text{C}$  NMR (125 MHz,  $\text{CDCl}_3$ ):  $\delta$  145.29, 144.29, 125.48, 124.05, 70.38, 32.11, 30.18, 30.04, 29.89, 29.83, 29.79, 29.56, 26.53, 22.91, 14.36.



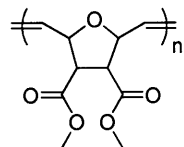
**P6.** This polymer was synthesized by the similar procedure as described for **P4** at reflux condition for the polymerization and 80 °C for the end-capping reaction using the following quantities of reagent: compound **9** (0.562 g, 1.02 mmol), compound **10** (0.642g, 0.998 mmol),  $\text{Pd}(\text{PPh}_3)_4$  (0) (3.0 mg, 2.6  $\mu\text{mol}$ ), 2M  $\text{Na}_2\text{CO}_3$  (2.0 mL), aliquat<sup>®</sup> 336 (0.06 g), toluene (4.5 mL), bicyclo[2.2.1]hepta-2,5-diene (0.40 mL, 3.9 mmol), formic acid (0.20 mL, 5.3 mmol), diisopropylamine (0.50 mL). This afforded 0.722 g of **P6** as a bright yellow solid.  $^1\text{H}$  NMR (500 MHz,  $\text{CDCl}_3$ ):  $\delta$  7.86 (br, d, 2H,  $J = 7.86$  Hz), 7.73 – 7.70 (br, m, 4H), 6.32, 6.22 (br, m, end group), 3.03, 2.97 (br, end group), 2.14 (br, 4H), 1.30 – 1.07 (br, m, 20H), 0.83 (br, t, 6H,  $J = 7.01$  Hz), 0.70 (br, 4H).  $^{13}\text{C}$  NMR (125 MHz,  $\text{CDCl}_3$ ):  $\delta$  152.02, 140.69, 140.22, 126.37, 125.75, 121.70, 120.19, 55.57, 40.61, 32.03, 30.54, 30.27, 29.47, 24.13, 22.84, 14.31.

**General Procedure for ROMP Homopolymerizations.** Under nitrogen atmosphere in a glove box, a solution of the monomer (norbornene, **11** or **12**) in  $\text{CH}_2\text{Cl}_2$  (0.1 g/mL concentration) was added in one portion to the vigorously stirred solution including the desired amount of the Grubbs' catalyst in  $\text{CH}_2\text{Cl}_2$ . The reaction mixture was stirred at room

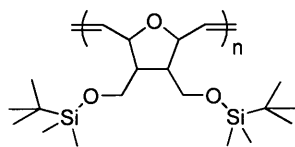
temperature for various periods of time before quenching with ethyl vinyl ether. The reaction mixture was poured into methanol or hexane to precipitate the polymer, which was dried *in vacuo*.



**Polynorbornene.** The polymer was obtained as a white solid (96.6% by **G1**, 95.6% by **G2**, 85.1% by **G3**) for 1 h reaction.  $^1\text{H}$  NMR (300 MHz,  $\text{CDCl}_3$ ):  $\delta$  5.35 ( $J = 1.9$  Hz), 5.21 ( $J = 6.0$  Hz) (br, d, 2H), 2.80, 2.45 (br, 2H), 1.89 – 1.78 (br, m, 3H), 1.36 (br, 2H), 1.05 (br, m, 1H).



**Poly(11).** The polymer was obtained as a white solid (83.8% by **G1**, 87.4% by **G3**) for 16 h reaction.  $^1\text{H}$  NMR (500 MHz,  $\text{CDCl}_3$ ):  $\delta$  5.90, 5.61 (br, m, 2H), 5.07, 4.71 (br, 2H), 3.69 (br, 6H), 3.09 (br, 2H).  $^{13}\text{C}$  NMR (125 MHz,  $\text{CDCl}_3$ ):  $\delta$  171.07, 170.84, 132.58, 131.03, 80.54, 53.38, 52.95, 52.68, 52.46, 52.37. The yield was 99% for 10 min reaction using catalyst **G2**.



**Poly(12).** The polymer was obtained as a white solid (91.6% by **G1**, 97.8% by **G2**, 97.0% by **G3**) for 1 h reaction.  $^1\text{H}$  NMR (300 MHz,  $\text{CDCl}_3$ ):  $\delta$  5.70, 5.54, 5.47 (br, m, 2H), 4.52, 4.36, 4.24 (br, m, 2H), 3.82 - 3.67 (br, m, 4H), 2.20, 2.15 (br, 2H), 0.89 (s, 18H), 0.04 (s, 12H).

$^{13}\text{C}$  NMR (125 MHz,  $\text{CDCl}_3$ ):  $\delta$  135.1, 133.7, 132.5, 81.62, 76.67, 76.05, 61.25, 60.61, 60.46, 50.14, 49.37, 26.20, 26.14, 18.35, -5.14.

**General Procedure for Block Copolymerizations.** A solution of the norbornene end-capped CP (**P4**, **P5** or **P6**) in  $\text{CH}_2\text{Cl}_2$  (concentration of solution depended on the CP's solubility) was added in one portion to the vigorously stirred solution including desired amount of the Grubbs' catalyst (2.2 – 10.0 equiv) in  $\text{CH}_2\text{Cl}_2$  under nitrogen. The reaction mixture was stirred at room temperature for 2 h before precipitation into hexanes. Isolated macroinitiator was dried *in vacuo* and redissolved in  $\text{CH}_2\text{Cl}_2$ . To this solution, the ROMP monomer solution of norbornene, **11** or **12** in  $\text{CH}_2\text{Cl}_2$  was added. The copolymerization was allowed to stir 20 h and quenched by addition of a drop of ethyl vinyl ether. The reaction mixture was poured into acetone or hexane to precipitate the block copolymer. Then, the polymer was dissolved in THF and reprecipitated in hexane and collected by a centrifuge, which was dried *in vacuo*. All protons of each block in copolymers corresponded to those of the appropriate homopolymers in  $^1\text{H}$  NMR spectra.

**References**

1. (a) Hatano, M.; Kambara, S.; Okamoto, S. *J. Polym. Sci.* **1961**, *51*, S26–S29. (b) Shirakawa, H.; Louis, E. J.; MacDiarmid, A. G.; Chiang, C. K.; Heeger, A. J. *J. Chem. Soc., Chem. Commun.* **1977**, 578–580. (c) *Handbook of Conducting Polymers*, 2nd ed.; Skotheim, T. A., Elsenbaumer, R. L., Reynolds, J. R., Eds.; Marcel Dekker: New York, 1998. (d) *Handbook of Organic Conductive Molecules and Polymers*; Nalwa, H. S., Ed.; Wiley: New York, 1997.
2. (a) Babudri, F.; Farinola, G. M.; Naso, F. *J. Mater. Chem.* **2004**, *14*, 11–34. (b) *Metal-Catalyzed Cross-Coupling Reactions*, 2nd ed.; Diederich, F., de Meijer, A., Eds.; Wiley-VCH: Weinheim, 2004.
3. (a) Hoeben, F. J. M.; Jonkheijm, P.; Meijer, E. W.; Schenning, A. P. H. J. *Chem. Rev.* **2005**, *105*, 1491–1546. (b) Bu, L.; Qu, Y.; Yan, D.; Geng, Y.; Wang, F. *Macromolecules* **2009**, *42*, 1580–1588.
4. (a) Zhong, X. F.; François, B. *Makromol. Chem.* **1991**, *192*, 2277–2291. (b) François, B.; Zhong, X. F. *Synth. Met.* **1991**, *41*, 955–958. (c) Widawski, G.; Rawiso, M.; François, B. *Nature* **1994**, *369*, 387–389. (d) Olinga, T.; François, B. *Makromol. Chem., Rapid Commun.* **1991**, *12*, 575–582. (e) François, B.; Olinga, T. *Synth. Met.* **1993**, *57*, 3489–3494.
5. (a) de Boer, B.; Stalmach, U.; Nijland, H.; Hadziioannou, G. *Adv. Mater.* **2000**, *12*, 1581–1583. (b) de Boer, B.; Stalmach, U.; van Hutten, P. F.; Melzer, C.; Krasnikov, V. V.; Hadziioannou, G. *Polymer* **2001**, *42*, 9097–9109.
6. (a) Francke, V.; Räder, H. J.; Geerts, Y.; Müllen, K. *Makromol. Chem., Rapid Commun.* **1998**, *19*, 275–281. (b) Marsitzky, D.; Brand, T.; Geerts, Y.; Klapper, M.; Müllen, K.

- Macromol. Chem., Rapid Commun.* **1998**, *19*, 385–389. (c) Marsitzky, D.; Klapper, M.; Müllen, K. *Macromolecules* **1999**, *32*, 8685–8688. (d) Leclère, P.; Calderone, A.; Marsitzky, D.; Francke, V.; Geerts, Y.; Müllen, K.; Brédas, J.-L.; Lazzaroni, R. *Adv. Mater.* **2000**, *12*, 1042–1046.
7. (a) Liu, J.; Sheina, E.; Kowalewski, T.; McCullough, R. D. *Angew. Chem., Int. Ed.* **2002**, *41*, 329–332. (b) Iovu, M. C.; Craley, C. R.; Jeffries-EL, M.; Krankowski, A. B.; Zhang, R.; Kowalewski, T.; McCullough, R. D. *Macromolecules* **2007**, *40*, 4733–4735.
8. (a) Craig, G. S. W.; Cohen, R. E.; Schrock, R. R.; Silbey, R. J.; Puccetti, G.; Ledoux, I.; Zyss, J. *J. Am. Chem. Soc.* **1993**, *115*, 860–867. (b) Wu, Z.; Grubbs, R. H. *Macromolecules* **1994**, *27*, 6700–6703.
9. (a) Risse, W.; Wheeler, D. R.; Cannizzo, L. F.; Grubbs, R. H. *Macromolecules* **1989**, *22*, 3205–3210. (b) Risse, W.; Grubbs, R. H. *Macromolecules* **1989**, *22*, 4462–4466. (c) Weck, M.; Schwab, P.; Grubbs, R. H. *Macromolecules* **1996**, *29*, 1789–1793. (d) Kitayama, T.; Ogawa, M.; Kawauchi, T. *Polymer* **2003**, *44*, 5201–5207.
10. (a) Kroeze, E.; de Boer, B.; ten Brinke, G.; Hadziioannou, G. *Macromolecules* **1996**, *29*, 8599–8605. (b) You, Y.; Bai, R.; Pan, C. *Macromol. Chem. Phys.* **2001**, *202*, 1980–1985. (c) Kuroda, K.; Swager, T. M. *Macromolecules* **2004**, *37*, 716–724. (d) Nomura, K.; Yamamoto, N.; Ito, R.; Fujiki, M.; Geerts, Y. *Macromolecules* **2008**, *41*, 4245–4249.
11. (a) Larock, R. C.; Johnson, P. L. *J. Chem. Soc., Chem. Commun.* **1989**, 1368–1370. (b) Arcadi, A.; Marinelli, F.; Bernocchi, E.; Cacchi, S.; Ortar, G. *J. Organomet. Chem.* **1989**, *368*, 249–256.
12. Cacchi, S. *Pure Appl. Chem.* **1990**, *62*, 713–722.
13. Bielawska, C. W.; Grubbs, R. H. *Prog. Polym. Sci.* **2007**, *32*, 1–29.

14. (a) Moon, J. H.; Deans, R.; Krueger, E.; Hancock, L. F. *Chem. Commun.* **2003**, 104–105. (b) Moon, J. H.; McDaniel, W.; MacLean, P.; Hancock, L. F. *Angew. Chem., Int. Ed.* **2007**, *46*, 8223–8225. (c) Pecher, J.; Mecking, S. *Macromolecules* **2007**, *40*, 7733–7735. (d) Wu, C.; Szymanski, C.; McNeill, J. *Langmuir* **2006**, *22*, 2956–2960. (e) We, C.; Peng, H.; Jiang, Y.; McNeill, J. *J. Phys. Chem. B* **2006**, *110*, 14148–14154.
15. (a) Bao, Z.; Chan, W.; Yu, L. *Chem. Mater.* **1993**, *5*, 2–3. (b) Yu, L.; Bao, Z.; Cai, R. *Angew. Chem., Int. Ed.* **1993**, *32*, 1345–1347. (c) Bao, Z.; Chan, W. K.; Yu, L. *J. Am. Chem. Soc.* **1995** *117*, 12426–12435. (d) Koeckelberghs, G.; Vangheluwe, M.; Persoons, A.; Verbiest, T. *Macromolecules* **2007**, *40*, 8142–8150.
16. (a) Yang, J.-S.; Swager, T. M. *J. Am. Chem. Soc.* **1998**, *120*, 5321–5322. (b) Yang, J.-S.; Swager, T. M. *J. Am. Chem. Soc.* **1998**, *120*, 11864–11873.
17. (a) Bernius, M.; Inbasekaran, M.; Woo, E.; Wu, W.; Wujkowski, L. *J. Mater. Sci.: Mater. Electron.* **2000**, *11*, 111–116. (b) Leclerc, M. *J. Polym. Sci., Part A: Polym. Chem.* **2001**, *39*, 2867–2873.
18. (a) Yamamoto, T. *Prog. Polym. Sci.* **1992**, *17*, 1153–1205. (b) Yamamoto, T.; Morita, A.; Miyazaki, Y.; Maruyama, T.; Wakayama, H.; Zhou, Z. H.; Nakamura, Y.; Kanbara, T.; Sasaki, S.; Kubota, K. *Macromolecules* **1992**, *25*, 1214–1223.
19. (a) Miyaura, N.; Yanagi, T.; Suzuki, A. *Synth. Commun.* **1981**, *11*, 513–519. (b) Miyaura, N.; Suzuki, A. *Chem. Rev.* **1995**, *95*, 2457–2483. (c) Inbasekaran, M.; Wu, W.; Woo, E. P. US Patent 5,777,070, July 7, 1998.
20. (a) Arnauld, T.; Barrett, A. G. M.; Hopkins, B. T.; Zécéri, F. J. *Tetrahedron Lett.* **2001**, *42*, 8215–8217. (b) Årstad, E.; Barrett, A. G. M.; Hopkins, B. T.; Köbberling, J. *Org. Lett.* **2002**, *4*, 1975–1977. (c) Barrett, A. G. M.; Hopkins, B. T.; Love, A. C.; Tedeschi, L. *Org.*

- Lett.* **2004**, *6*, 835–837.
21. Igarashi, T.; Swager, T. M. Unpublished work, 2005.
22. Shin, S.; Park, J.; Park, J.; Kim, H. *Synthetic Metals* **1999**, *102*, 1060–1062.
23. Zhu, Z.; Swager, T. M. *Org. Lett.* **2001**, *3*, 3471–3474.
24. (a) Ranger, M.; Rondeau, D.; Leclerc, M. *Macromolecules* **1997**, *30*, 7686–7691. (b) Chen, X.; Liao, J.-L.; Liang, Y.; Ahmed, M. O.; Tseng H.-E.; Chen, S.-A. *J. Am. Chem. Soc.* **2003**, *125*, 636–637. (c) Cho S.; Grimsdale, A. C.; Jones, D. J.; Watkins, S. E.; Holmes A. B. *J. Am. Chem. Soc.* **2007**, *129*, 11910–11911.
25. Janietz S.; Bradley, D. D. C.; Grell, M.; Giebeler, C.; Inbasekaran, M.; Woo, E. P. *Appl. Phys. Lett.* **1998**, *73*, 2453–2455.
26. Brion, F. *Tetrahedron Lett.* **1982**, *23*, 5299–5302.
27. Arjona, O.; Medel, R.; Plumet, J.; Herrera, R.; Jiménez-Vázquez, H. A.; Tamariz, J. *J. Org. Chem.* **2004**, *69*, 2348–2354.
28. Weder, C.; Wrighton, M. S. *Macromolecules* **1996**, *29*, 5157–5165.
29. Bao, Z.; Chen, Y.; Cai, R.; Yu, L. *Macromolecules* **1993**, *26*, 5281–5286.
30. Kilbinger, A. F. M.; Feast, W. J. *J. Mater. Chem.* **2000**, *10*, 1777–1784.

## **CHAPTER 3**

# **Liquid Crystalline Gels Using Iptycene-PPEs Through Hydrogen Bonding**



## Introduction

Liquid crystals (LCs), first discovered in the 1850s, are anisotropic fluids, combining the flow properties of an ordinary liquid with the anisotropic physical parameters generally only found for crystals (Figure 3-1). In 1889 Lehmann used the term “liquid crystal” to describe this new state of matter.<sup>1</sup> LCs are generally distinguished between “thermotropic phases”, which are observed solely by temperature variation (at constant pressure) and “lyotropic phases”, which are formed by addition of an isotropic solvent.<sup>2</sup> Thermotropic LCs are further categorized by the shape of their constituent molecules: “calamitic” for rod-like, “discotic” for disk-like, and “sanicic” for lath-like molecular shapes. Calamitic LCs exhibit nematic and smectic phases which have been applied for informational displays in televisions and personal computers, while discotic compound shows a columnar phase that has been used for semiconductors (Figure 3-1).<sup>3</sup>

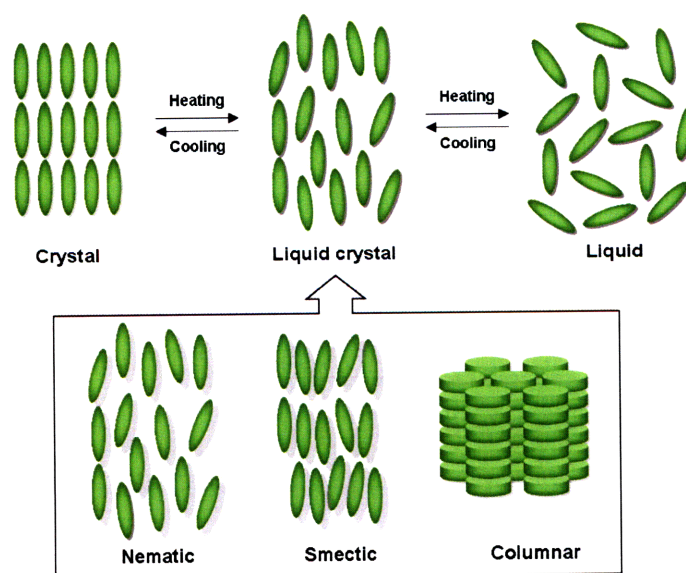


**Figure 3-1.** Schematic illustration of phase transition behavior and the molecular order of LCs and their different structural representation (adapted from ref 3).

The first liquid crystal displays (LCDs) were developed in 1968 based on the dynamic scattering mode.<sup>4</sup> However, they did not succeed commercially due to various limitations of the dynamic scattering mode such as relatively high power consumption, short lifetime, and poor contrast ratio. In 1972, the invention of the cyanobiphenyls, which have a stable phase with a large positive dielectric anisotropy and a strong birefringence enabled the production of commercial displays and rapid development in the display industry.<sup>1</sup>

Among various LCDs such as twist nematic (TN) and in-plane switching (IPS) mode, vertically aligned nematic LCDs (VAN-LCDs) have lately achieved excellent viewing angles in full color. Since the cell gap is not critical, these VAN-LCDs are also easy to manufacture. Major disadvantages for VAN-LCDs are the limited temperature range, low response time and low transmission. For TV applications, a switching time under the so-called frame time of 16 ms is required, along with high brightness, high contrast and good color quality.<sup>5</sup>

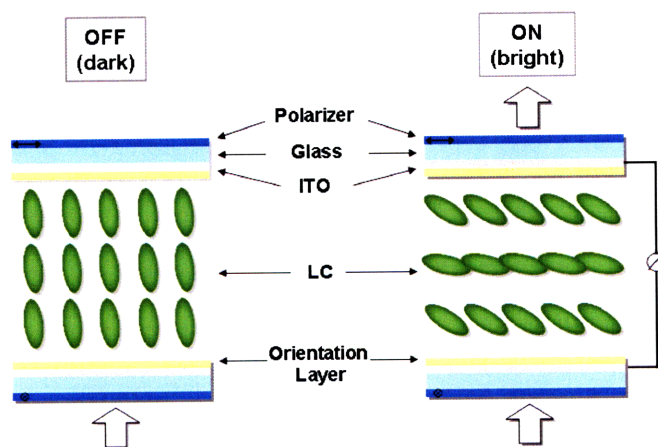


**Figure 3-2.** Setup and basic principle of the VA switching mode (adapted from ref 5).

The basic principle of the vertically aligned (VA) switching mode is schematically shown in Figure 3-2. This mode requires LC materials with negative dielectric anisotropy. The definition of dielectrically negative LCs is that lateral polar substituents induce a dominant dipole moment perpendicular to the long axis of the molecule. Compounds containing lateral dipole groups often exhibit a higher viscosity than those with axial groups due to the larger moment of inertia. Commercial dielectrically negative LCs are based on the 1,2-difluorobenzene building block as shown in Figure 3-3. Since a single LC compound cannot fulfill the complex requirements of the displays, typically mixtures of 10 to 20 LC compounds are required for the wide operating temperature range in combination with other properties.<sup>5</sup>

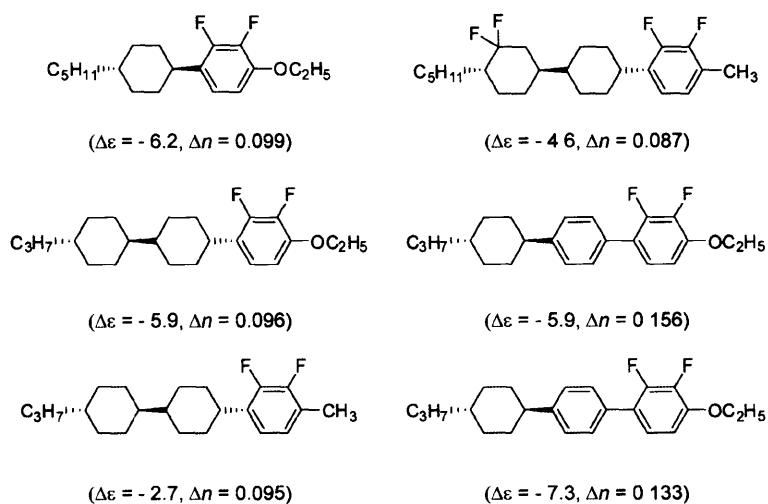


**Figure 3-3.** Representative LCs with negative dielectric anisotropy ( $\Delta \epsilon$ ) and medium birefringence ( $\Delta n$ ).<sup>5</sup>

In the field-off state, LC molecules are aligned vertically to the substrate surfaces, via

elastic forces, by the surface-director orientation layer (surfactants such as lecithin or hexadecyl trimethyl ammonium bromide are commonly used) coated on the substrate surfaces. With this homeotropic orientation and crossed polarizers, the VA mode operates in a normally black mode, which allows high device contrast ratio across the entire spectrum of visible light. Application of an electric field to the VA mode causes the LC molecules to orientate perpendicular to the electric field (parallel to the substrate). This movement of the molecules allows light to pass through and create a white display. After removal of the external field, the LC molecules near the surface-director alignment layer relax to their initial field-off orientation, due to the solid surface/LC interactions. The relaxation of the LC molecules in this region affects, via elastic forces, the orientation of the more remote LC bulk molecules and the initial uniform field-off homeotropic alignment is restored. However, the relaxation to field-off orientation is rather slow, thus resulting in a rather long decay time ( $\tau_{\text{decay}}$ ). The decay time of this device is generally about 20-100 ms.<sup>6</sup> Therefore, it is desirable to decrease the time period needed to relax the LC molecules to a field-off orientation state to optimize the performance of VAN-LCDs.

LCs are often combined with polymers to influence the LCs' orientation and mechanical properties.<sup>7</sup> LC anisotropic gels are a new class of LC compositions containing small amounts of additives (0.2 ~ 1.0 wt %). The LC gels are obtained by the self-assembly of fibrous solid networks of gelators or polymers in LCs that is driven by noncovalent interactions such as hydrogen bonding,  $\pi$ - $\pi$  interactions or van der Waals interactions. The formation of anisotropic phase-separated structures leads to the induction of new functions by the enhancement of the physical properties and dynamic behavior of the LC molecules.<sup>8</sup> The electro-optical properties of LC gels can be tuned by chemical modification of the

components and changing the choice and the concentration of the gelators.<sup>3</sup>

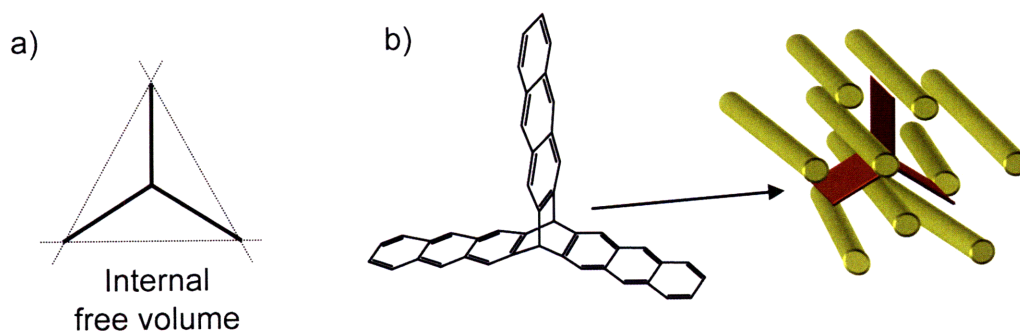


**Figure 3-4.** (a) Definition of “internal free volume” and (b) “minimization of free volume” alignment of iptycene in nematic LCs (adapted from ref 8(a)).

Our group has been interested in the alignment and conformation of conjugated polymer (CP) chains since they are crucial factors for the efficient implementation of CPs in electro-optical systems such as electroluminescent devices, sensors, and field-effect transistors. These characteristics of CP chains strongly depend on the chemical structures of the repeat units and the molecular weights of the polymers. In previous studies, fluorescent dyes, poly(phenyleneethynylene)s (PPEs), and poly(phenylenevinylene)s (PPVs) containing rigid iptycene units were shown to align along the nematic LC’s director due to the minimization of “internal free volume”, resulting in significant anisotropic ordering (Figure 3-4).<sup>9</sup> These methods could produce electronic polymers with chain-extended planar conformations for improved properties.<sup>9-10</sup> Among various iptycene containing polymers, the PPE incorporated with elaborate iptycene scaffolds (shown in Figure 3-5(a)) displayed the greatest ordering (order parameter ( $S$ ) = 0.86, dichroic ratio ( $D$ ) = 19.0), and the global and

local chain conformation could be aligned uniaxially more effectively with increasing molecular weight.<sup>9(e)</sup>

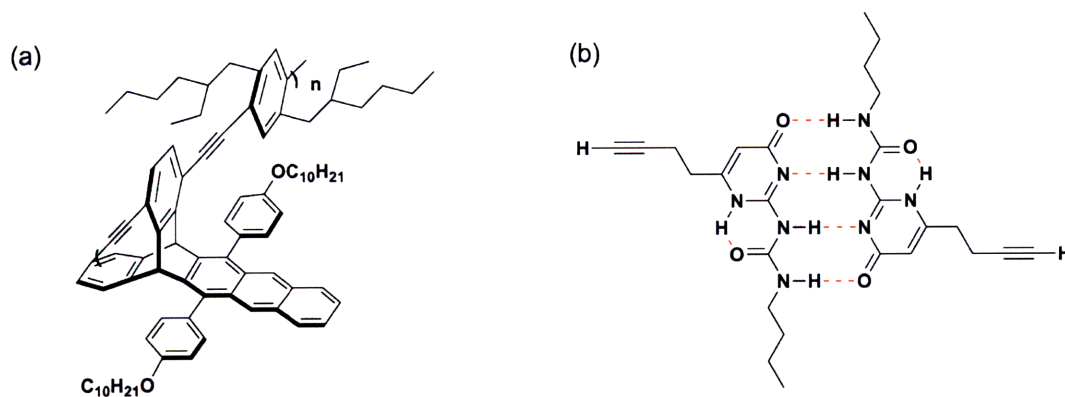


**Figure 3-5.** (a) The PPE structure having the highest anisotropic ordering in nematic LCs<sup>9(e)</sup> and (b) the dimerization of the Upy functional group via quadruple hydrogen bonding (keto tautomer).<sup>11(b)</sup>

The director of the LCs also can be influenced by the presence of an extended rigid polymer just as the polymer's alignment can be influenced by LCs. As a result, it is attractive to construct shape-persistent polymers in networks or ultrahigh molecular weight forms that can span the gaps between critical features (such as electrodes) in electro-optic devices, and thereby produce a homogeneous anchoring element for alignment of LCs. The physical properties of linear polymers and organic molecules can be strongly modified when they are provided with associating end groups. Noncovalent interactions are increasingly being used in the molecular self-assembly of well-defined supramolecular structures and materials.

Hydrogen bonds, used most frequently in noncovalent architectures, are thermally reversible and the strength of hydrogen bonded complexes can be tuned easily by changing solvent or temperature, or altering the acidity and/or basicity of the donor and acceptor moieties. The quadruple hydrogen bonding unit, ureidopyrimidinone (Upy), first introduced by the Meijer group, is a prime example. It dimerizes strongly (the dimerization constant,  $K_{dim}$ , is  $>10^7 \text{ M}^{-1}$  in  $\text{CHCl}_3$ ) since the rich tautomerism inherent within Upy allows for self-complementary associations as shown in Figure 3-5(b).<sup>11</sup> A wide range of polymers have been functionalized with Upy end groups since Upy has proven effective in the preparation of telechelic polymers as well as pendant units off a polymer backbone to improve material properties. By integrating hydrogen bonding groups into conventional polymers through functional initiators or monomers, a versatile platform for designing new materials is envisaged. These developments pave the way to combine the properties of conjugated oligomers and polymers by incorporating well-defined  $\pi$ -conjugated moieties in these hydrogen-bonded polymeric assemblies that exhibit real macroscopic polymeric properties.

Recently, our group has reported that the hydrogen bonding interactions between PPEs dramatically improve their alignment in LCs, increase the anisotropic ordering of the system, and the stability of LC solutions.<sup>9(d)</sup> In this chapter, we report the effect of these iptycene-PPEs having high “virtual” weight molecular through hydrogen bonding interactions on the VAN-LCD’s switching speed, particularly relaxation time. A commercial dielectrically negative LC, MLC-6884 which is an experimental mixture from Licristal<sup>®</sup>, was chosen for switching measurements and its physical properties are shown in Table 3-1.

**Table 3-1.** Physical properties of MLC-6884

$T_{\text{iso}}$	$\Delta n$	$\Delta \epsilon$	$K_1$	$K_3$	$\gamma_1$
74.5 °C	0.0970	- 5.0	13.3 pN	14.8 pN	209 mPa s

$T_{\text{iso}}$ ; Isotropic temperatures,  $K_i$ ; elastic constants,  $\gamma_1$ ; rotational viscosity.



## Results and Discussion

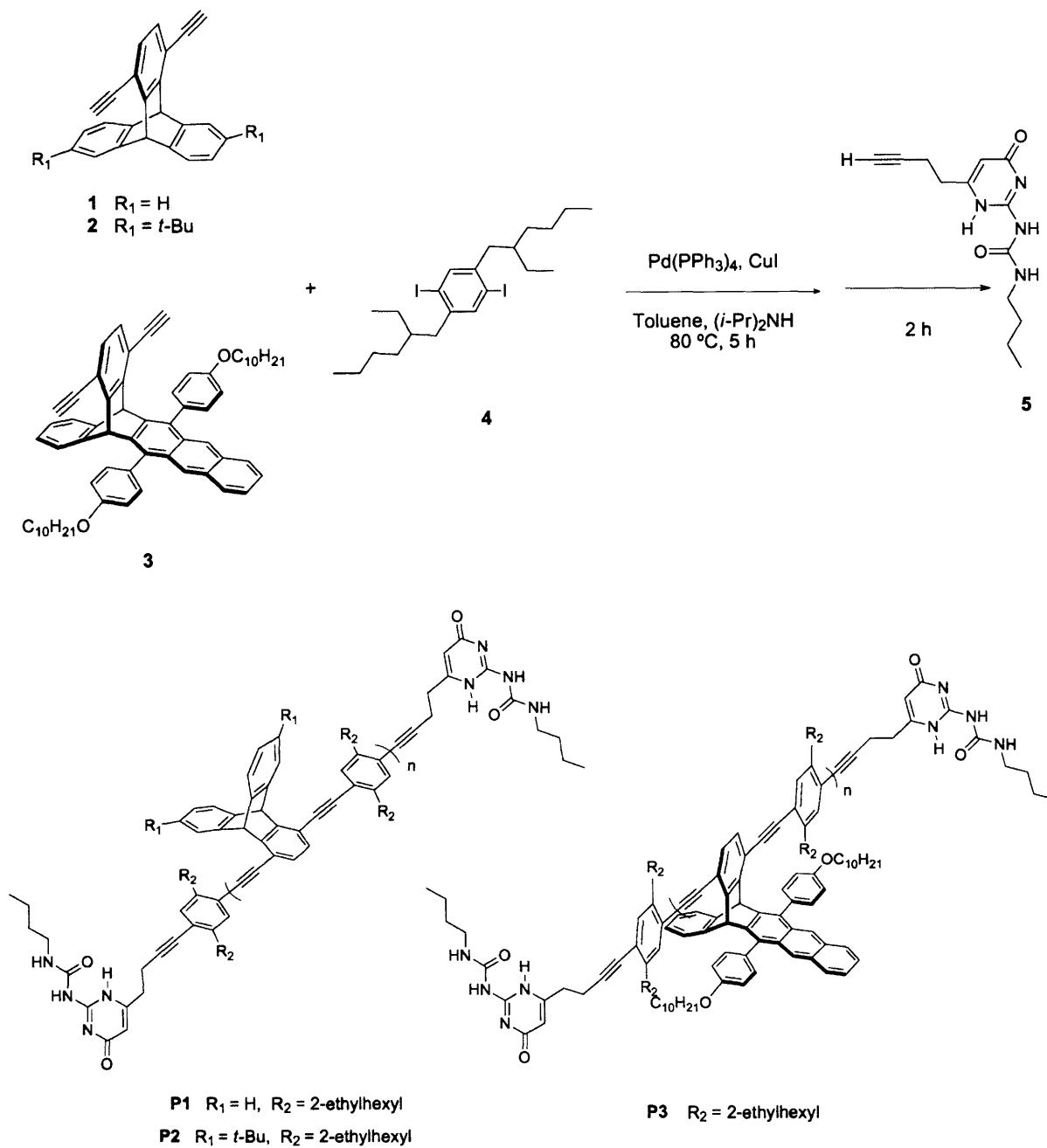
### Polymer Synthesis

To produce LC-polymer gels, three different PPEs, **P1**, **P2** and **P3**, containing rigid iptycene structures end-capped with a hydrogen bonding unit (**5**) were synthesized using the Sonogashira coupling reactions (Scheme 3-1).<sup>9(c)-(e)</sup> A small excess of the dialkyl diiodo benzene monomer **4** (1.01 – 1.08 equiv) was used to ensure that an aryl iodide is at the end of each polymer chain and to allow reactive end-capping with hydrogen bonding units, and to synthesize moderate molecular weight polymers. The NH proton signals of the end group were found at 13.5, 12.0 and 10.2 ppm, indicative of extensive hydrogen bonding by <sup>1</sup>H NMR spectroscopy (see Appendix 3).<sup>11(b)</sup>

Table 3-2 summarizes the GPC results of these polymerizations. Polymers' molecular weights were slightly decreased and PDIs were slightly increased after end-capping reactions. If the oligomers have  $M_n$  less than 5,000 g/mol for hydrogen bonding end functional materials, the hydrogen bonding end group constitutes a larger fraction of the mass of the macromolecules, and it has been shown that not only hydrogen bonding but also phase separation or crystallization of the end groups have a significant influence on the bulk properties of the materials.<sup>12</sup> By increasing the molecular weight of the polymer and thereby decreasing the relative contribution of the end group, such complicating factors could be minimized.

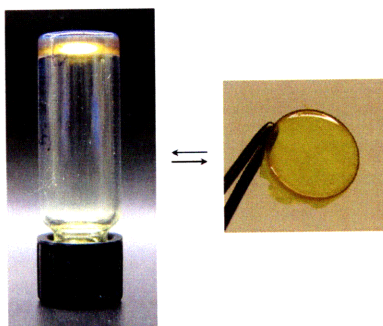
All three polymers formed gels in CHCl<sub>3</sub> which also indicated the existence of hydrogen bonding interactions (Figure 3-6). Flexible polymer films could be obtained when the solvent evaporated. If these films were added into the solvent, they immediately reverted to the gel state.

Scheme 3-1.



**Table 3-2.** GPC results of polymerizations

polymer	hydrogen bonding end group ( <b>5</b> )	$M_n$	PDI
<b>P1</b>	w/o	20,900	2.0
	w	18,200	2.0
<b>P2</b>	w/o	10,000	1.5
	w	8,300	1.6
<b>P3</b>	w/o	15,800	1.8
	w	10,500	2.0

**Figure 3-6.** Gelated **P1** in  $\text{CHCl}_3$  (4.0 mg of **P1** in 0.2 ml  $\text{CHCl}_3$ ) and dried polymer film.

### LC-Polymer gels

MLC-6884 having negative dielectric anisotropy was chosen for our switching experiments. Four different concentrations of LC-polymer solutions between 0.05 - 0.5 weight % (wt %) were prepared. Polymers were dissolved in  $\text{CH}_2\text{Cl}_2$  before addition to MLC-6884 due to the low solubility of polymers in the LC solvent. **P2** had the highest

solubility in the LC, which is consistent with its low molecular weight. The LC-polymer solution became homogeneous after slow evaporation of the  $\text{CH}_2\text{Cl}_2$  at room temperature. If the solution was dried at elevated temperature under vacuum, small weight loss (3.6 wt % loss of LC at 60 °C for 10 h) was observed. The physical gel state was only observed at room temperature when the concentration was 0.5 wt % solution (Figure 3-7). When these gels were heated into the isotropic phase, they reversibly turned into viscous fluids. We also prepared LC mixtures with monomers (1 – 3) and polymers without hydrogen bonding end groups to see the effect of gelation on the switching speeds. All monomers were soluble in MLC-6884 at 0.5 wt % concentration.

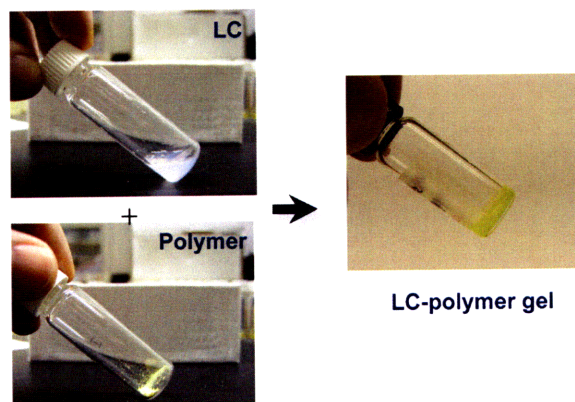


**Figure 3-7.** Preparation of LC-polymer gel.

The isotropic temperatures of each LC mixtures were measured by DSC at a scan rate of 10 °C/min (Table 3-3). Since MLC-6884 is a mixture of LC compounds, the transition peak is broad (about 1 °C width) compared with a single LC compound. Therefore,  $T_{iso}$

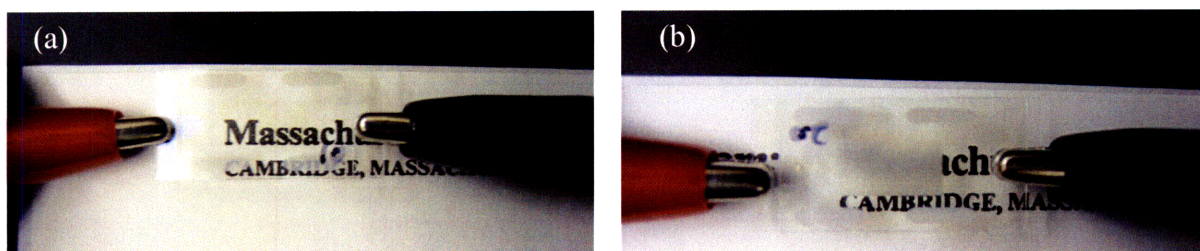
was taken at the maximum value of the transition peak. The phase transition temperatures of the LC mixtures did not deviate significantly from pure MLC-6884. The maximum of the transition peaks on heating roughly increased and those on cooling were decreased upon increasing the wt % of polymer, but the transition peaks were almost identical as a whole.

**Table 3-3.**  $T_{iso}$  of LC mixtures

LC mixture	wt %	$T_{iso}$ on heating (°C)	$T_{iso}$ on cooling (°C)
MLC-6884	-	76.2	74.5
<b>1</b>	0.50	75.6	73.6
P1 (w/o end group)	0.20	76.4	73.4
P1 (w/o end group)	0.50	76.5	72.1
P1 (w/ end group)	0.050	76.0	73.8
P1 (w/ end group)	0.10	76.6	73.4
P1 (w/ end group)	0.20	76.8	73.8
P1 (w/ end group)	0.50	76.5	73.6
<b>2</b>	0.50	75.1	72.5
P2 (w/o end group)	0.20	76.3	73.4
P2 (w/o end group)	0.50	76.6	72.7
P2 (w/ end group)	0.050	76.2	73.8
P2 (w/ end group)	0.10	76.3	73.5
P2 (w/ end group)	0.20	76.4	74.5
P2 (w/ end group)	0.50	77.2	73.0
<b>3</b>	0.50	76.5	73.3
P3 (w/o end group)	0.20	76.2	74.0
P3 (w/o end group)	0.50	76.9	73.3
P3 (w/ end group)	0.050	76.1	73.7
P3 (w/ end group)	0.10	76.5	73.5
P3 (w/ end group)	0.20	76.4	73.3
P3 (w/ end group)	0.50	76.4	73.7

### Switching Off Speed Measurements

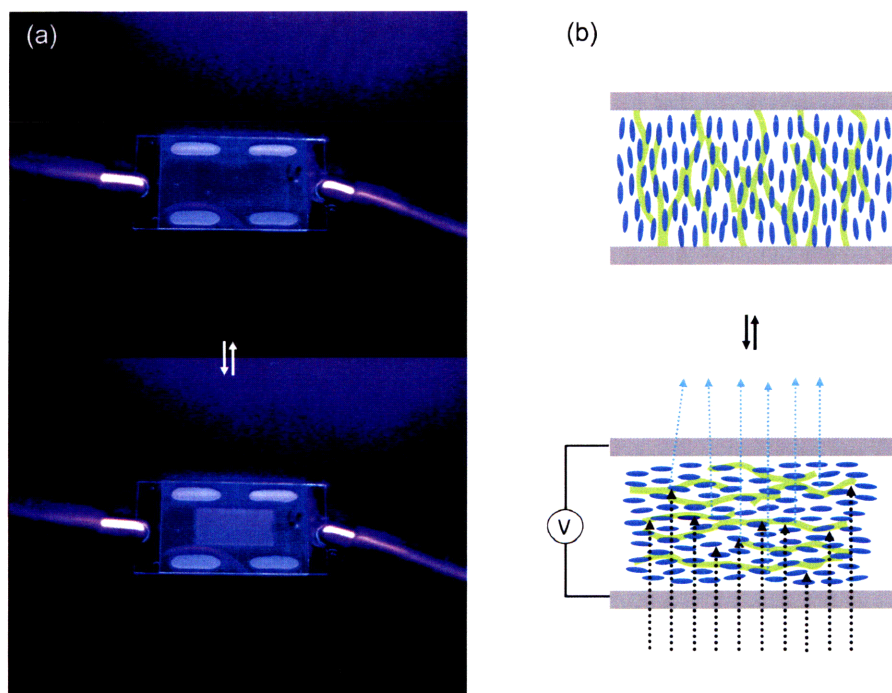
Presumably, at lower temperatures some of the end groups have been “frozen” in a non-hydrogen bonding state.<sup>13</sup> However, there would be enough thermal energy in the system for these moieties to rearrange, allowing the end groups’ hydrogen bonding to be maximized upon reaching the isotropic temperature. Therefore, prepared LC mixtures were heated to the isotropic phase on a hot stage and loaded by capillary action into 10  $\mu\text{m}$  gap of LC test cells designed for vertical alignment. The cell was cooled to 75  $^{\circ}\text{C}$ , equilibrated at this temperature for 30 min, and then slowly cooled to room temperature.



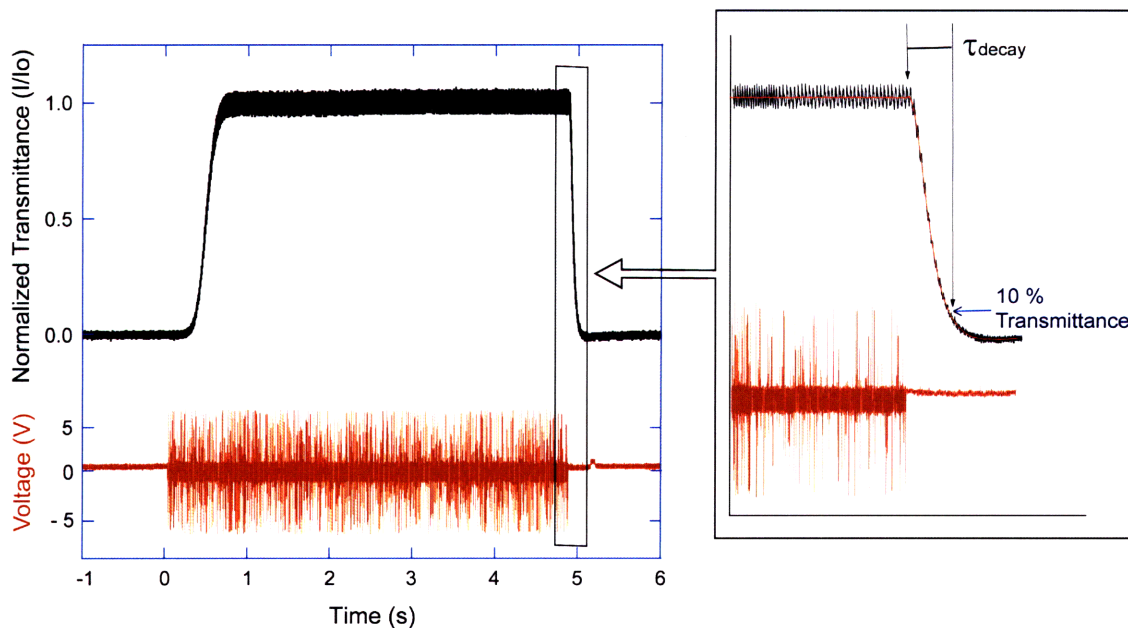
**Figure 3-8.** The LC test cell filled with MLC-6884 (a) light transmission state (0 V) (b) light scattering state (10 V).

Figure 3-8 shows the electro-optical switching in the light scattering mode. At the left, homeotropically aligned LCs in the LC test cell transmitted incident light (Figure 3-8(a)). At the right, 10 V was applied across the LC test cell that realigned the LCs parallel to the glass slides, resulting in light scattering states (Figure 3-8(b)). The fluorescent images of the LC test cell filled with LC-polymer gel containing 0.5 wt % **P1** are shown in Figure 3-9. We had expected the fluorescence to not switch upon application of an electric field since the

fluorescent polymer was tied up in the LC gel. Contrary to our planned design, the polymers also realigned with the nematic director when a voltage was applied, and polymer's fluorescence became apparent. This observation means that a physical gel state, if produced inside the LC test cell, breaks down with the movement of the LC host. All three LC polymer gels showed reversible fluorescence switching in response to the applied voltage. We assume that hydrogen bonding interactions between the end groups of polymer chains were not effective enough in VA mode and/or interrupted by the alignment layer (cetyltrimethyl ammonium bromide) within the LC test cell.



**Figure 3-9.** (a) Fluorescent image of a LC test cell filled with **P1** in MLC-6884 under illumination with 365 nm light and (b) schematic illustration of the LC test cell.



**Figure 3-10.** The electro-optic response of MLC-6884 when a square wave driving voltage (1 kHz AC, 2.25 V) was applied for approximately 5 seconds. (The noise in the voltage was caused by the data acquisition device due to the high frequency of the square wave. The small peak after 5s was induced by switching the power off.)

The transmittance was observed as a function of voltage (1 KHz AC) to find the voltage required for maximum transmittance for each sample. An alternating electric field at 1 KHz frequency was applied to avoid the induced separation of charged impurities.<sup>15</sup> After we decided the applying voltage (2.2 – 2.4 V), the transmittance was recorded while the voltage was applied for about 5 seconds and removed.  $\tau_{\text{decay}}$  is the time when the transmittance reaches 10 % of its maximum value after removal of the field (Figure 3-10). For each sample 5 to 10 measurement was taken, and  $\tau_{\text{decay}}$  of each LC mixture was averaged



over five different samples. The  $\tau_{\text{decay}}$  of MLC-6884 was determined to be 108.4 ( $\pm$  9.5) ms under our experimental condition. The switching time of an LCD is proportional to the rotational viscosity ( $\gamma_1$ ) of the LC.<sup>14</sup> Since MLC-6884 has relatively high rotational viscosity ( $\gamma_1 = 209$ ), compared to LCs used in LCD TVs ( $\gamma_1 \sim 100$ ), the measured switching times in this chapter were slower than the state-of-the-art technology. Table 3-4 summarizes the measured switching time of LC mixtures.

**Table 3-4.**  $\tau_{\text{decay}}$  of LC mixtures

LC mixtures	$\tau_{\text{decay}}$ of <b>P1</b> (ms)	$\tau_{\text{decay}}$ of <b>P2</b> (ms)	$\tau_{\text{decay}}$ of <b>P3</b> (ms)
monomer (0.5 wt %)	119.1 ( $\pm$ 3.0)	127.6 ( $\pm$ 4.1)	130.4 ( $\pm$ 3.8)
w/o end group (0.5 wt %)	134.1 ( $\pm$ 3.6)	157.3 ( $\pm$ 5.2)	139.4 ( $\pm$ 6.0)
w/ end group (0.1 wt %)	121.7 ( $\pm$ 2.3)	135.5 ( $\pm$ 7.4)	127.6 ( $\pm$ 3.2)
w/ end group (0.5 wt %)	140.4 ( $\pm$ 9.6)	180.7 ( $\pm$ 3.9)	137.5 ( $\pm$ 7.7)

For LC mixtures with monomers, the higher the molecular weight of the compound (**3** > **2** > **1**), the slower the switching speed was (but not linearly proportional). For LC mixtures with polymers, on the contrary, the higher  $M_n$  of the polymer (see Table 3-2), the faster the switching speed was at the same concentration except the LC mixture having 0.5 wt % of end-capped **P3**. Polymer mixtures were slower than monomer mixtures for **P1** and **P2** even at lower concentration. It seemed that long polymer chains needed more time to restore than small compounds. LC mixtures having **P3** showed the smallest difference in  $\tau_{\text{decay}}$  from the mixture with the monomer. Polymer, **P3** is known to show the highest alignment among various ipycene-PPEs and align uniaxially more effectively with increasing

molecular weight in nematic LCs.<sup>9(e)</sup> The switching energy of the applied electric field is lower with more uniform alignment.<sup>17</sup> The ability of **P3** to align more uniformly in LC might therefore result in an orientation that more closely tracks the LC dynamics.

All LC mixtures switched off slower than pure LC. The general idea for this study was the stabilization of alignment of a low molecular weight LC by interactions between the polymer network and LC. Since the polymer moves (reorients) with the LC instead of forming a static network inside the cell, the polymer impedes the realignment of LC and slows down the switching speed relative to pure LC. If hydrogen bonding interactions can span two surfaces of the cell, a gel state might be stable enough within the cell and improve the switching speed of the LC.

## Conclusions

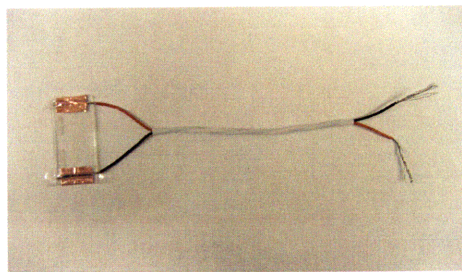
Three different end capped ipitycene-PPEs capable of strong hydrogen bonding were synthesized, and mixed with nematic LC to see the effect of LC-polymer gel on the VAN-LCDs' switching speed, particularly relaxation time. Prepared LC mixtures had similar phase transition temperature to pure LC. Unfortunately, the polymers could not improve the LC's switching time in the VA mode probably because these polymers could not form a stable physical gel state within the LC test cell with even though the same LC polymer mixtures could form a strong gel stage in the bulk at 0.5 wt % concentration. The research to realize a LC gel state within a cell using polymers end-capped with hydrogen bonding unit is under investigation in our group.

## Experimental Section

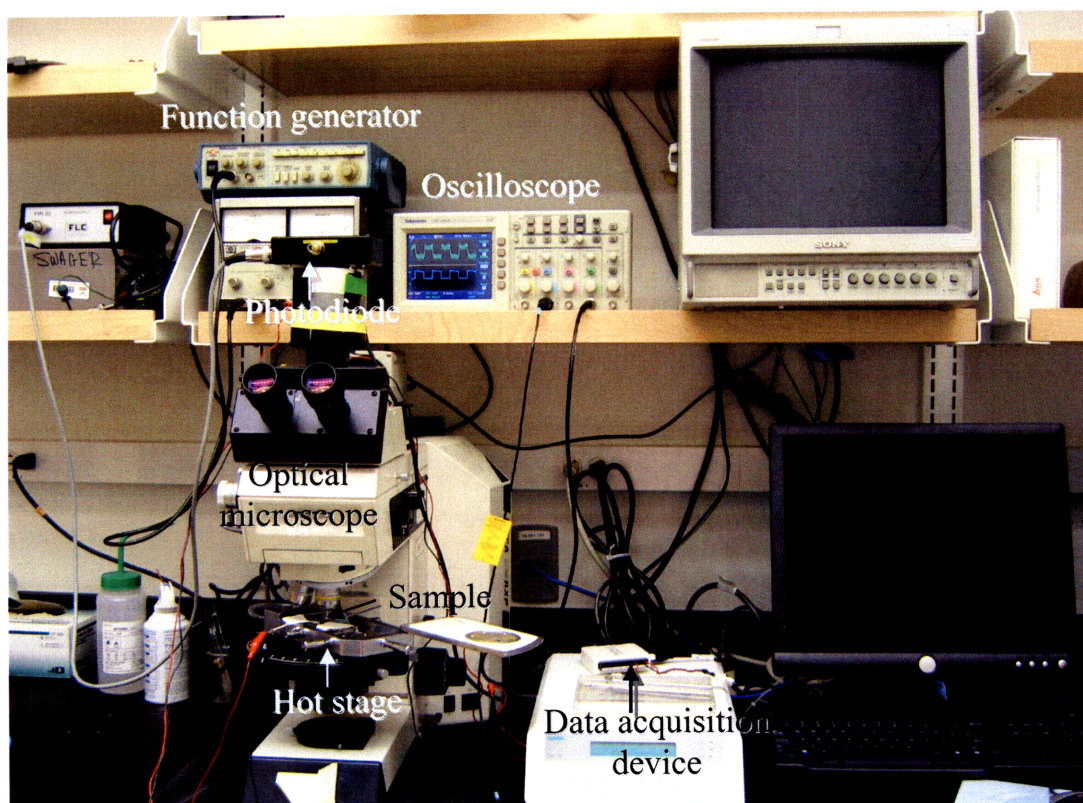
**Materials.**  $\text{CH}_2\text{Cl}_2$  and toluene were purified by passage through solvent purification columns containing activated alumina. Diisopropylamine was distilled from  $\text{CaH}_2$ . 1,4-Diethynyl-9,10-dihydro-9,10[1',2']benzenoanthracene (**1**),<sup>16</sup> 6,14-di-*tert*-butyl-1,4-diethynyl-9,10-dihydro-9,10[1',2']benzenoanthracene (**2**)<sup>9(c)</sup>, 6,13-bis[4-(decyloxy)phenyl]-1,4-diethynyl-5,14-dihydro-5,14[1',2']benzenopentacene (**3**)<sup>9(e)</sup> and 1-[6-(but-3-ynyl)-4-oxo-1,4-dihydropyrimidin-2-yl]-3-butylurea (**5**)<sup>9(d)</sup> were prepared according to the literature procedures. Liquid crystal, MLC-6884, was obtained from Merck Chemicals Ltd. All other reagents were used without further purification unless otherwise noted.

**Instrumentation.** NMR spectra were recorded on Varian Inova 500 MHz spectrometer. Chemical shifts were reported in ppm and referenced to residual NMR solvent peaks ( $\text{CDCl}_3$ :  $\delta$  7.27 ppm for  $^1\text{H}$ ,  $\delta$  77.23 ppm for  $^{13}\text{C}$ ). Number average molecular weight ( $M_n$ ) and polydispersity index (PDI) of polymers were obtained on a HP series 1100 gel permeation chromatography (GPC) system in THF and calibrated with polystyrene standards. Glass transition temperature ( $T_g$ ) and isotropic temperature ( $T_{\text{iso}}$ ) were determined using a TA Instruments Q100 differential scanning calorimetry (DSC) at scan rate of 10 °C/min under nitrogen atmosphere. Liquid crystal test cells were obtained from E.H.C. Co. Ltd, Tokyo, Japan. LC polymer solutions were prepared using the following procedure: A weighted polymer was dissolved in small amount of  $\text{CH}_2\text{Cl}_2$  and added to MLC-6884. Evaporation of solvent at reduced pressure for one day resulted in generation of homogeneous LC polymer solutions. LC Solutions were heated to the isotropic phase on a Linkham 350 Hot Stage and infused by capillary action into LC test cells. The cell was cooled to 75 °C, equilibrated at

this temperature for 30 min, and then slowly cooled to room temperature. Wires were attached to each electrode part of the cell with copper tape and sealed over with transparent tape (Figure 3-11).

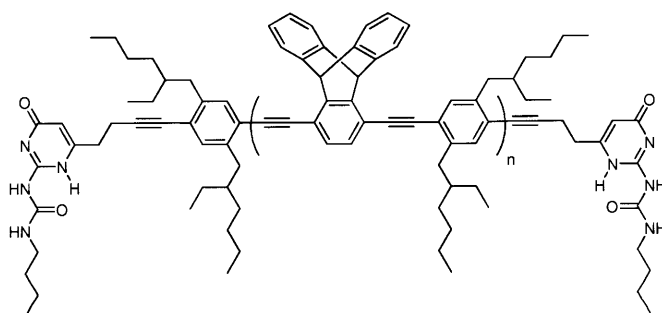


**Figure 3-11.** Wire attached LC test cell.



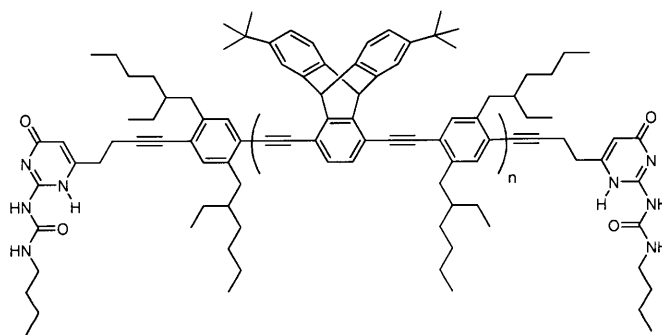
**Figure 3-12.** Experimental setup for switching tests.

Figure 3-12 shows the experimental setup for switching time measurements. The prepared LC cell was mounted on the hot stage controlled by Linkham TMS 94 Temperature Controller. Voltage required for maximum transmittance was applied across the cells, perpendicular to the glass plates, as a square wave potential using a Tektronix CFG253 Function Generator. Applied voltage was measured by Fluke 114 true RMS Multimeter. A FLC Electronics PIN 20 detector was mounted on a Leica DM RXP Optical Microscope to collect the intensity of white light that passes through the experimental setup. The optical response was monitored on the oscilloscope via a photodetector. Data was collected using a National Instruments VI Logger through USB digital I/O. Switching time ( $\tau_{\text{decay}}$ ) is quoted as the time taken to reach 90 % off the maximum transmission.



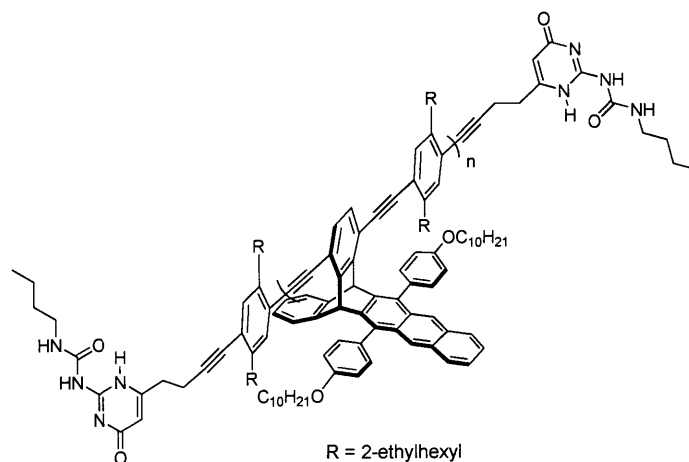
**P1.** 1,4-Diethynyl-9,10-dihydro-9,10[1',2']benzenoanthracene (105 mg, 0.35 mmol), 1,4-bis(2-ethylhexyl)-2,5-diiodobenzene (212 mg, 0.38 mmol), Pd(PPh<sub>3</sub>)<sub>4</sub> (0) (31.0 mg, 0.027 mmol) and CuI (4.2 mg, 0.022 mmol) were placed in a Schlenk flask with a stir bar. The flask was evacuated and backfilled with argon three times before the addition of 2.5 mL of toluene and 1.5 mL of diisopropylamine. Then this reaction flask was subjected to three cycles of freeze-pump-thaw. The reaction mixture was stirred and heated at 80 °C for 5 h

before addition of 1 mL toluene solution of end-capping hydrogen bonding unit, **5** (15 mg, 0.057 mmol). A small sample (about 0.5 mL) was taken just before the addition of end-capping unit and the reaction was allowed to stir another 2 h. Then the mixture was cooled to room temperature, diluted with  $\text{CHCl}_3$  and washed with saturated ammonium chloride solution and water several times. After drying over  $\text{MgSO}_4$ , the solution was filtered, and the solvent was distilled off under reduced pressure. The residue was dissolved in a minimum amount of  $\text{CHCl}_3$  and reprecipitated in acetone. The filtration and drying in *vacuo* afforded a polymer as a yellow solid (88%).  $^1\text{H}$  NMR (500 MHz,  $\text{CDCl}_3$ ):  $\delta$  13.47 (s, end group), 11.97 (s, end group), 10.20 (s, end group), 7.58 (br, 2H), 7.53 (br, 4H), 7.25 (br, 2H), 7.10 (br, 4H), 6.09 (br, 2H), 3.01 (br, 4H) 1.97 (br, m, 2H), 1.54 – 1.34 (br, m, 16H), 1.03 (t, 6H), 0.95 (m, end group), 0.85 (t, 6H).



**P2.** This polymer was synthesized by the same procedure as described for **P1** using the following quantities of reagent: 6,14-di-*tert*-butyl-1,4-diethynyl-9,10-dihydro-9,10[1',2'] benzeneanthracene (38.6 mg, 0.099 mmol), 1,4-bis(2-ethylhexyl)-2,5-diiodobenzene (58.1 mg, 0.10 mmol),  $\text{Pd}(\text{PPh}_3)_4$  (0) (5.0 mg, 0.0043 mmol),  $\text{CuI}$  (2.0 mg, 0.010 mmol), compound **5** (20 mg, 0.076 mmol), 1.3 mL of toluene and 0.7 mL diisopropylamine. The polymer was obtained as a yellow solid (50%).  $^1\text{H}$  NMR (500 MHz,  $\text{CDCl}_3$ ):  $\delta$  13.48 (s, end group),

11.98 (s, end group), 10.21 (s, end group), 7.60 (br, 2H), 7.54 (br, 2H), 7.45 – 7.41 (br, 2H), 7.23 (br, 2H), 7.11 (br, 2H), 6.03 (br, 2H), 3.04 (br, 4H), 1.98 (br, 2H), 1.56 – 1.29 (br, m, 34H), 1.04 (t, 6H), 0.97 (m, end group), 0.84 (m, 6H).



**P3.** This polymer was synthesized by the same procedure as described for **P1** using the following quantities of reagent: 6,13-bis[4-(decyloxy)phenyl]-1,4-diethynyl-5,14-dihydro-5,14[1',2']benzenopentacene (75.0 mg, 0.086 mmol), 1,4-bis(2-ethylhexyl)-2,5-diiodobenzene (50.6 mg, 0.091 mmol), Pd(PPh<sub>3</sub>)<sub>4</sub> (0) (6.0 mg, 0.0052 mmol), CuI (2.0 mg, 0.010 mmol), compound **5** (20 mg, 0.076 mmol), 1.3 mL of toluene and 0.7 mL diisopropylamine. The polymer was obtained as a bright green solid (72%). <sup>1</sup>H NMR (500 MHz, CDCl<sub>3</sub>): δ 13.51 (s, end group), 12.00 (s, end group), 10.24 (s, end group), 8.04 (br, 2H), 7.76 (br, 2H), 7.38 – 7.17 (br, m, 16H), 6.71 – 6.60 (br, m, 2H), 6.24 (br, 2H), 3.72 – 2.64 (br, m, 8H), 1.80 (br, 6H), 1.41 – 0.86 (br, m, 62H).

## References

1. Hikmet, R. A. M. *Liquid Crystals* **2006**, *33*, 1407–1409.
2. (a) Collings, P. J., Hird, M. *Introduction to Liquid Crystals: Chemistry and Physics*; Taylor & Francis: Philadelphia, 1997. (b) Dierking, I. *Adv. Mater.* **2000**, *12*, 167–181.
3. Kato, T.; Hirai, Y.; Nakaso, S.; Moriyama, M. *Chem. Soc. Rev.* **2007**, *36*, 1857–1867.
4. Helmeier, G. H.; Zannoni, L. A.; Barton, L. A. *Appl. Phys. Lett.* **1968**, *13*, 46–47.
5. Pauluth, D.; Tarumi, K. *J. Mater. Chem.* **2004**, *14*, 1219–1227.
6. Komitov, L.; Helgee, B.; Felix, J. A liquid Crystal Device and A Method for Manufacturing Thereof. WO/2004/11405, Dec 29, 2004.
7. (a) Hikmet, R. A. *Adv. Mater.* **1992**, *4*, 679–683. (b) Hikmet, R. A.; Higgins, J. A. *Liquid Crystals* **1992**, *12*, 831–845. (c) Hikmet, R. A.; Kemperman, H. *Nature* **1998**, *392*, 476–479. (d) Kempe, M. D.; Scruggs, N. R.; Verduzco, R.; Lal, J.; Kornfield, J. A. *Nature Materials* **2004**, *3*, 177–182. (e) Xia, Y.; Verduzco, R.; Grubbs, R. H.; Kornfield, J. A. *J. Am. Chem. Soc.* **2008**, *130*, 1735–1740.
8. (a) Mizoshita, N.; Hanabusa, K.; Kato, T. *Adv. Mater.* **1999**, *11*, 392–394. (b) Mizoshita, N.; Hanabusa, K.; Kato, T. *Adv. Funct. Mater.* **2003**, *13*, 313–317. (c) Mizoshita, N.; Suzuki, Y.; Kishimoto, K.; Hanabusa, K.; Kato, T. *J. Mater. Chem.* **2002**, *12*, 2197–2201. (d) Suzuki, Y.; Mizoshita, N.; Hanabusa, K.; Kato, T. *J. Mater. Chem.* **2003**, *13*, 2870–2874. (e) Tong, X.; Zhao, Y.; An, B.-K.; Park, S. Y. *Adv. Funct. Mater.* **2006**, *16*, 1799–1804. (f) Tong, X.; Zhao, Y. *J. Am. Chem. Soc.* **2007**, *129*, 6372–6373. (g) Mizoshita, N.; Suzuki, Y.; Hanabusa, K.; Kato, T. *Adv. Mater.* **2005**, *17*, 692–696.
9. (a) Long, T. M.; Swager, T. M. *Adv. Mater.* **2001**, *13*, 601–604. (b) Long, T. M.; Swager, T. M. *J. Am. Chem. Soc.* **2002**, *124*, 3826–3827. (c) Zhu, Z.; Swager, T. M. *J. Am. Chem.*



- Soc.* **2002**, *124*, 9670–9671. (d) Hoogboom, J.; Swager, T. M. *J. Am. Chem. Soc.* **2006**, *128*, 15058–15059. (e) Ohira, A.; Swager, T. M. *Macromolecules* **2007**, *40*, 19–25.
10. (a) Nesterov, E. E.; Zhu, Z. Z.; Swager, T. M. *J. Am. Chem. Soc.* **2005**, *127*, 10083–10088. (b) Thomas, S. W.; Long, T. M.; Pate, B. D.; Kline, S. R.; Thomas, E. L.; Swager, T. M. *J. Am. Chem. Soc.* **2005**, *127*, 17976–17977.
11. (a) Sijbesma, R. P.; Beijer, F. H.; Brunsveld, L.; Folmer, B. J. B.; Hirschberg, J. H. K. K.; Lange, R. F. M.; Lowe, J. K. L.; Meijer, E. W. *Science* **1997**, *278*, 1601–1604. (b) Beijer, F. H.; Sijbesma, R. P.; Kooijman, H.; Spek, A. L.; Meijer, E. W. *J. Am. Chem. Soc.* **1998**, *120*, 6761–6769. (c) Hirschberg, J. H. K. K.; Beijer, F. H.; van Aert, H. A.; Magusin, P. C. M. M.; Sijbesma, R. P.; Meijer, E. W. *Macromolecules* **1999**, *32*, 2696–2705. (d) El-ghayoury, A.; Schenning, A. P. H. J.; van Hal, P. A.; van Duren, J. K. J.; Janssen, R. A. J.; Meijer, E. W. *Angew. Chem., Int. Ed.* **2001**, *40*, 3660–3663. (e) Dudek, S. P.; Pouderoijen, M.; Abbel, R.; Schenning, A. P. H. J.; Meijer, E. W. *J. Am. Chem. Soc.* **2005**, *127*, 11763–11768.
12. (a) Sivakova, S.; Bohnsack, D. A.; Mackay, M. E.; Suwanmala, P.; Rowan, S. J. *J. Am. Chem. Soc.* **2005**, *127*, 18202–18211. (b) Dankers, P. Y. W.; Zhang, Z.; Wisse, E.; Grijpma, D. W.; Sijbesma, R. P.; Feijen, J.; Meijer, E. W. *Macromolecules* **2006**, *39*, 8763–8771.
13. de Greef, T. F. A.; Ligthart, G. B. W. L.; Lutz, M.; Spek, A. L.; Meijer, E. W.; Sijbesma, R. P. *J. Am. Chem. Soc.* **2008**, *130*, 5479–5486.
14. Tarumi, K.; Finkenzeller, U.; Schuler, B. *Jpn. J. Appl. Phys.* **1992**, *31*, 2829–2836.
15. Wu, K.-J.; Chu, K.-C.; Chao, C.-Y.; Chen, Y.-F.; Lai, C.-W.; Kang, C.-C.; Chen, C.-Y.; Chou, P.-T. *Nano Lett.* **2007**, *7*, 1908–1913.

16. Zhu, Z.; Swager, T. M. *Org. Lett.* **2001**, *3*, 3471–3474.
17. Konovalov, V.; Chigrinov, V.; Kwok, H.; Takada, H.; Takatsu, H. *Jpn. J. Appl. Phys.* **2004**, *43*, 261–266.

# CURRICULUM VITAE

## HYUN A KANG

### EDUCATION

- 9/2001 - present *Massachusetts Institute of Technology*, Cambridge, MA  
Ph.D., Chemistry  
Research Advisor: Timothy M. Swager
- 3/1998 - 2/2000 *Korea Advanced Institute of Science and Technology*, Daejeon, Korea  
M.S., Chemistry  
Research Advisor: Sang Youl Kim
- 3/1994 - 2/1998 *Korea Advanced Institute of Science and Technology*, Daejeon, Korea  
B.S., Chemistry

### EXPERIENCE

- 1/2002 - present *Massachusetts Institute of Technology*, Cambridge, MA  
*Research Assistant, Advisor: Timothy M. Swager*
- Synthesized processable conductive polymers by block copolymerization via ring-opening metathesis polymerization and studied their properties
  - Investigated LC-polymer gel materials to improve LCD's switching speed
- 9/2001 - 5/2002 *Teaching Assistant, Undergraduate chemistry laboratory*
- Instructed and supervised laboratory techniques for intermediate and advanced chemical experimentation and instrumentation
- 3/1998 - 2/2000 *Korea Advanced Institute of Science and Technology*, Daejeon, Korea  
*Research Assistant in Macromolecular Synthesis Lab, Advisor: Song Youl Kim*
- Synthesized and characterized polyimides from unsymmetrical diamines containing cyano group
  - Synthesized linear and star-shaped polymers using tin and aluminum compounds
- 7/1997 *Samyang, Corp.*, Daejeon, Korea  
*Intern, Analysis center of the Central R&D*
- Analyzed new materials for cloth, macromolecular synthetic fibers for industrial use and engineering plastics
- 9/1997 - 12/1997 *Korea Advanced Institute of Science and Technology*, Daejeon, Korea  
*Undergraduate Research in Biochemistry Lab, Advisor: Younghoon Lee*
- Assisted the development of novel antifungal proteins
- 6/1996 - 8/1996 *Undergraduate Research in Polymer Chemistry Lab, Advisor: Hong-Ku Shim*
- Synthesized monomers used for LED polymers

### PRESENTATIONS

1. **Hyun A Kang**, Rachel Z. Pytel and Timothy M. Swager, "Nanostructured Conducting Block Copolymers Integrated into Polynorbornene-Derived Scaffolds", Sixth International Symposium on Functional  $\pi$ -Electron Systems, Ithaca, NY (June 2004).

2. Rachel Z. Pytel, **Hyun A Kang**, Patrik A. Anquetil, Timothy M. Swager, Ian W. Hunter, Edwin L. Thomas, "Novel Conducting Block Copolymers for Actuator Applications", SPIE International Symposium on Smart Materials and Structures, San Diego, CA (March 2004).
3. **Hyun A Kang** and Timothy M. Swager, "Nanostructured Actuators: Conducting Polymers Integrated into Polynorbornene-Derived Scaffolds", Materials Research Society 2005 Fall Meeting, Boston, MA (November 2003).
4. **Hyun A Kang** and Timothy M. Swager, "Toward Block Copolymer Actuators: Synthesis and Electrochemical Properties of Conducting Polymers Integrated Into Polynorbornene-derived Scaffolds", American Chemical Society 226th National Meeting, New York, NY (September 2003).
5. Youn Ku Kim, **Hyun A Kang**, Sang Youl Kim, "Polymerization of Acrylamides by Aluminum Alkyls", 2000 Annual Meeting of The Polymer Society of Korea, South Korea (April 2000).
6. **Hyun A Kang**, Sang Youl Kim, "Synthesis and Properties of Linear and Star Poly( $\epsilon$ -caprolactone)", 1999 Annual Meeting of The Polymer Society of Korea, South Korea (October 1999).
7. **Hyun A Kang**, Im Shik Jung, Sang Youl Kim, "Synthesis and Properties of Aromatic Polyimides Containing Cyano Groups", 1998 Annual Meeting of The Polymer Society of Korea, South Korea (October 1998).

## PUBLICATIONS

1. **Hyun A Kang**, Hindy E. Bronstein and Timothy M. Swager, "Conductive Block Copolymers Integrated into Polynorbornene-Derived Scaffolds", *Macromolecules* **2008**, *41*, 5540-5547.
2. **Hyun A Kang**, Im Shik Jung, Masa-aki Kakimoto and Sang Youl Kim, "Synthesis and Characterization of Polyimides from Unsymmetrical Diamine with Cyano Groups", *Polymer Journal* **2001**, *33*, 284-289.

## Acknowledgments

I never expected that my life at MIT was going to be such a long journey when I first came here. Now, I arrived at the finish line after many difficulties and I cannot help being grateful to the many people who helped me to finish my study, since I could not do this without their help.

I can never thank Professor Tim Swager enough. He is an amazing academic advisor with an extraordinary sense of humanity. He guided my research with his creative ideas whenever I could not find solutions. He is also supportive, patient and takes good care of his group members. I also would like to thank Professor Greg Fu and Ned Thomas for their valuable advice, suggestions on my research and comments on my thesis. I also need to thank my former advisor Professor Sang Youl Kim at KAIST. He advised me during my first research experience in polymer chemistry and convinced me to pursue a full Ph.D.

I was blessed to be a Swager group member. Every group member I have met has been willing to help with research projects and never refused or ignored me when I had questions. Since I have had the pleasure of working with wonderful colleagues, I want to thank all the people I interacted with during my time at MIT. Hindy Bronstein initiated my first research project, so I could follow up on her work when I started working in the Swager lab. The great results that Akihiro Ohira, Takeshi Igarashi and Johan Hoogboom had demonstrated were also good references for my research projects.

I want to express my gratitude to the so-called Korean Gang in the Swager group: Youngmi Kim, Dongwhan Lee, Taehyun Kim, Jihho Oh, Inja Song, Changsik Song and Jeewoo Lim. I especially want to thank Dongwhan, my first bench mate. He taught me many important lab techniques, kindly advised me on every question I had.

Bruce Yu and Phoebe Kwan helped me a lot to learn electrochemistry. Alex Paraskos, Karen Martin, Craig Breen, Zhihua Chen, Koushik Venkatesan and Julian Chan were members of my subgroup and gave me numerous advices on my chemistry. Jean Bouffard was a good bench mate especially during late night in lab. ISN members, Paul Byrne, Brad Holiday, Michael Büchel, Jocelyn Nadeau, Yong Yang, Lokman Torun and Ivory Hills were also fun people to discuss chemistry and hang out with. I also had great classmates, Gigi Bailey, John Amara, Sam Thomas, Nate Vandesteeg, and Rob Eaton in the Swager group.

I always enjoyed the company of the Japanese members of our lab such as Kenichi Kuroda, Koji Arimitsu, Masashi Hasegawa, Koji Miki, Ryo Takita and Kazunori Sugiyasu because they reminded me of my childhood in Japan and fed my interest in Japanese culture.

I have to give special thanks to Trisha Andrew. She is the most enthusiastic person I ever met, and she became my best friend ever since we shared the “night shift” together in lab. We entertained each other whenever one of us needed it and she willingly proof-read any document I gave her. She also provided motivation when I most needed it.

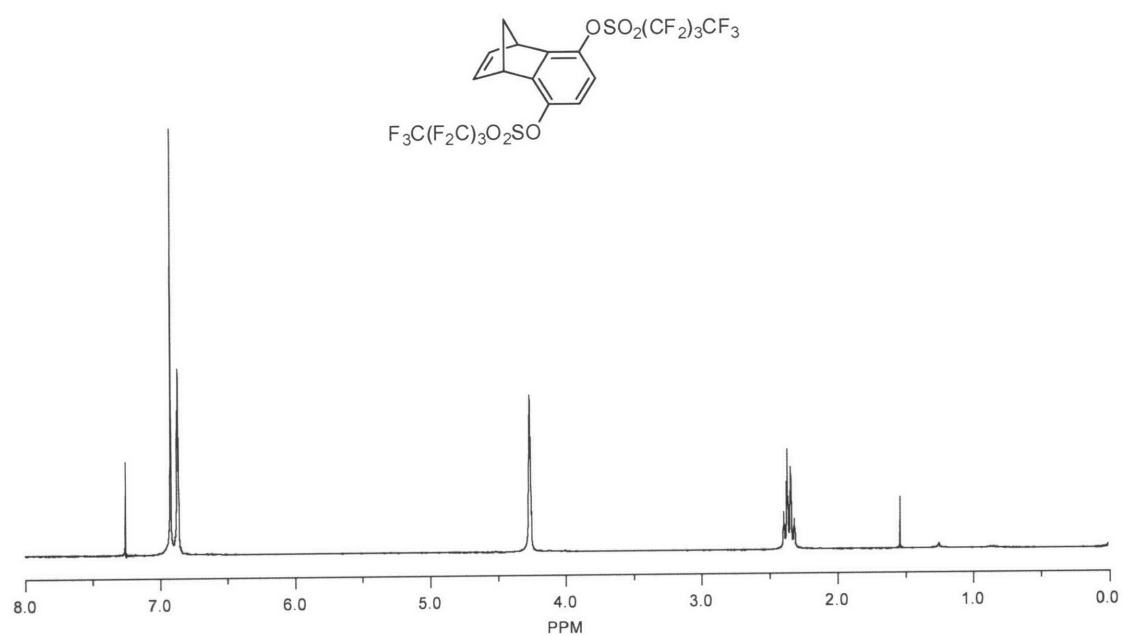
I want to thank the rest of group members, Aimee Rose, JD Tovar, Jordan Wosnick, Juan Zheng, Andrew Satrijo, Jessica Liao, Scott Meek, Eric Dane, Fei Wang, Brett VanVeller, Jose Lobez, Shuang Liu, Evgueni Nesterov, Paul Kouwer, Guy Joly, Anne McNeil, Mark Taylor, Dahui Zhao, Wei Zhang and Becky Bjork for fruitful discussions.

I had two Korean classmates, Soonsil Hyun and Hoisung Chung. I could start school more easily with them. I spent most of my first semester with Soonsil by taking classes and vacations together. She helped, encouraged and comforted me especially when I was down. I also want to thank my fellow alumni, Jaehyuk Choi, Yongwon Jung and Yoon-aa Choi for being good friends.

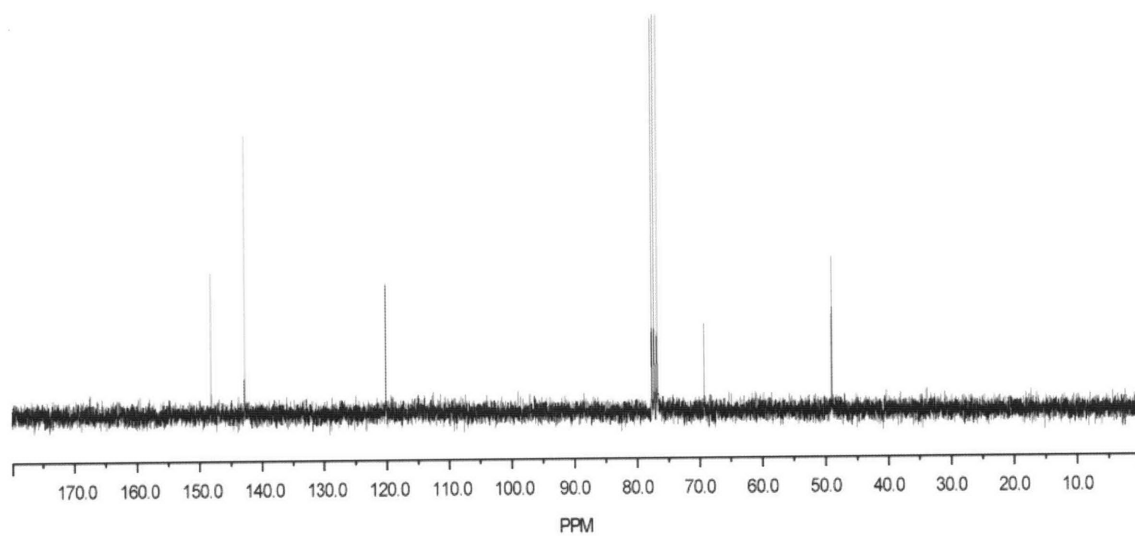
I am mostly thankful to my family. My parents taught me to live honestly and warmly, and they pray for me everyday. They encouraged me to continue my study when I was disappointed and never gave up their faith in me. I cannot pay back their love enough. My brother and my sister are also supportive for my decision and helped me to do my work.

I still remember my prayer before I applied for the science high school, which was my first step to become a scientist. I can live only with God's blessing and I believe that God always prepares my way.

**Appendix 1**  
**NMR Spectra for Chapter 1**

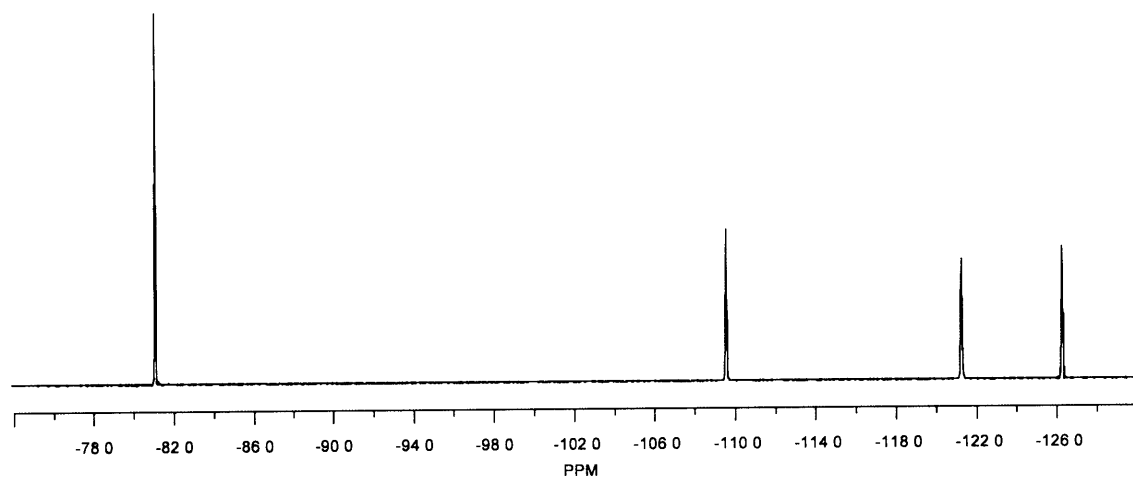


<sup>1</sup>H NMR spectrum of **3** (300 MHz,  $\text{CDCl}_3$ )

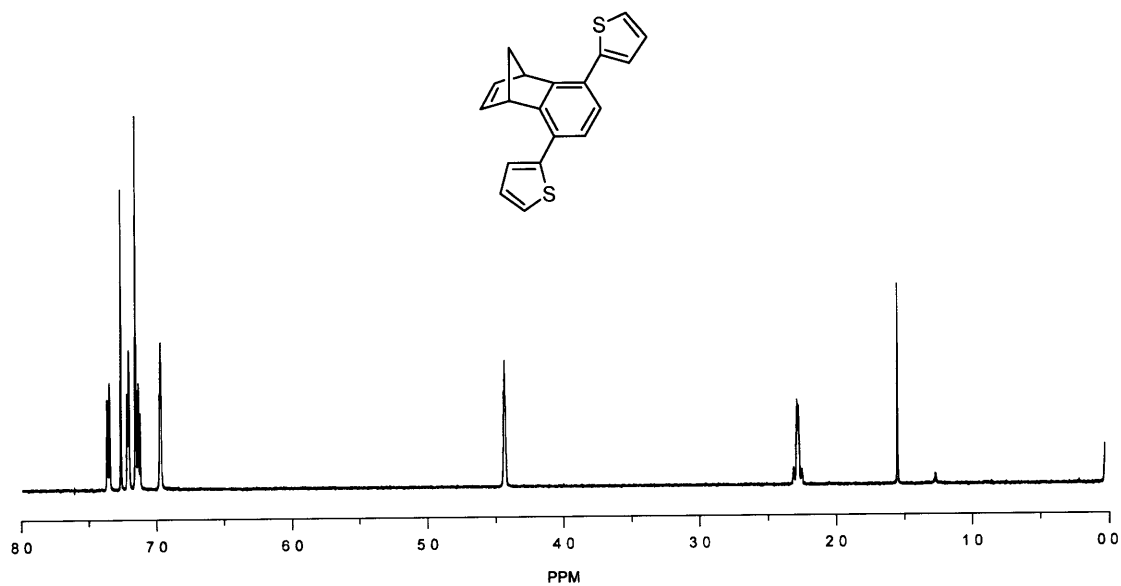


<sup>13</sup>C NMR spectrum of **3** (75 MHz,  $\text{CDCl}_3$ )

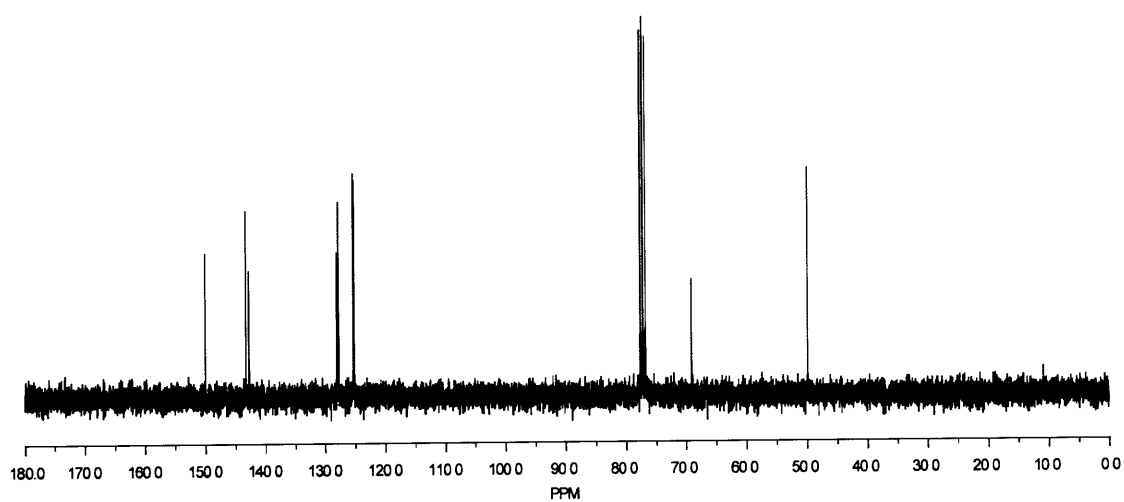




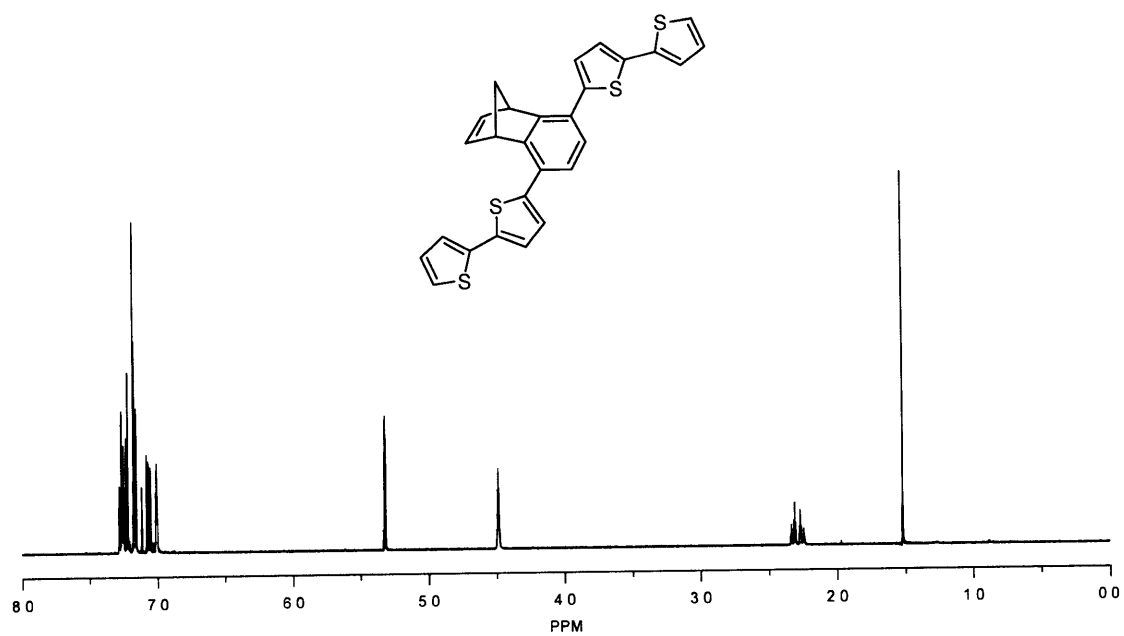
$^{19}\text{F}$  NMR spectrum of **3** (188 MHz,  $\text{CDCl}_3$ )



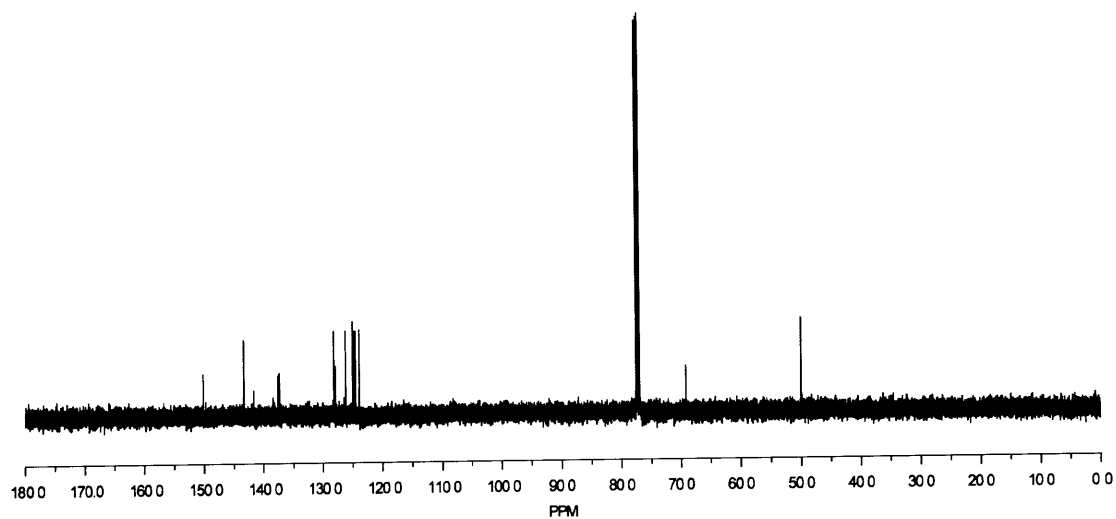
<sup>1</sup>H NMR spectrum of 4 (300 MHz, CDCl<sub>3</sub>)



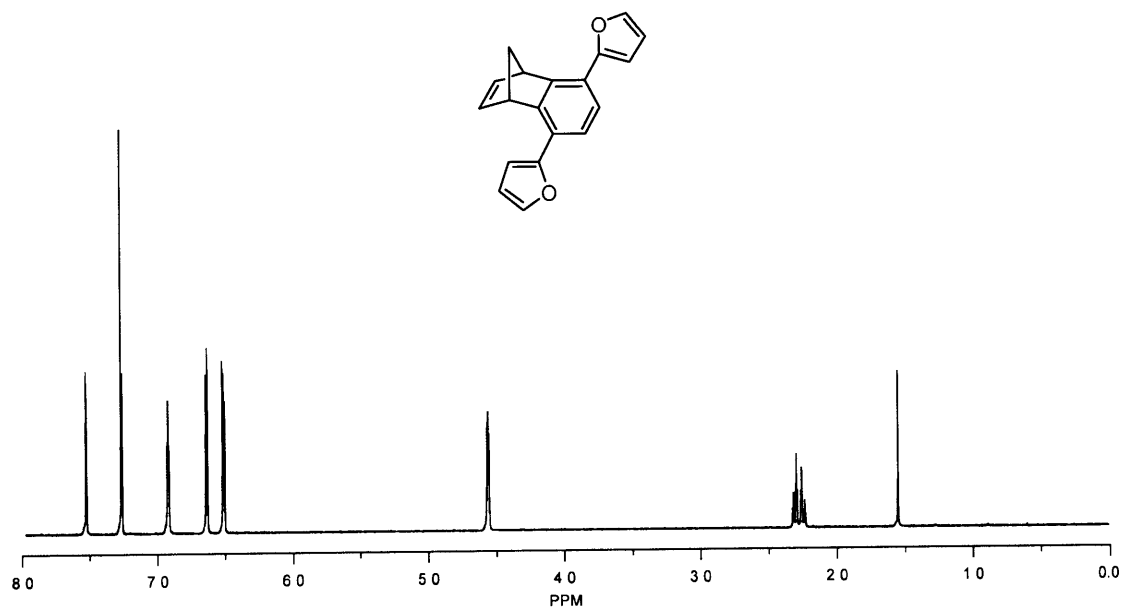
<sup>13</sup>C NMR spectrum of 4 (75 MHz, CDCl<sub>3</sub>)



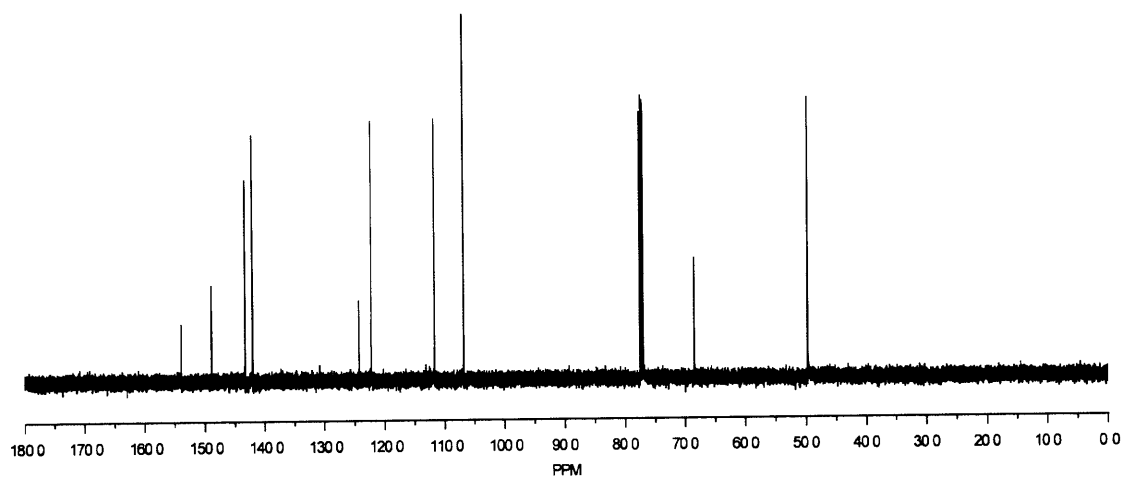
$^1\text{H}$  NMR spectrum of **5** (300 MHz,  $\text{CDCl}_3$ )



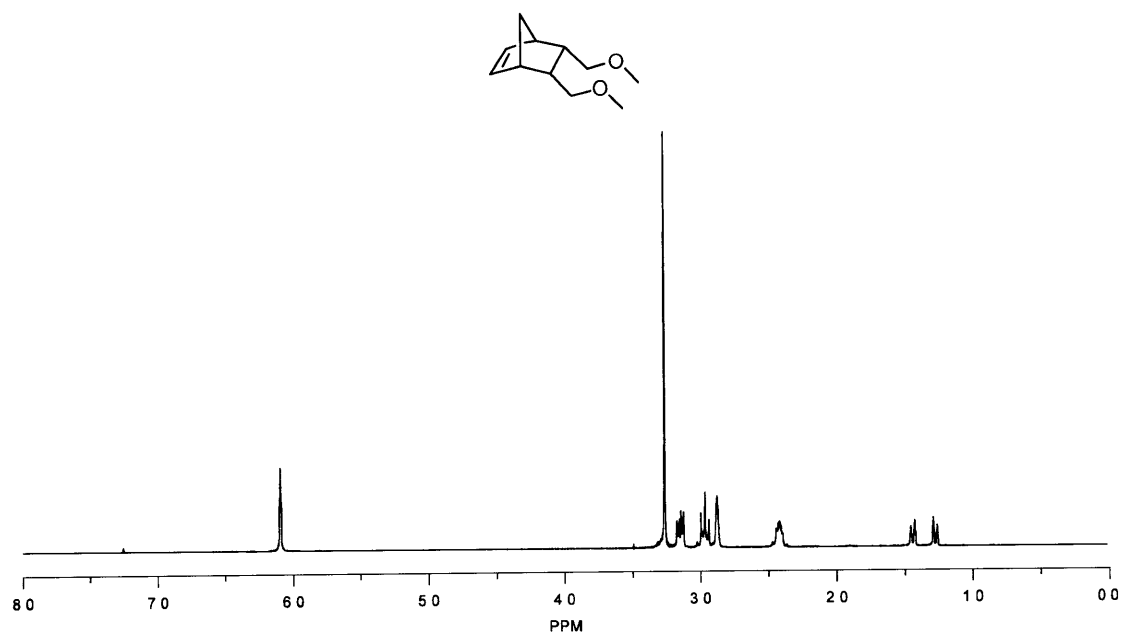
$^{13}\text{C}$  NMR spectrum of **5** (75 MHz,  $\text{CDCl}_3$ )



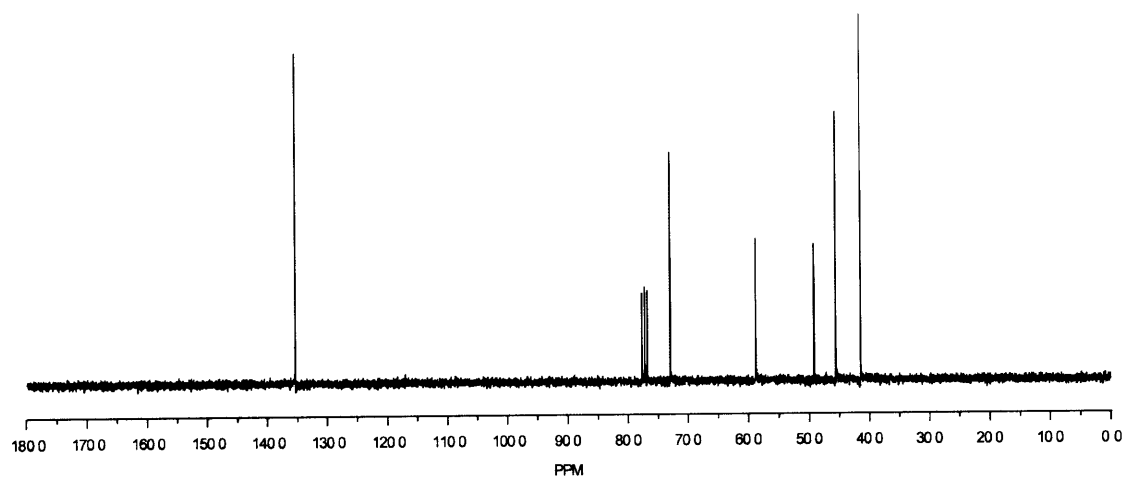
<sup>1</sup>H NMR spectrum of **6** (300 MHz, CDCl<sub>3</sub>)



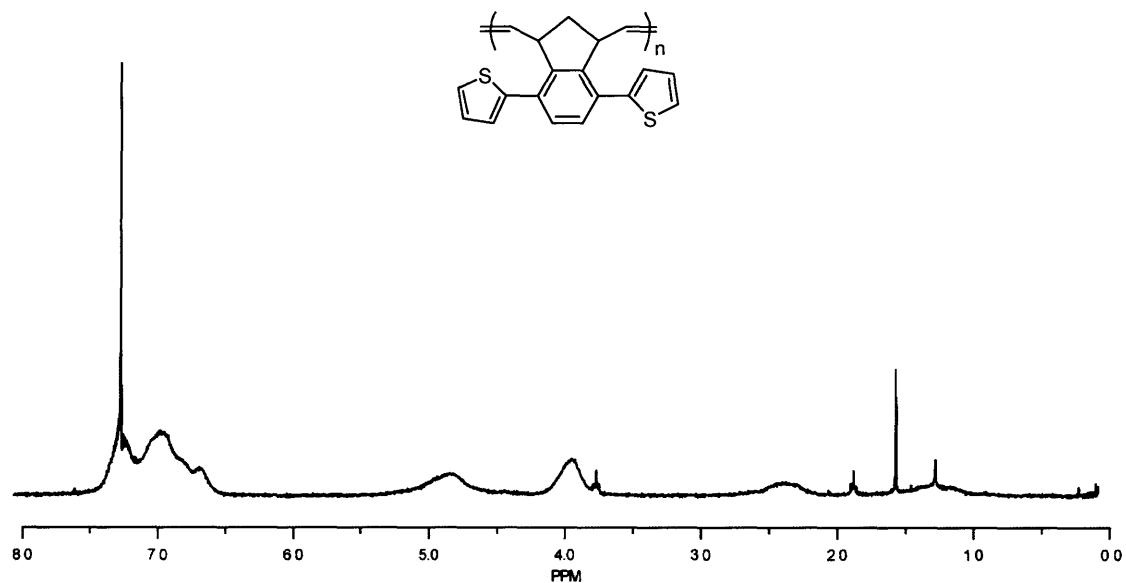
<sup>13</sup>C NMR spectrum of **6** (75 MHz, CDCl<sub>3</sub>)



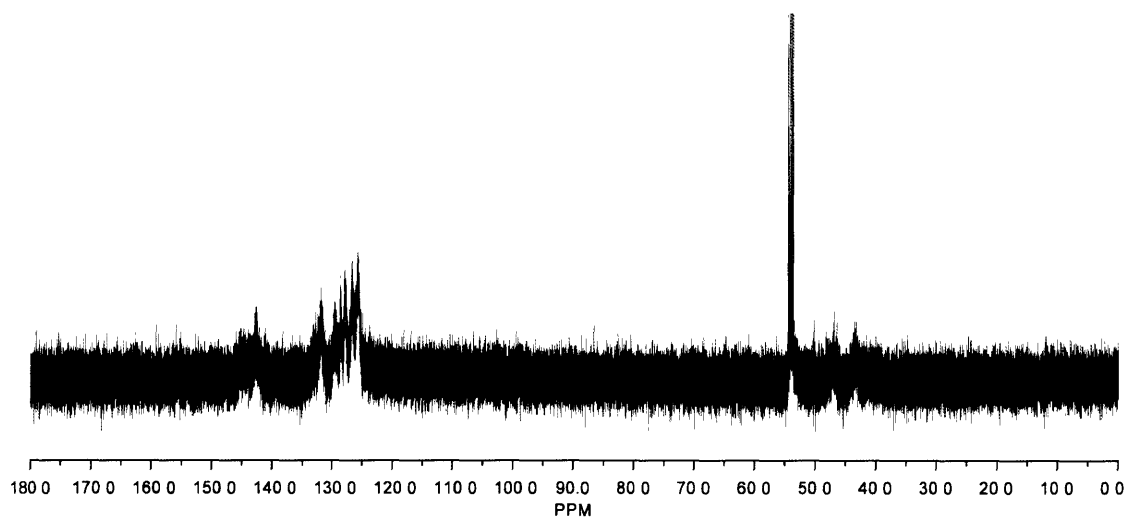
<sup>1</sup>H NMR spectrum of 12 (300 MHz, CDCl<sub>3</sub>)



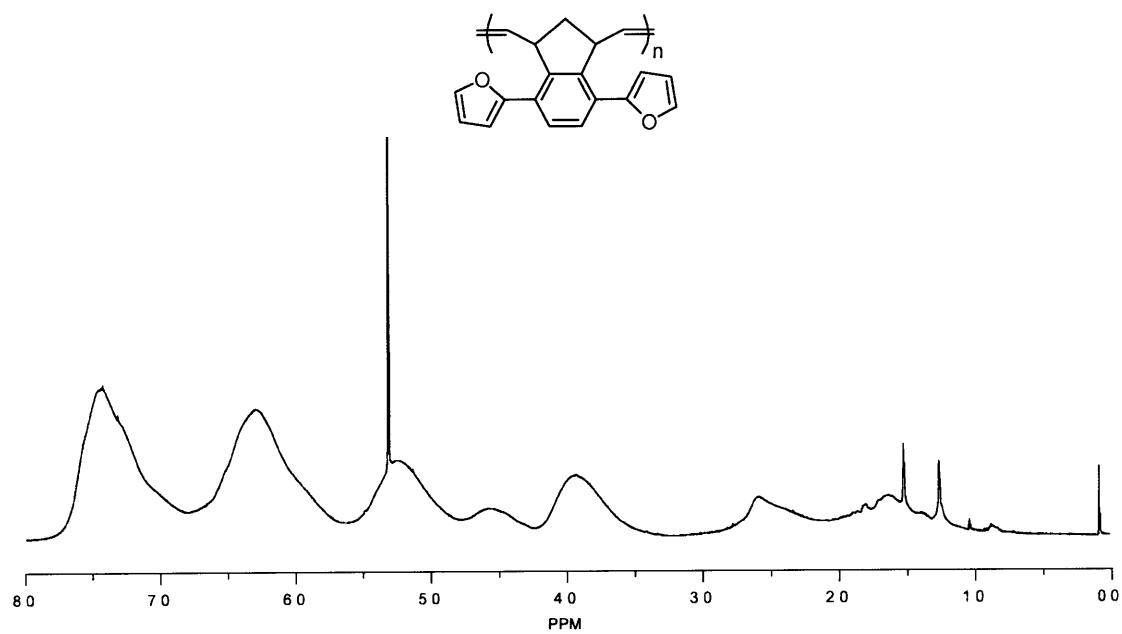
<sup>13</sup>C NMR spectrum of 12 (75 MHz, CDCl<sub>3</sub>)



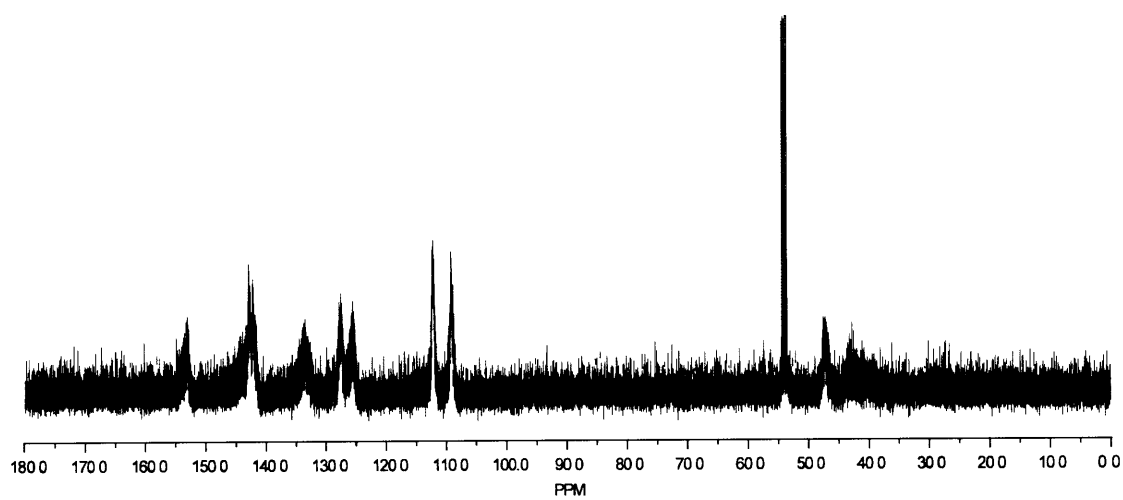
$^1\text{H}$  NMR spectrum of poly(4) (300 MHz,  $\text{CDCl}_3$ )



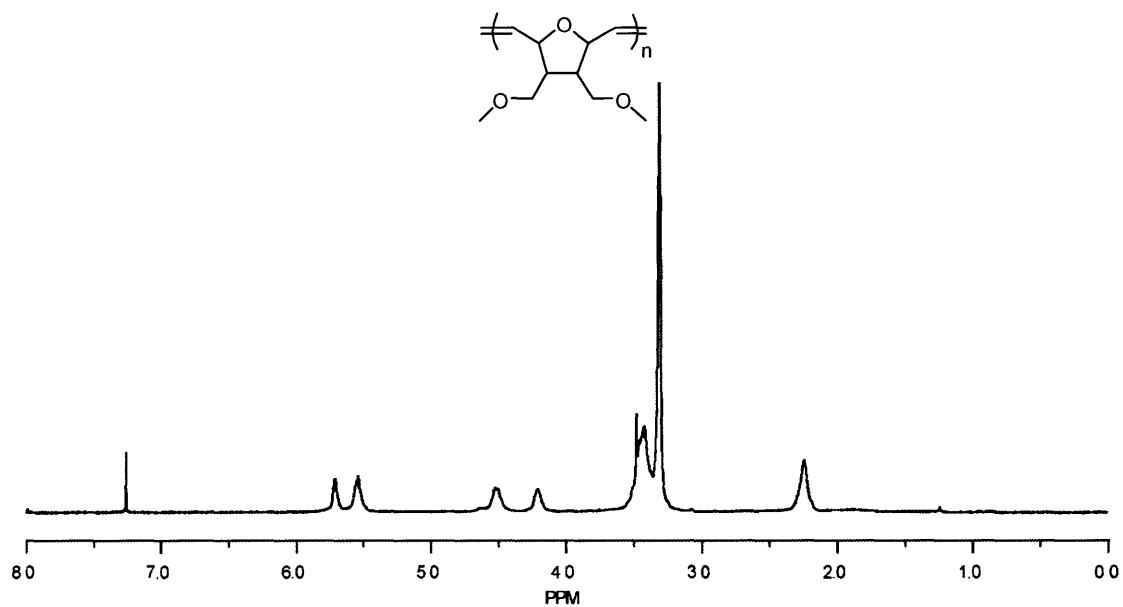
$^{13}\text{C}$  NMR spectrum of poly(4) (125 MHz,  $\text{CD}_2\text{Cl}_2$ )



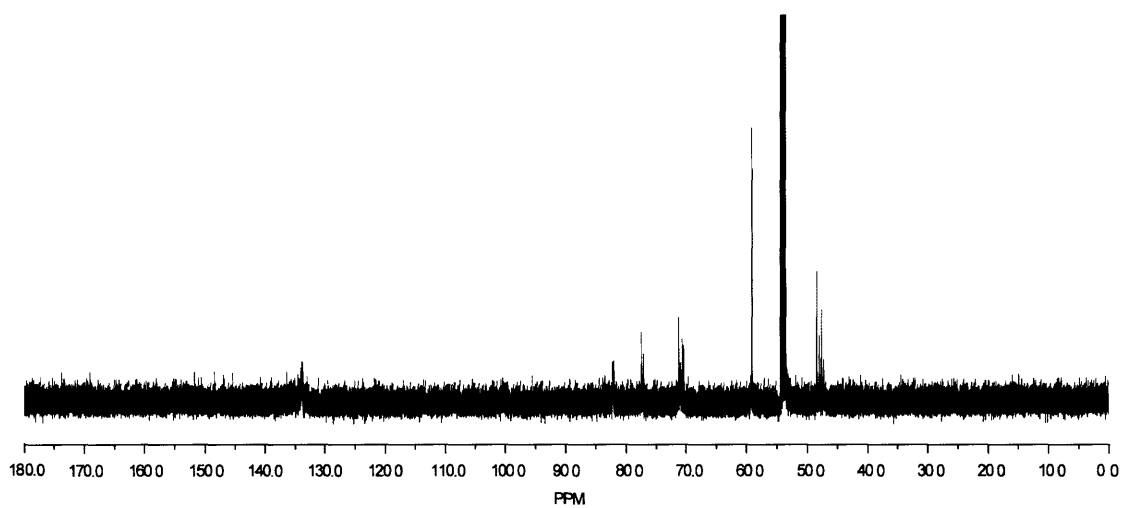
$^1\text{H}$  NMR spectrum of poly(6) (300 MHz,  $\text{CD}_2\text{Cl}_2$ )



$^{13}\text{C}$  NMR spectrum of poly(6) (125 MHz,  $\text{CD}_2\text{Cl}_2$ )

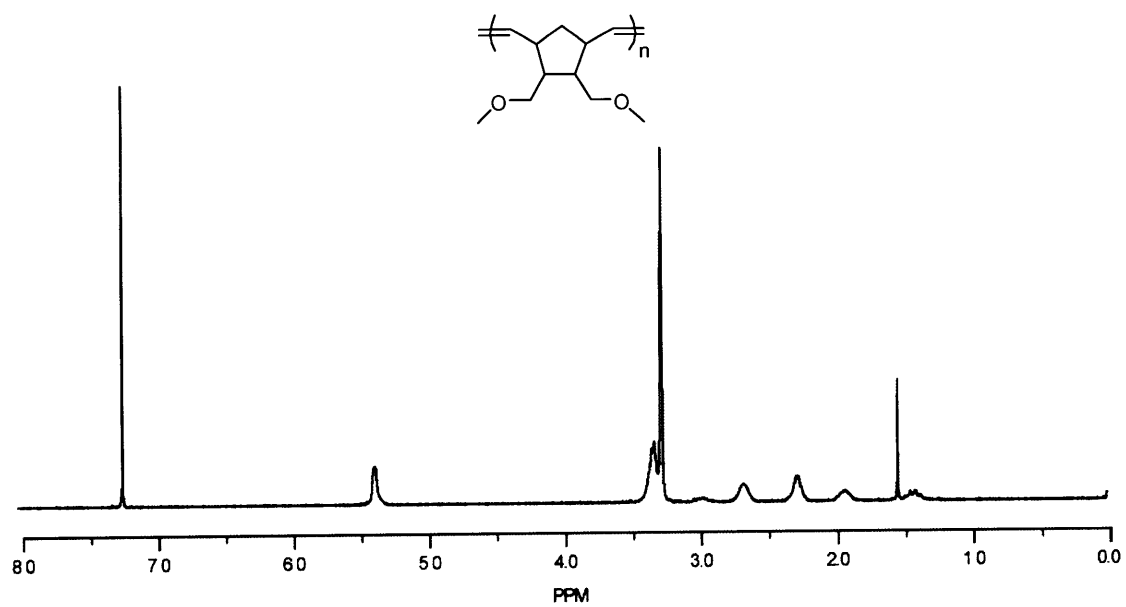


$^1\text{H}$  NMR spectrum of poly(9) (500 MHz,  $\text{CDCl}_3$ )

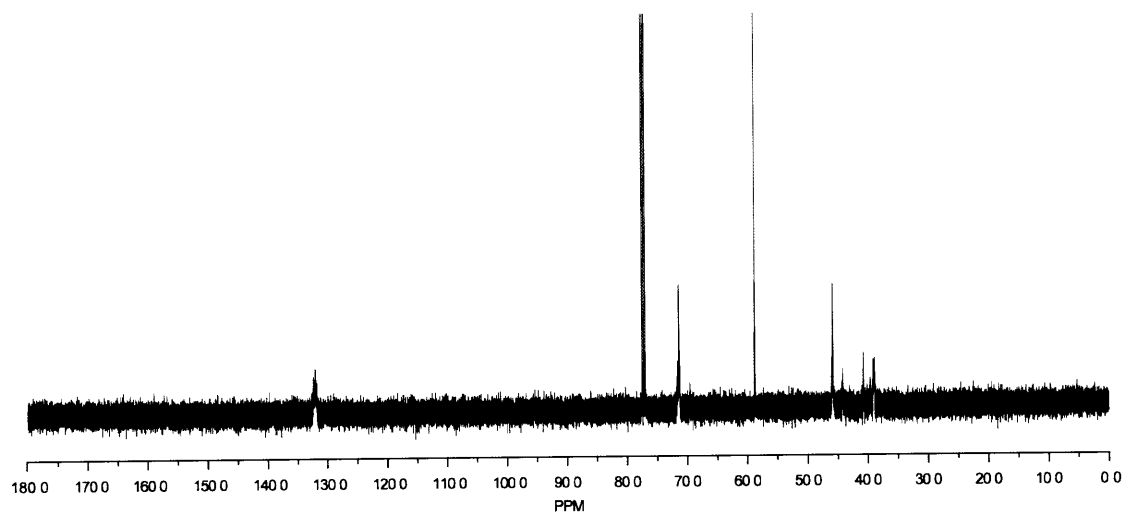


$^{13}\text{C}$  NMR spectrum of poly(9) (125 MHz,  $\text{CD}_2\text{Cl}_2$ )

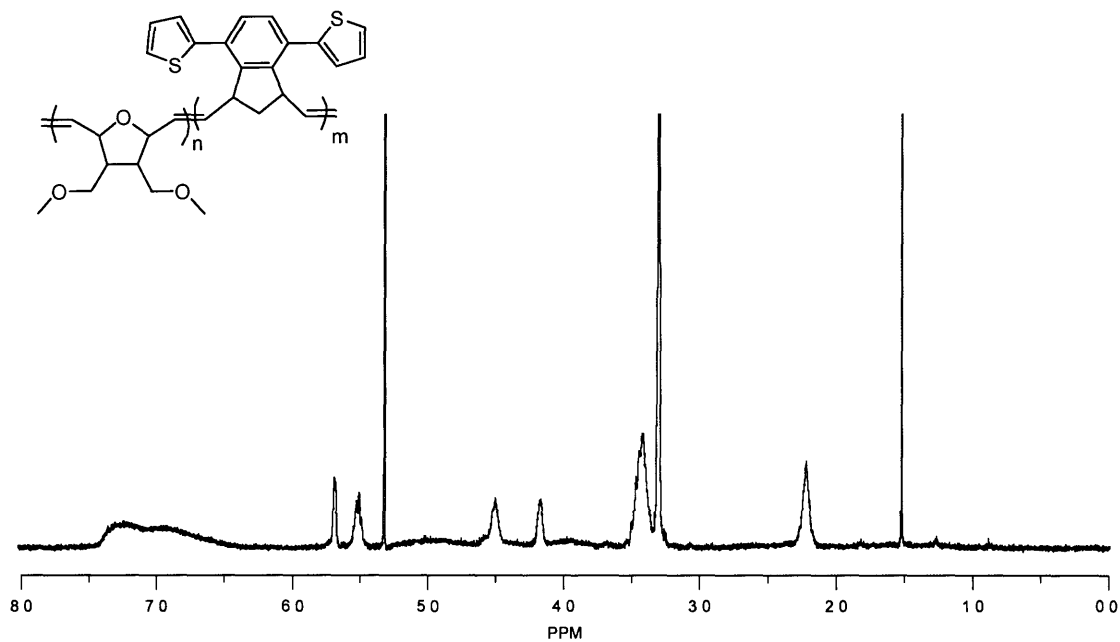




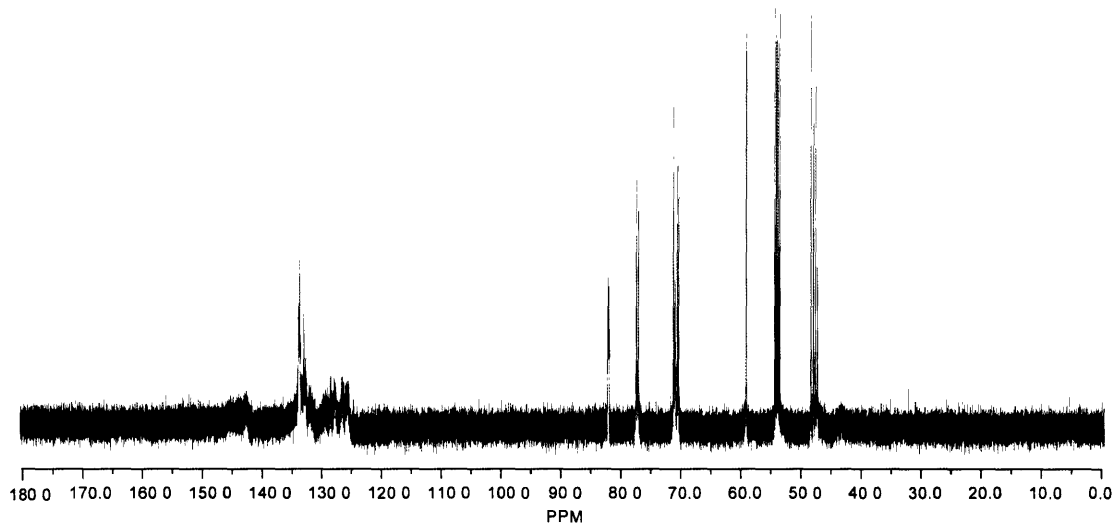
$^1\text{H}$  NMR spectrum of poly(12) (500 MHz,  $\text{CDCl}_3$ )



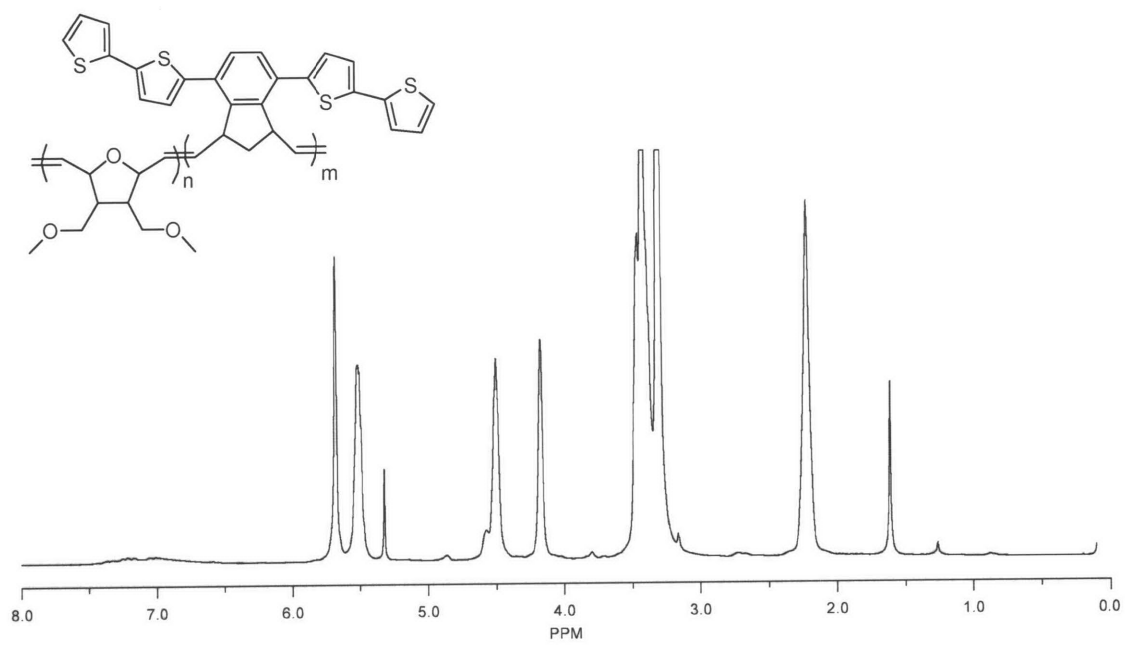
$^{13}\text{C}$  NMR spectrum of poly(12) (125 MHz,  $\text{CDCl}_3$ )



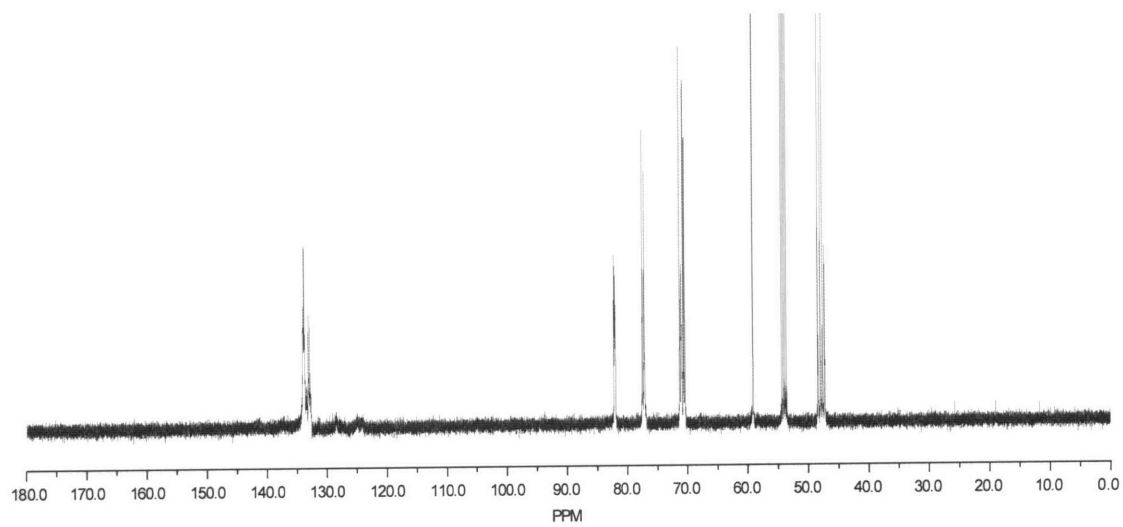
<sup>1</sup>H NMR spectrum of **BCP1** (300 MHz, CD<sub>2</sub>Cl<sub>2</sub>)



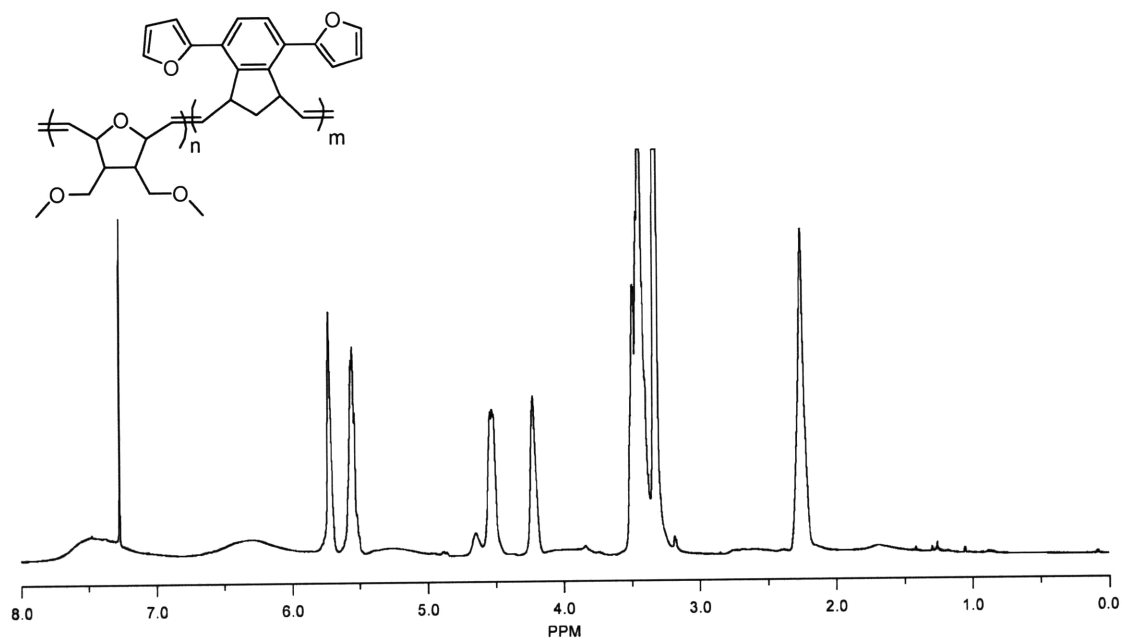
<sup>13</sup>C NMR spectrum of **BCP1** (125 MHz, CD<sub>2</sub>Cl<sub>2</sub>)



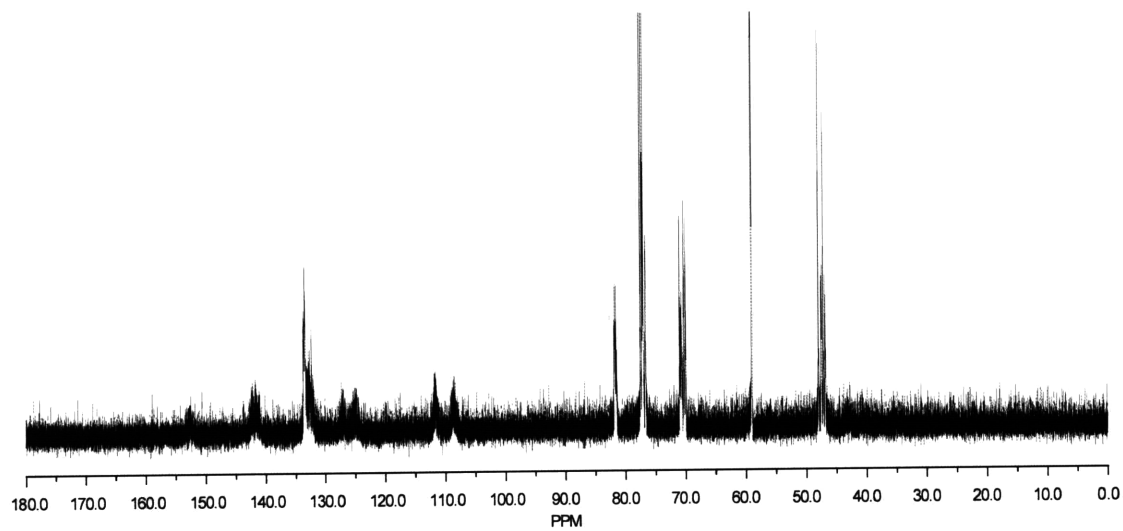
<sup>1</sup>H NMR spectrum of **BCP2** (300 MHz, CD<sub>2</sub>Cl<sub>2</sub>)



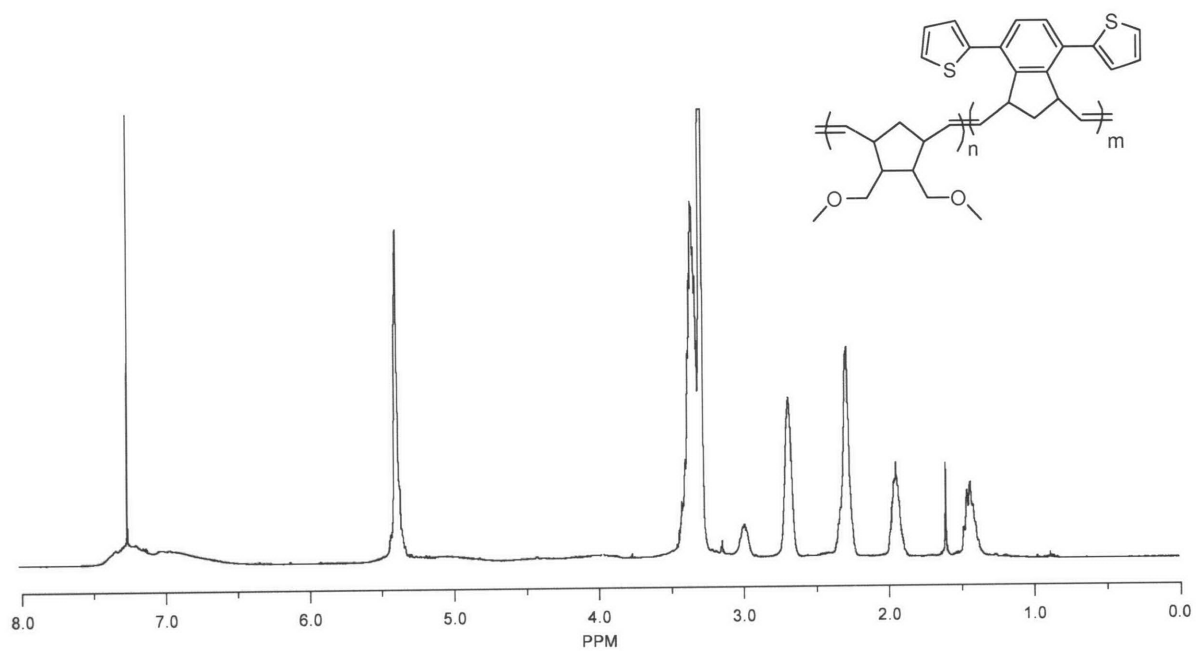
<sup>13</sup>C NMR spectrum of **BCP2** (125 MHz, CD<sub>2</sub>Cl<sub>2</sub>)



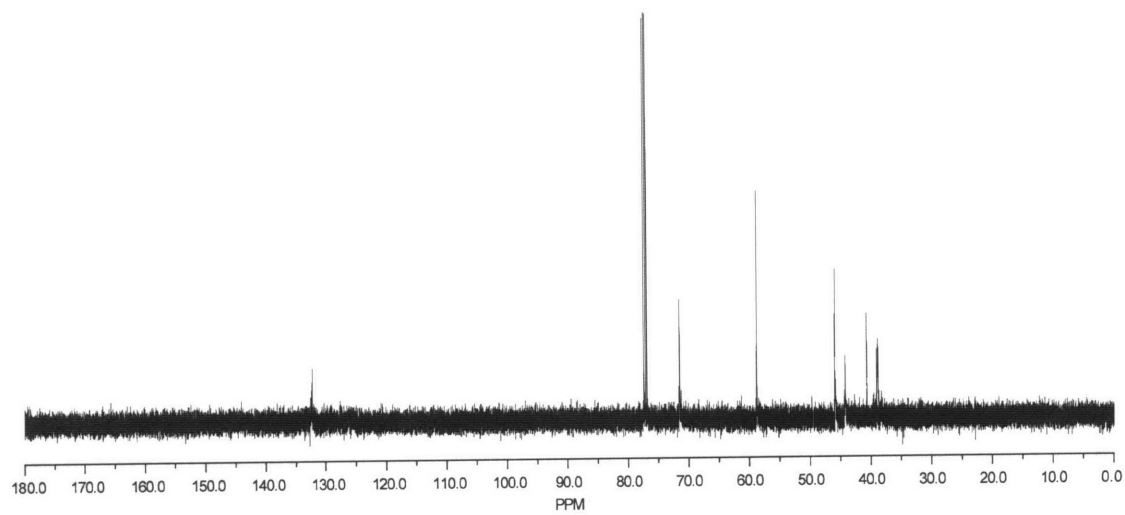
<sup>1</sup>H NMR spectrum of **BCP3** (300 MHz, CDCl<sub>3</sub>)



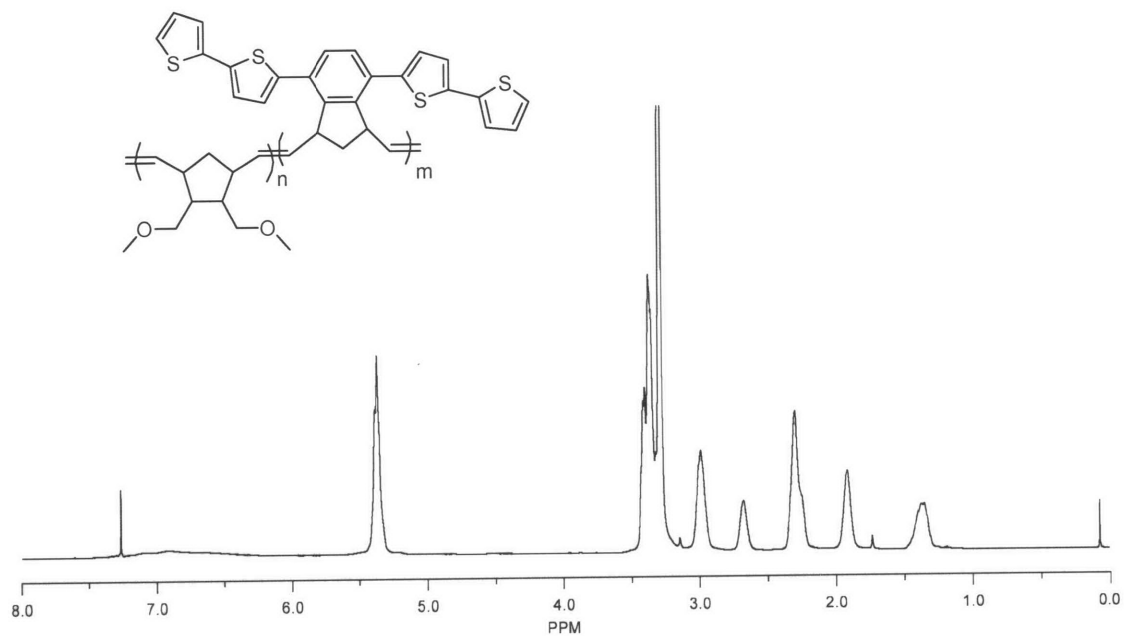
<sup>13</sup>C NMR spectrum of **BCP3** (125 MHz, CDCl<sub>3</sub>)



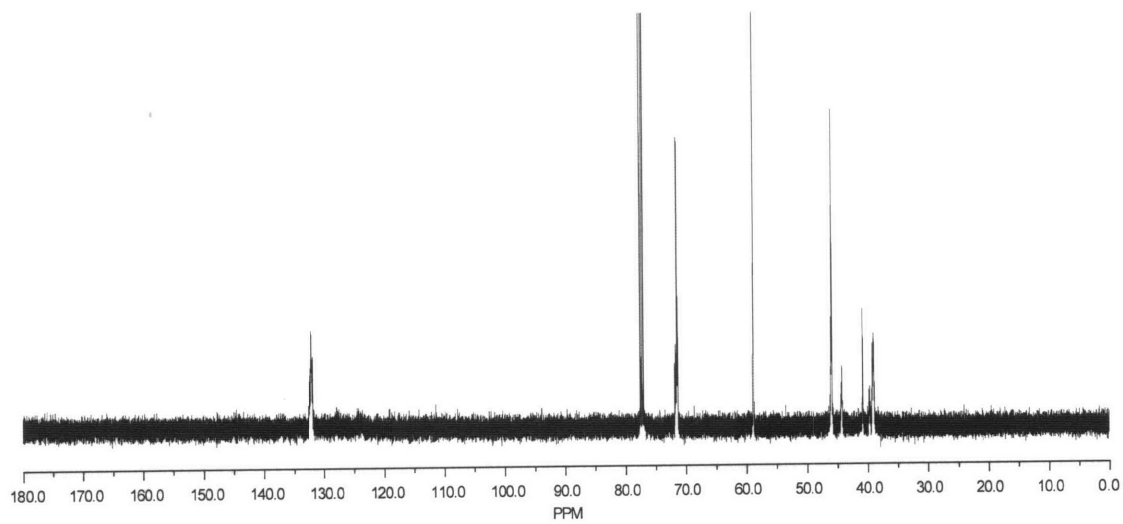
$^1\text{H}$  NMR spectrum of **BCP4** (500 MHz,  $\text{CDCl}_3$ )



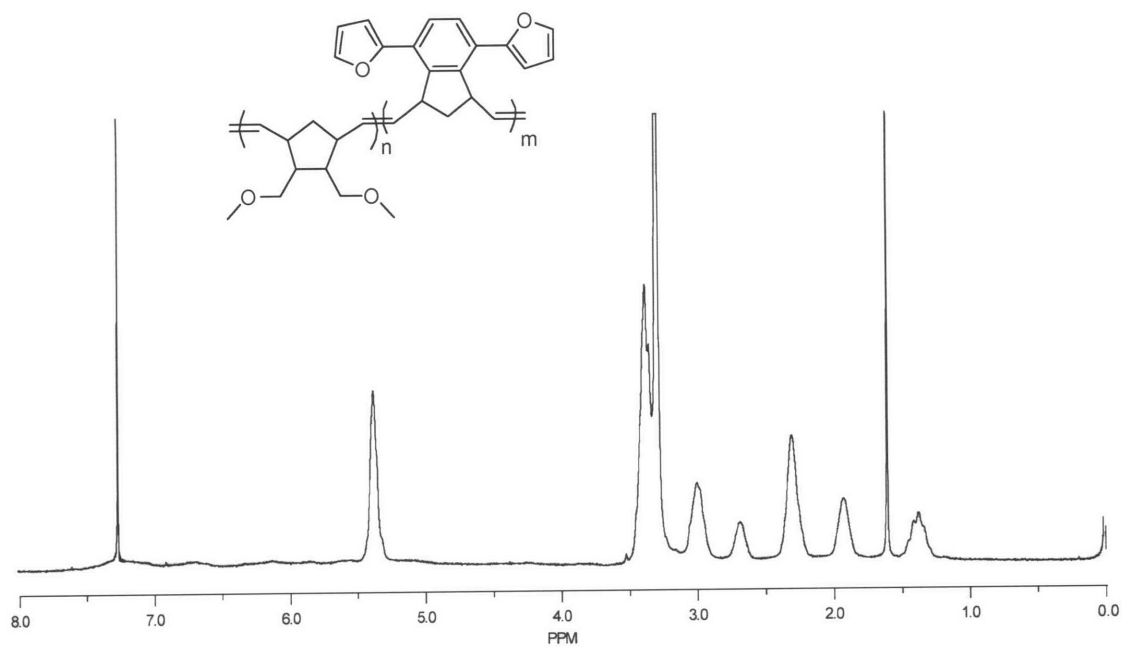
$^{13}\text{C}$  NMR spectrum of **BCP4** (125 MHz,  $\text{CDCl}_3$ )



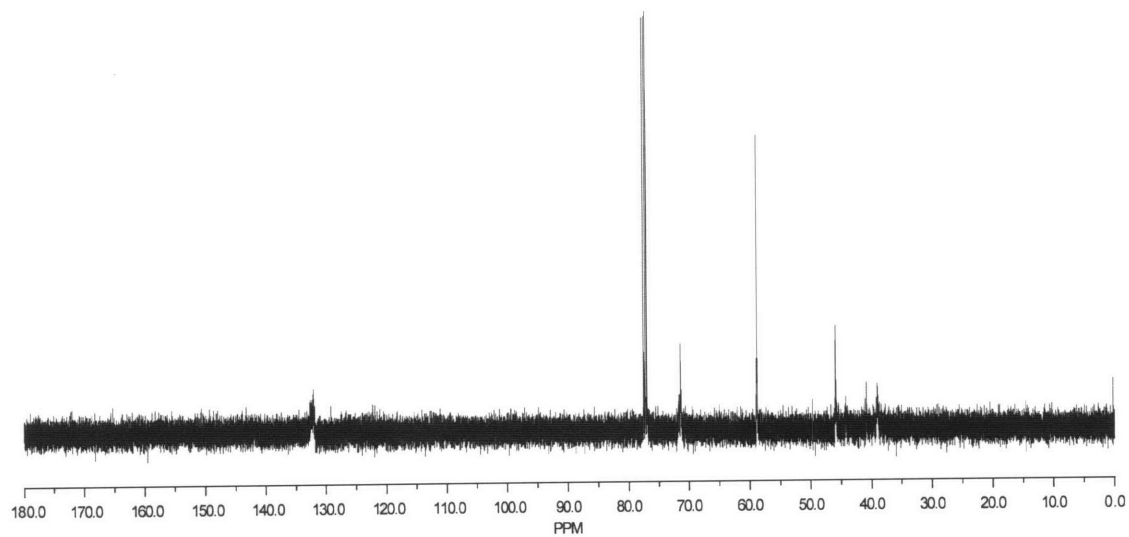
<sup>1</sup>H NMR spectrum of **BCP5** (300 MHz, CDCl<sub>3</sub>)



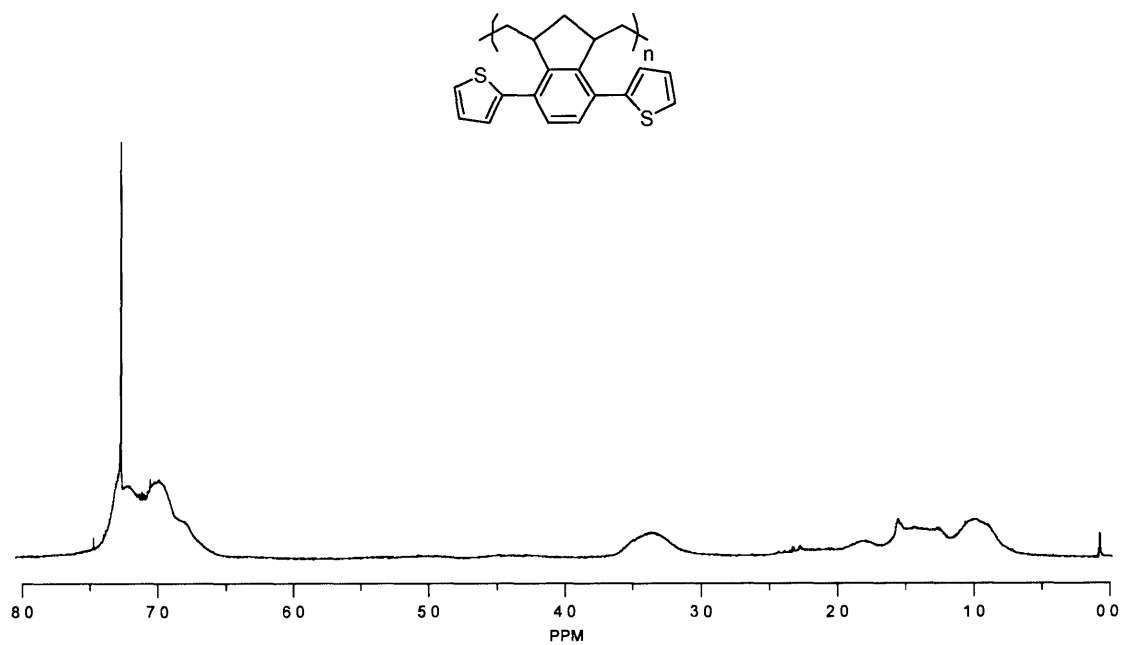
<sup>13</sup>C NMR spectrum of **BCP5** (125 MHz, CDCl<sub>3</sub>)



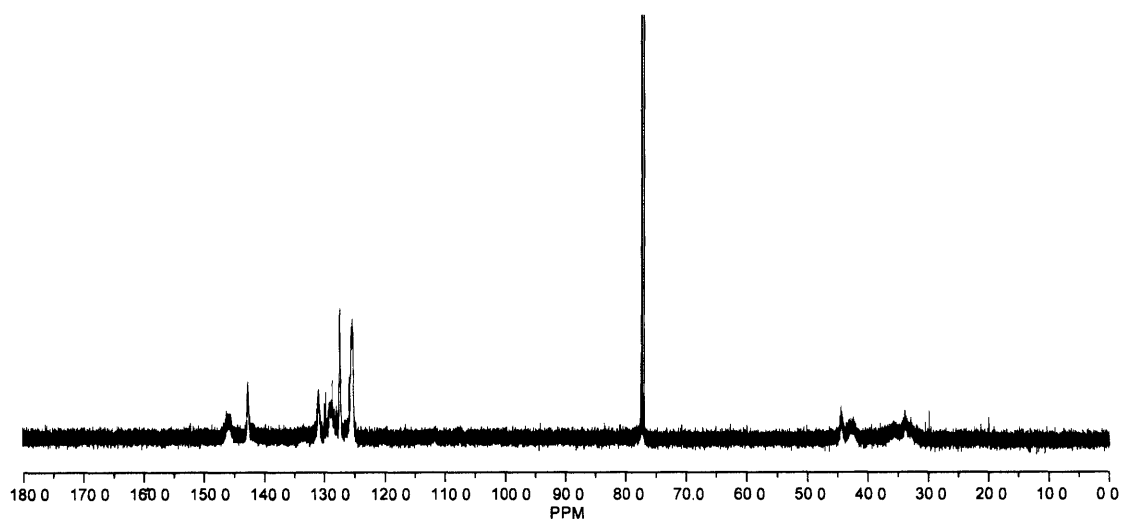
<sup>1</sup>H NMR spectrum of **BCP6** (300 MHz, CDCl<sub>3</sub>)



<sup>13</sup>C NMR spectrum of **BCP6** (125 MHz, CDCl<sub>3</sub>)

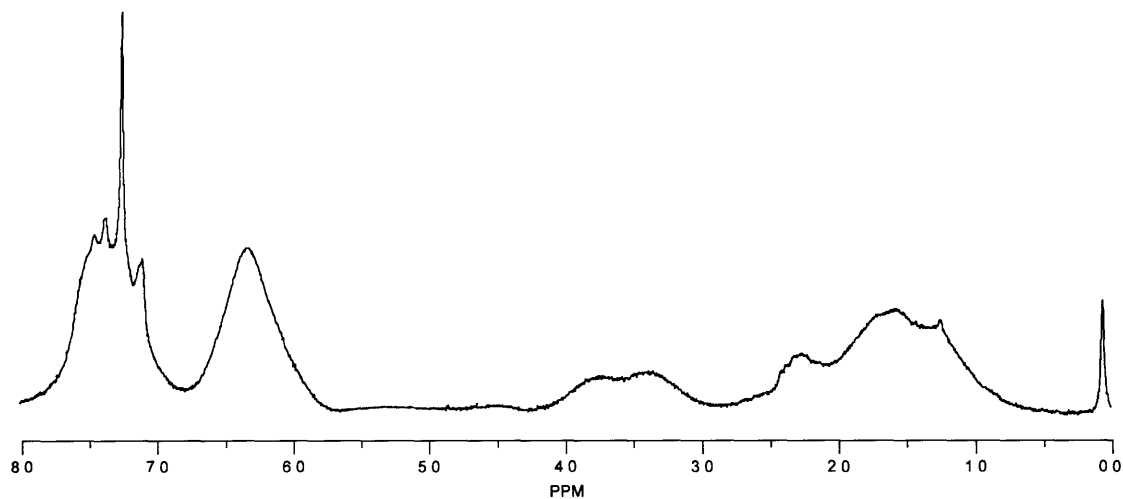
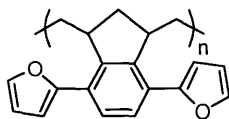


<sup>1</sup>H NMR spectrum of hydrogenated poly(4) (500 MHz, CDCl<sub>3</sub>)

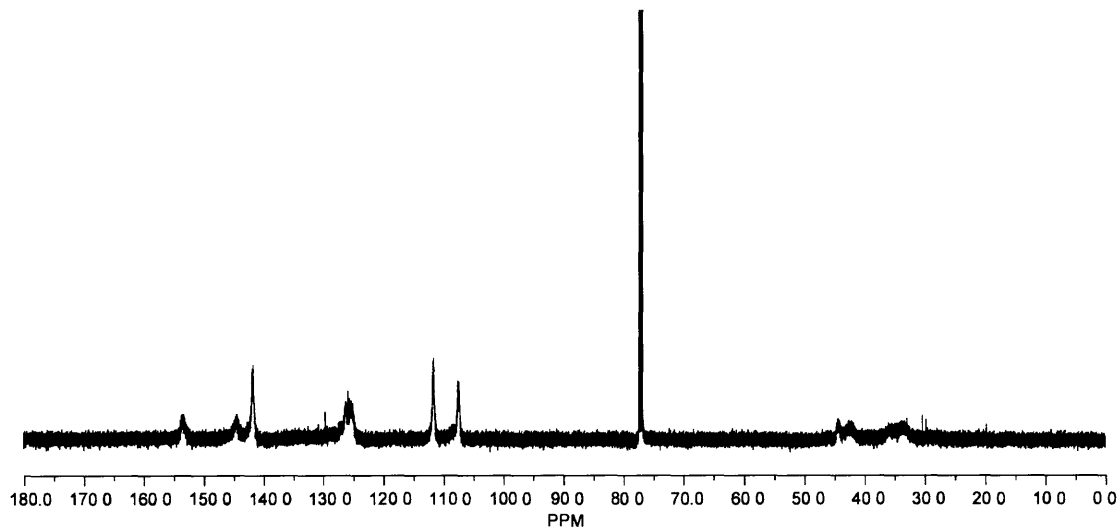


<sup>13</sup>C NMR spectrum of hydrogenated poly(4) (125 MHz, CDCl<sub>3</sub>)

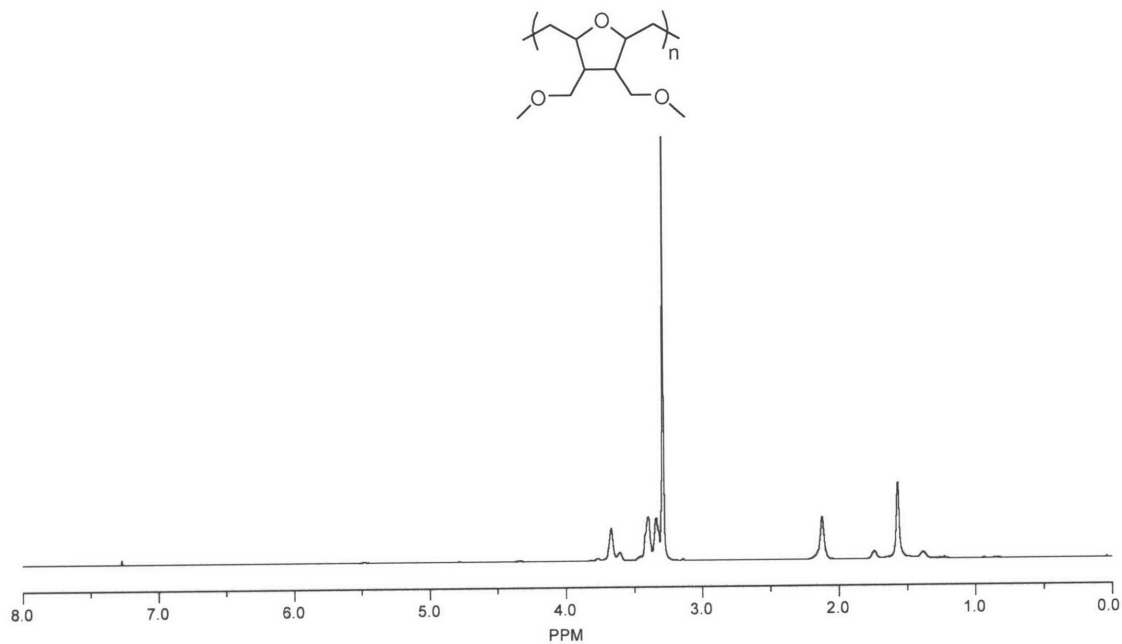




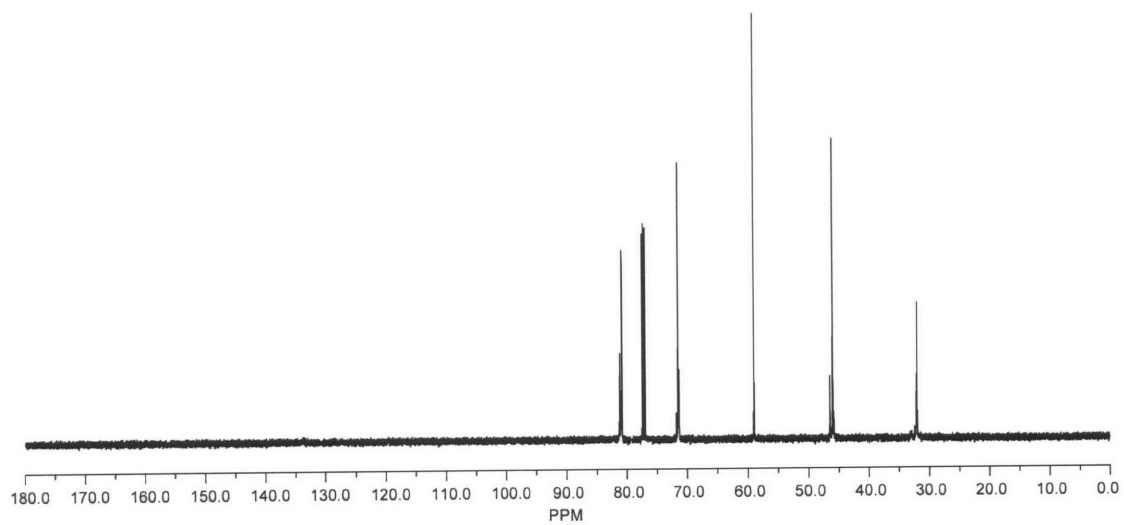
$^1\text{H}$  NMR spectrum of hydrogenated poly(6) (500 MHz,  $\text{CDCl}_3$ )



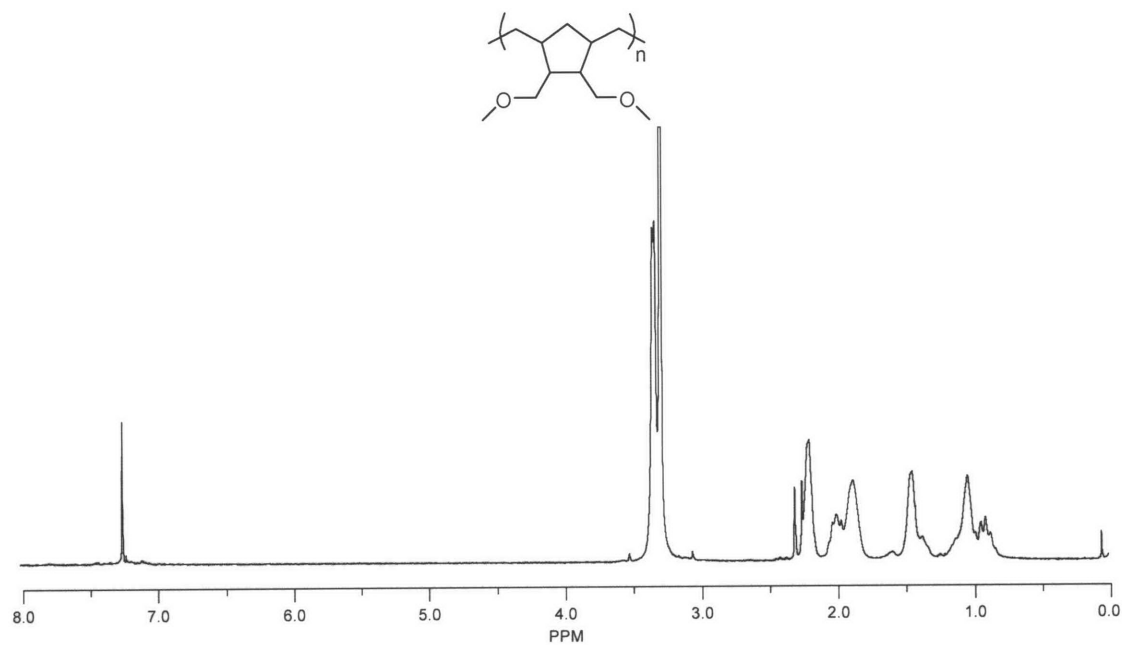
$^{13}\text{C}$  NMR spectrum of hydrogenated poly(6) (125 MHz,  $\text{CDCl}_3$ )



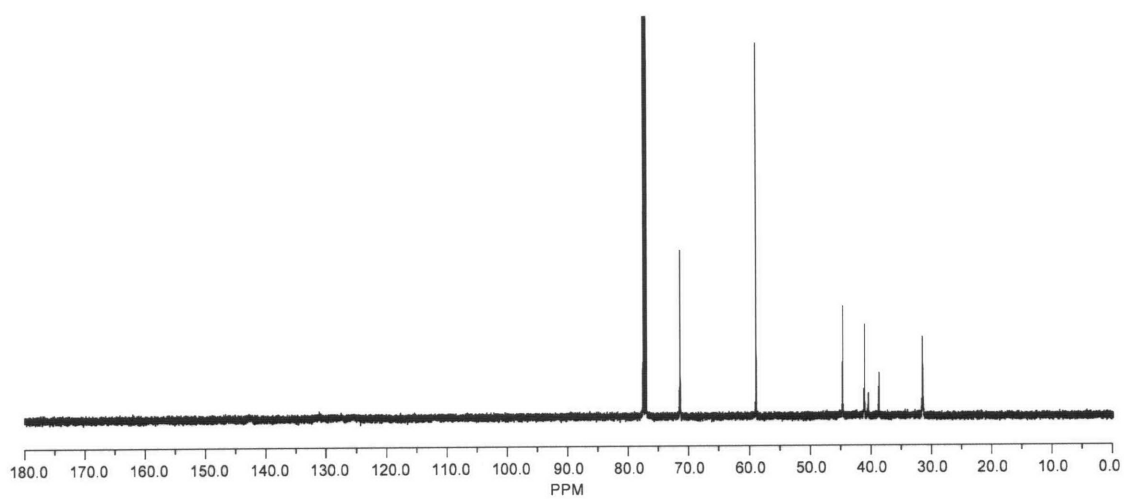
<sup>1</sup>H NMR spectrum of hydrogenated poly(9) (500 MHz, CDCl<sub>3</sub>)



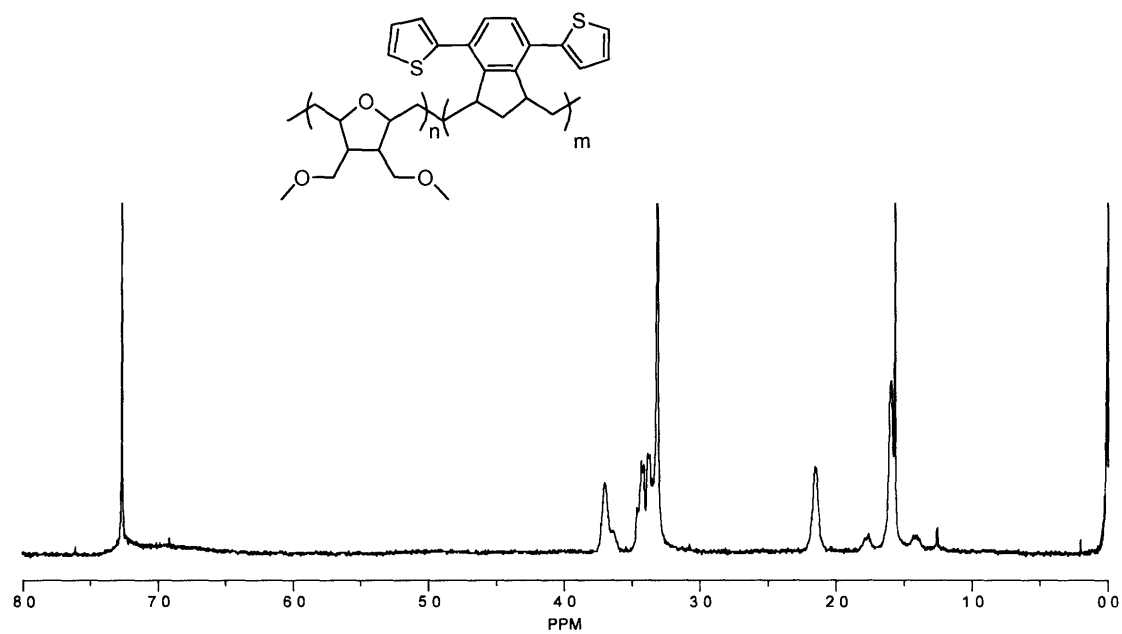
<sup>13</sup>C NMR spectrum of hydrogenated poly(9) (125 MHz, CDCl<sub>3</sub>)



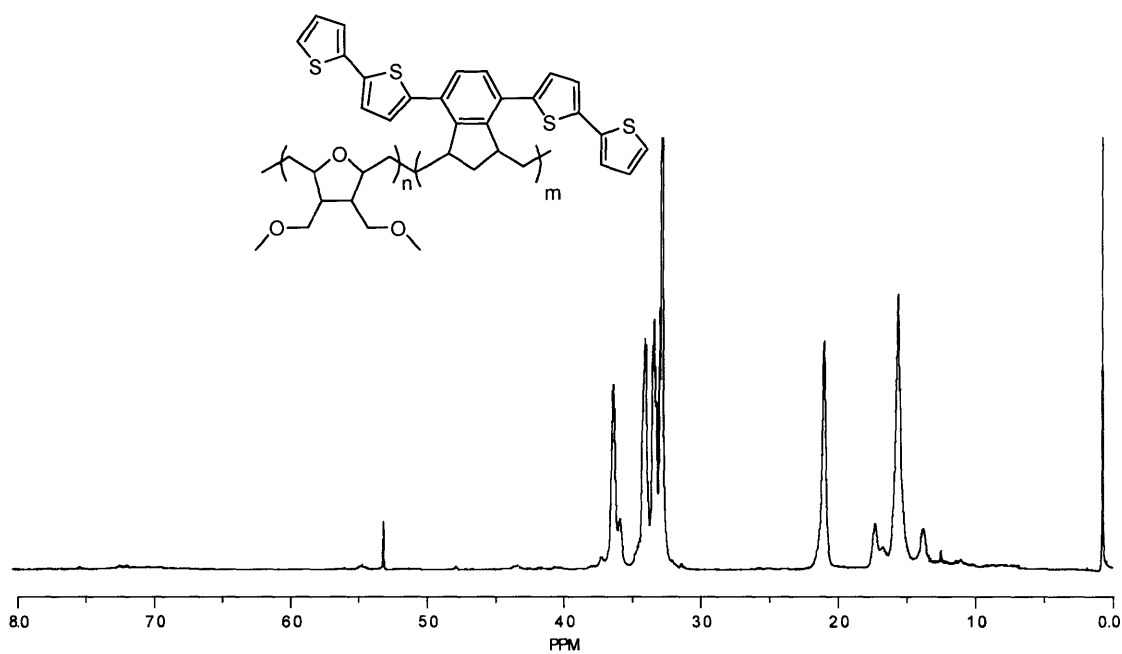
$^1\text{H}$  NMR spectrum of hydrogenated poly(**12**) (500 MHz,  $\text{CDCl}_3$ )



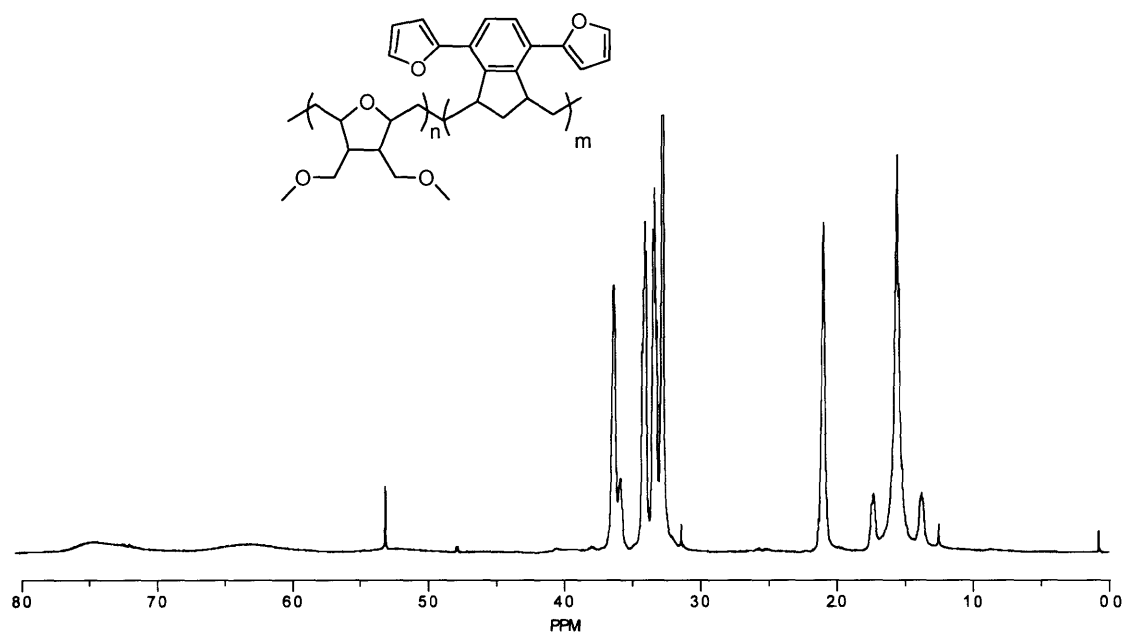
$^{13}\text{C}$  NMR spectrum of hydrogenated poly(**12**) (125 MHz,  $\text{CDCl}_3$ )



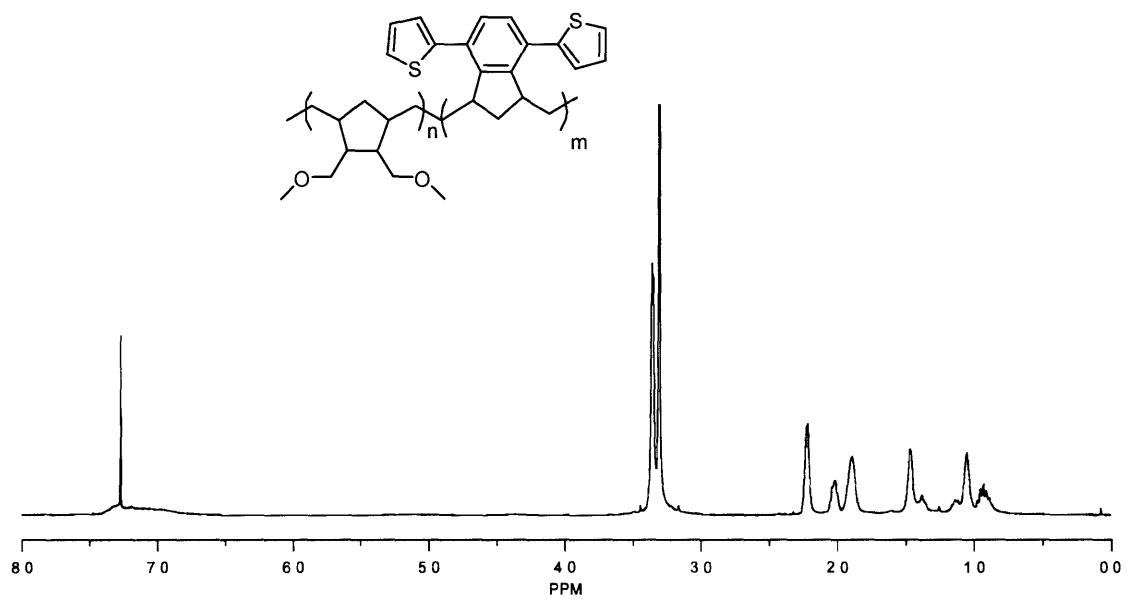
<sup>1</sup>H NMR spectrum of hydrogenated **BCP1** (300 MHz, CDCl<sub>3</sub>)



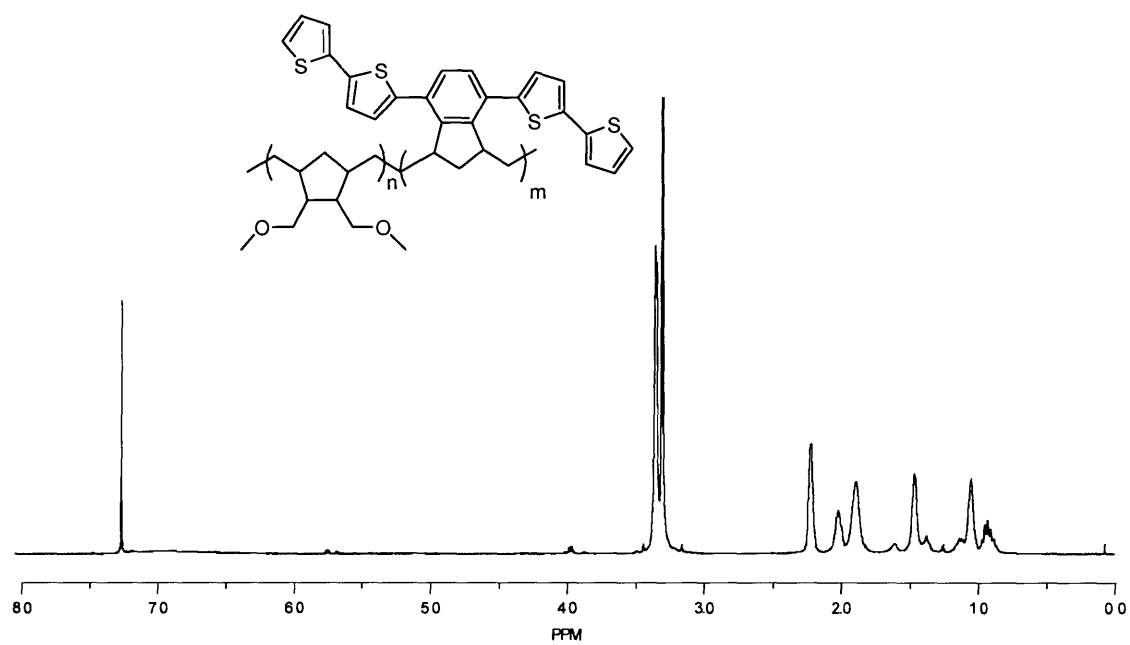
<sup>1</sup>H NMR spectrum of hydrogenated **BCP2** (500 MHz, CD<sub>2</sub>Cl<sub>2</sub>)



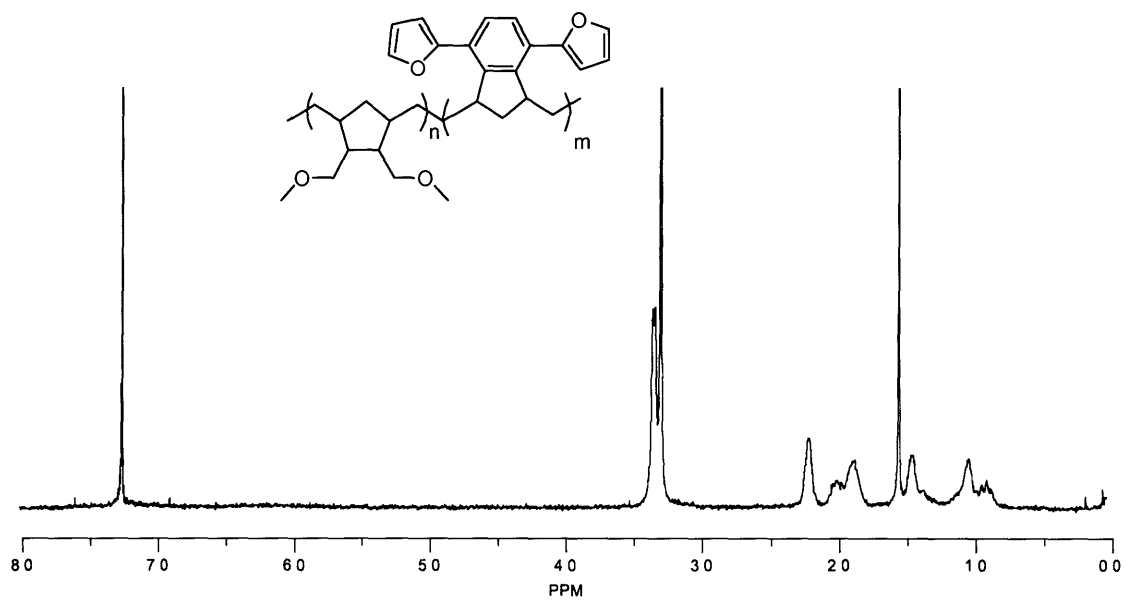
<sup>1</sup>H NMR spectrum of hydrogenated **BCP3** (500 MHz, CD<sub>2</sub>Cl<sub>2</sub>)



<sup>1</sup>H NMR spectrum of hydrogenated **BCP4** (500 MHz, CDCl<sub>3</sub>)

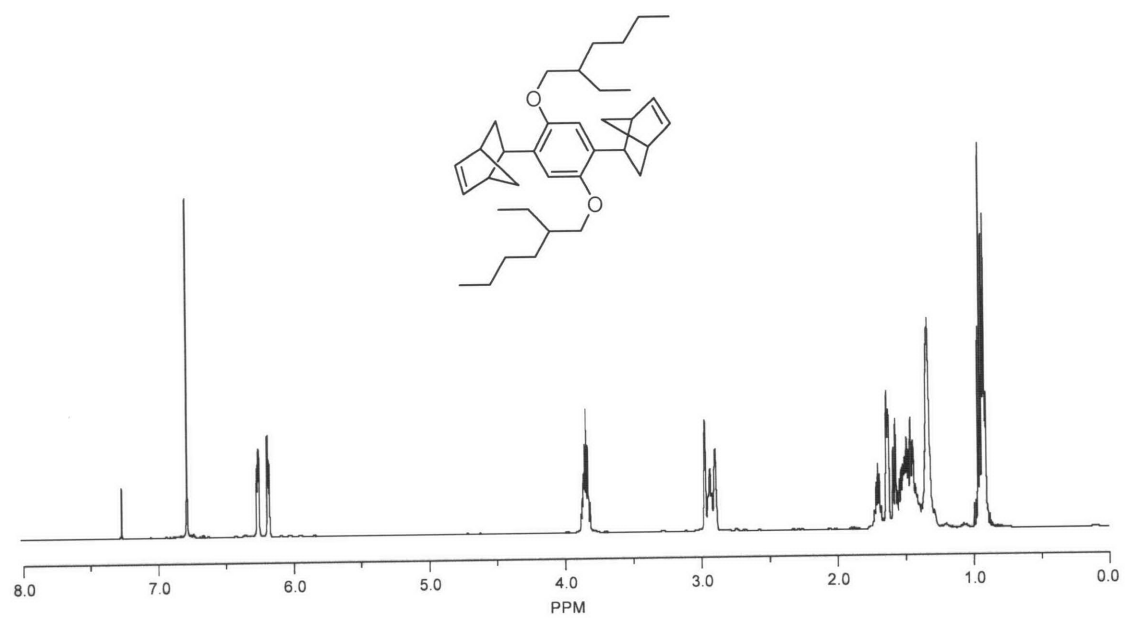


<sup>1</sup>H NMR spectrum of hydrogenated **BCP5** (500 MHz, CDCl<sub>3</sub>)

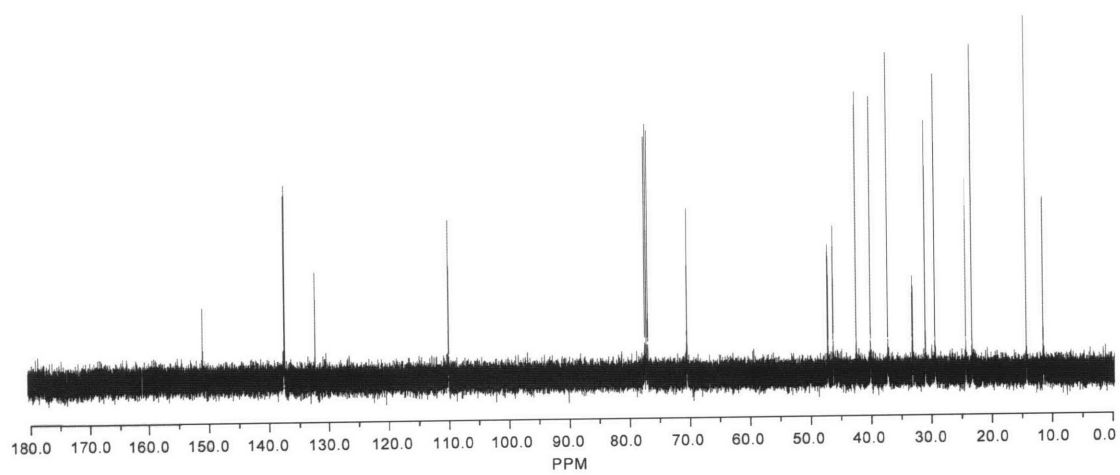


<sup>1</sup>H NMR spectrum of hydrogenated **BCP6** using (300 MHz, CDCl<sub>3</sub>)

**Appendix 2**  
**NMR Spectra for Chapter 2**

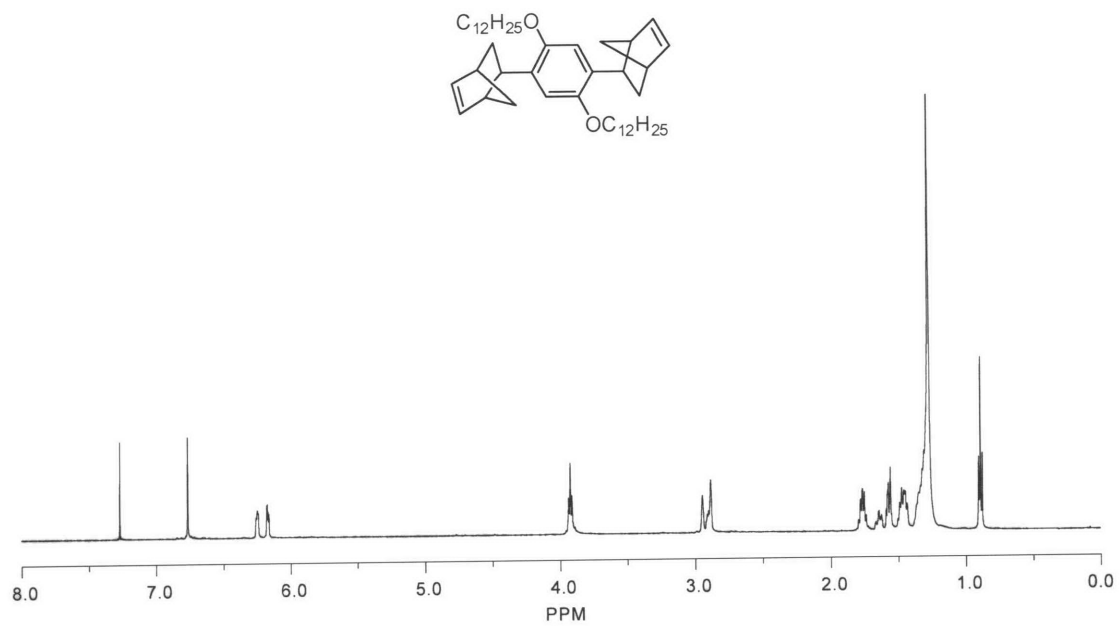


$^1\text{H}$  NMR spectrum of **4** (500 MHz,  $\text{CDCl}_3$ )

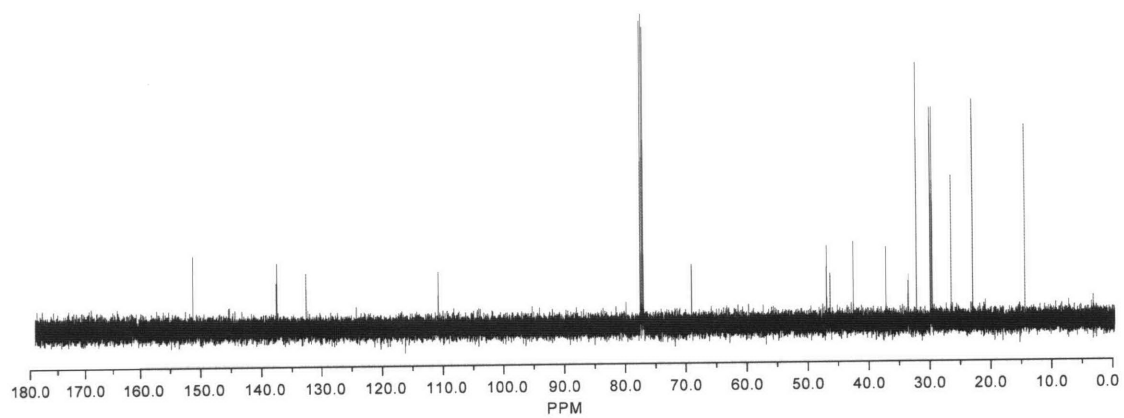


$^{13}\text{C}$  NMR spectrum of **4** (125 MHz,  $\text{CDCl}_3$ )

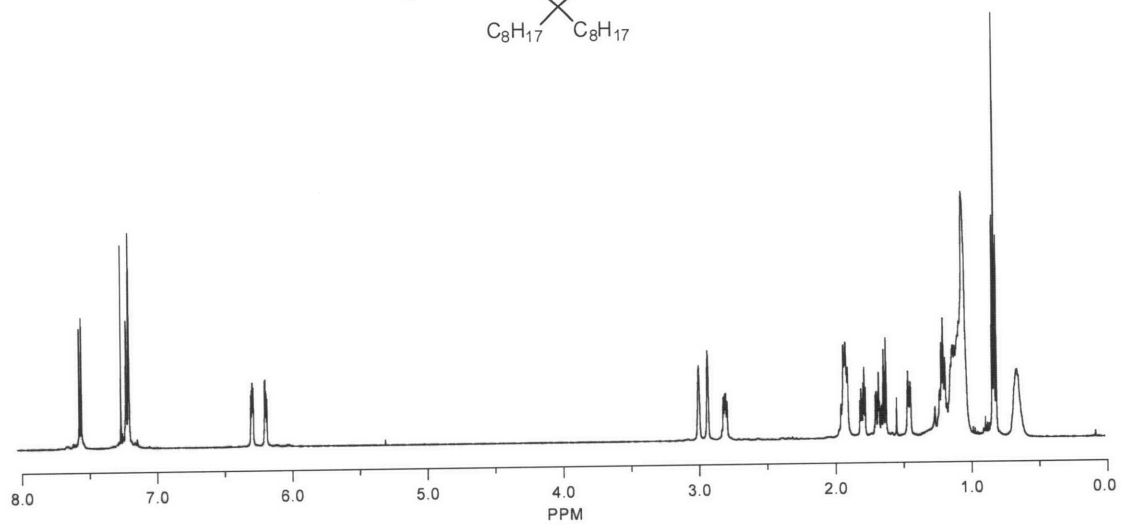
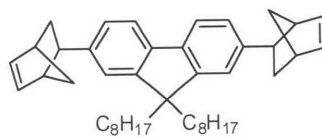




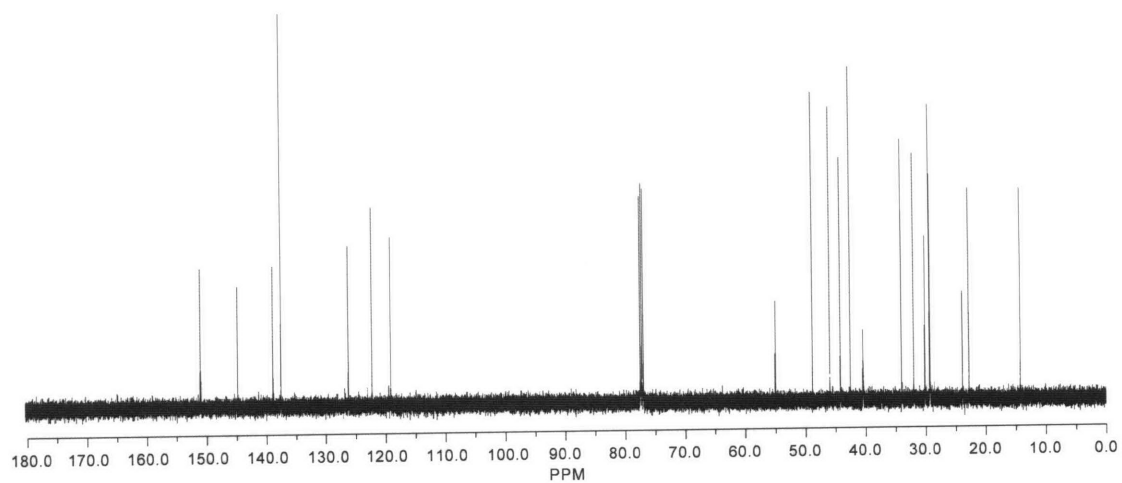
$^1\text{H}$  NMR spectrum of **5** (500 MHz,  $\text{CDCl}_3$ )



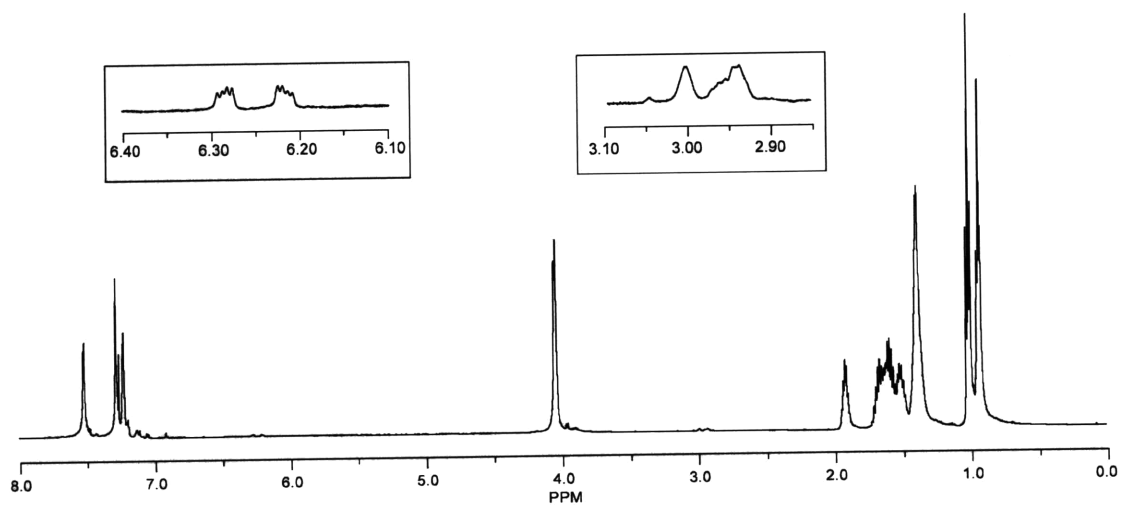
$^{13}\text{C}$  NMR spectrum of **5** (125 MHz,  $\text{CDCl}_3$ )



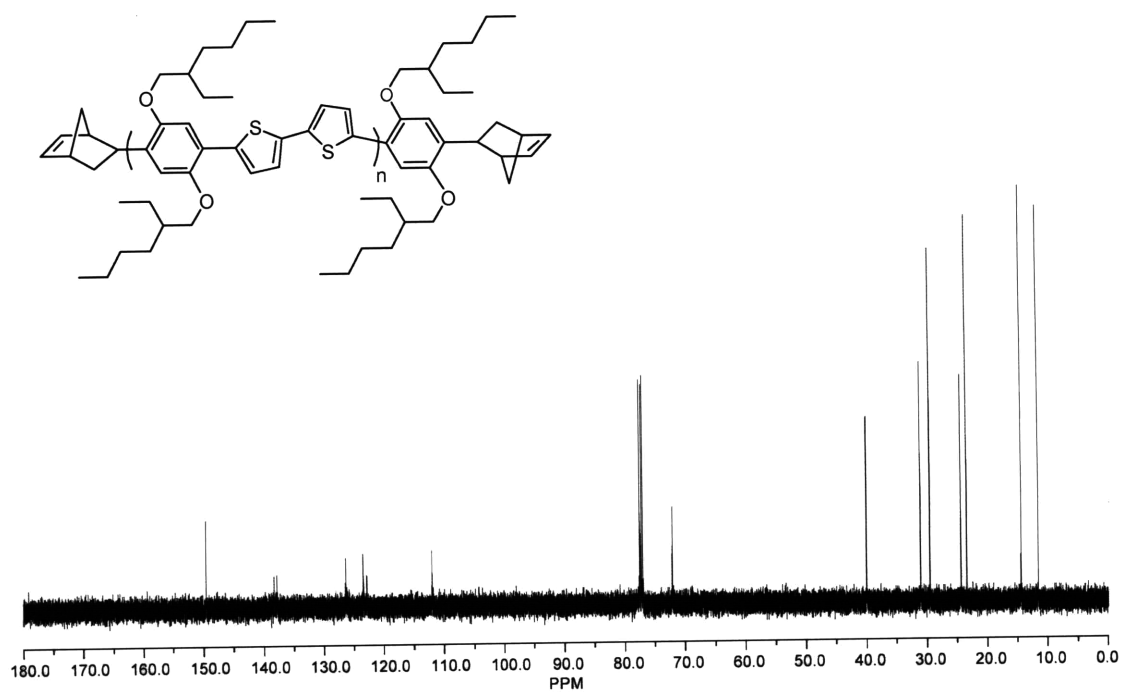
<sup>1</sup>H NMR spectrum of **6** (500 MHz, CDCl<sub>3</sub>)



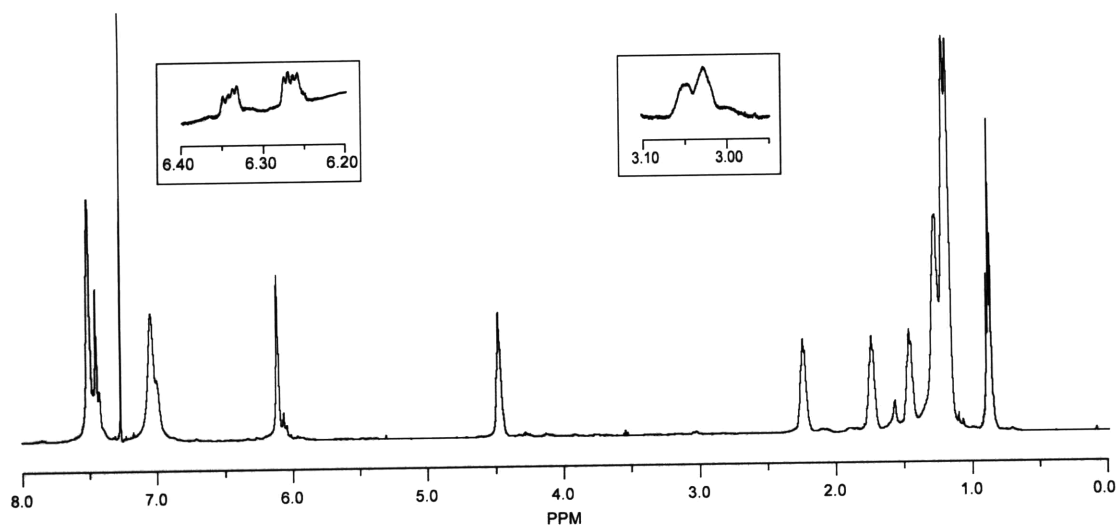
<sup>13</sup>C NMR spectrum of **6** (125 MHz, CDCl<sub>3</sub>)



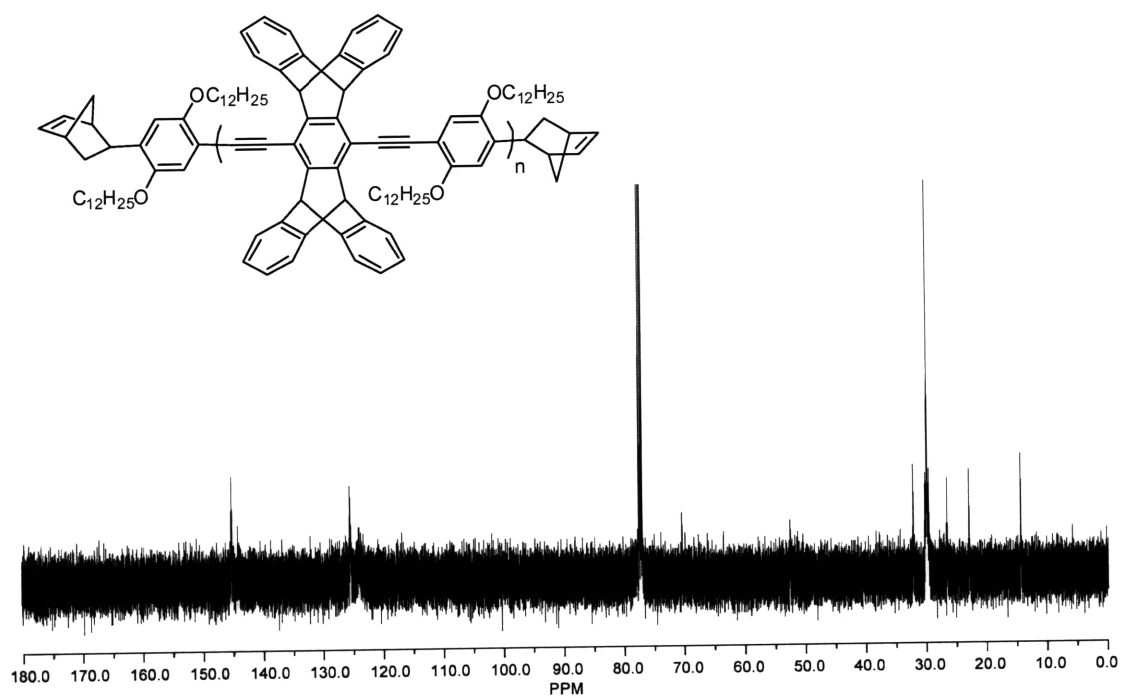
$^1\text{H}$  NMR spectrum of **P4** (500 MHz,  $\text{CDCl}_3$ )



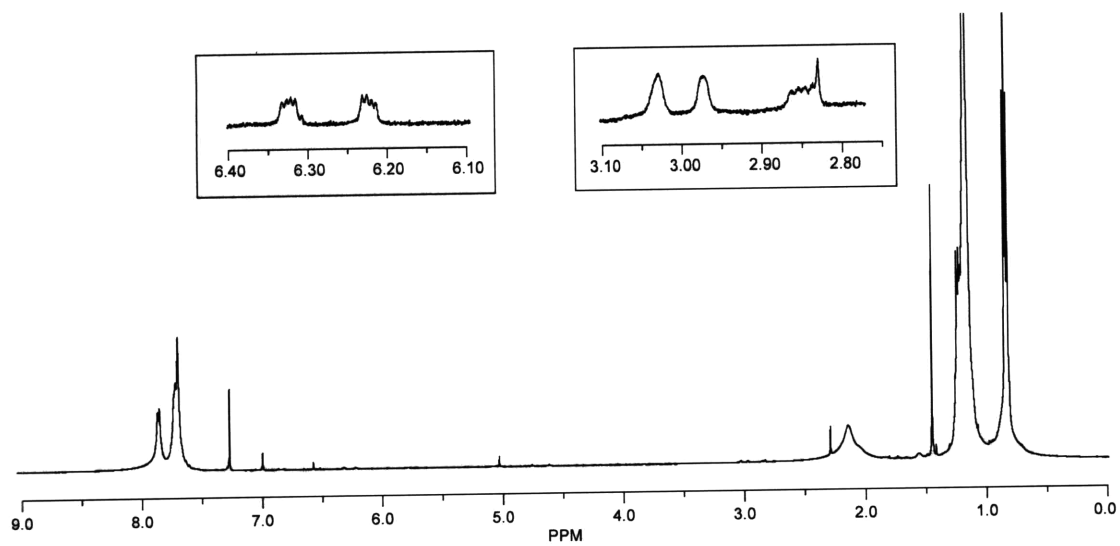
$^{13}\text{C}$  NMR spectrum of **P4** (125 MHz,  $\text{CDCl}_3$ )



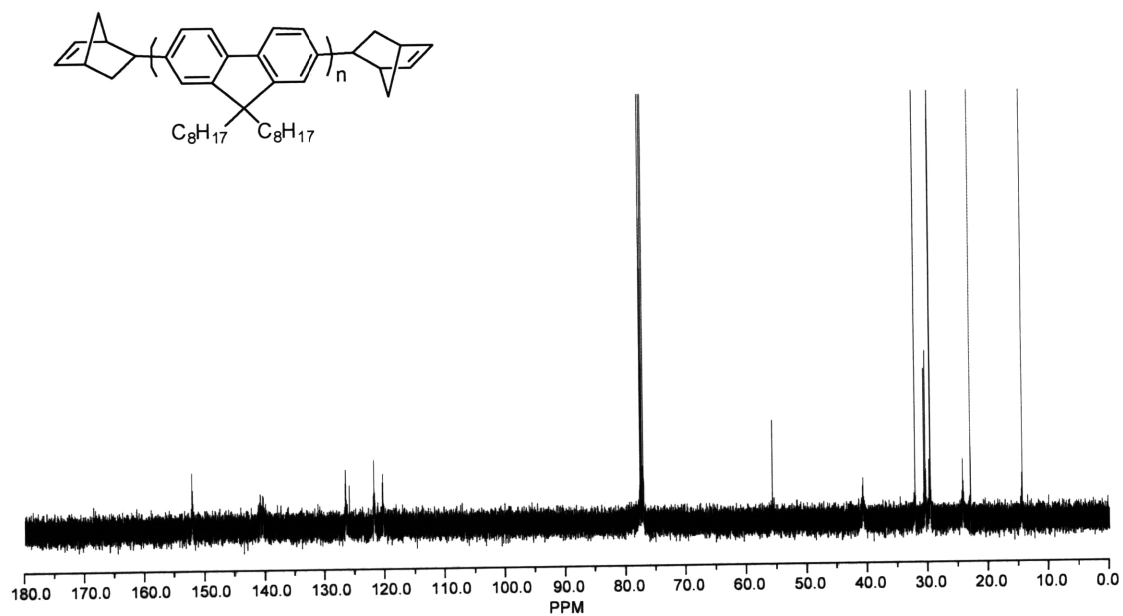
$^1\text{H}$  NMR spectrum of **P5** (500 MHz,  $\text{CDCl}_3$ )



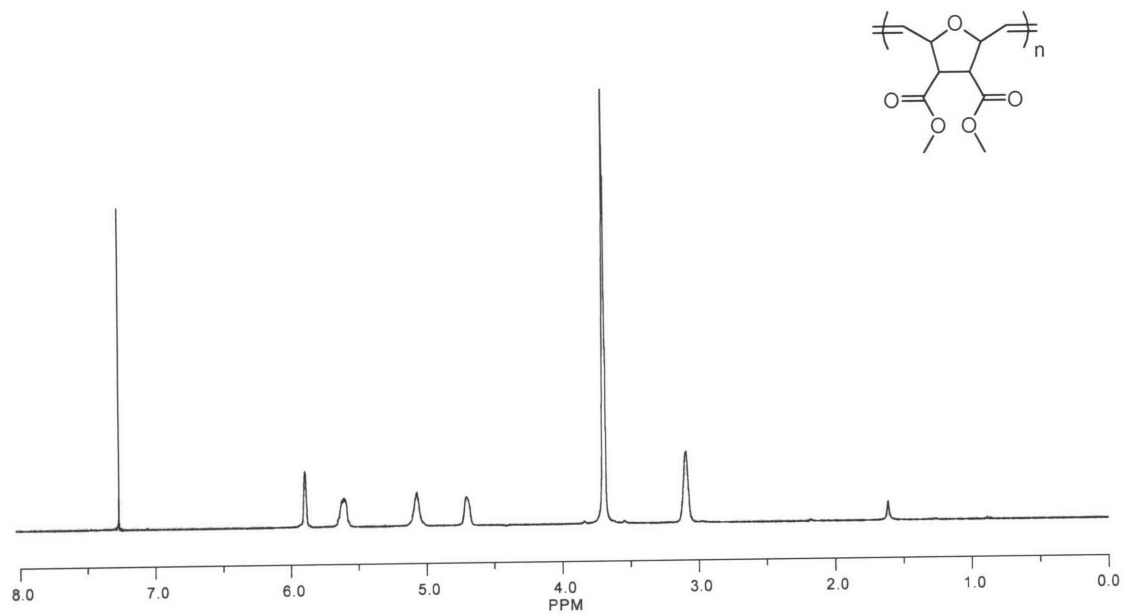
$^{13}\text{C}$  NMR spectrum of **P5** (125 MHz,  $\text{CDCl}_3$ )



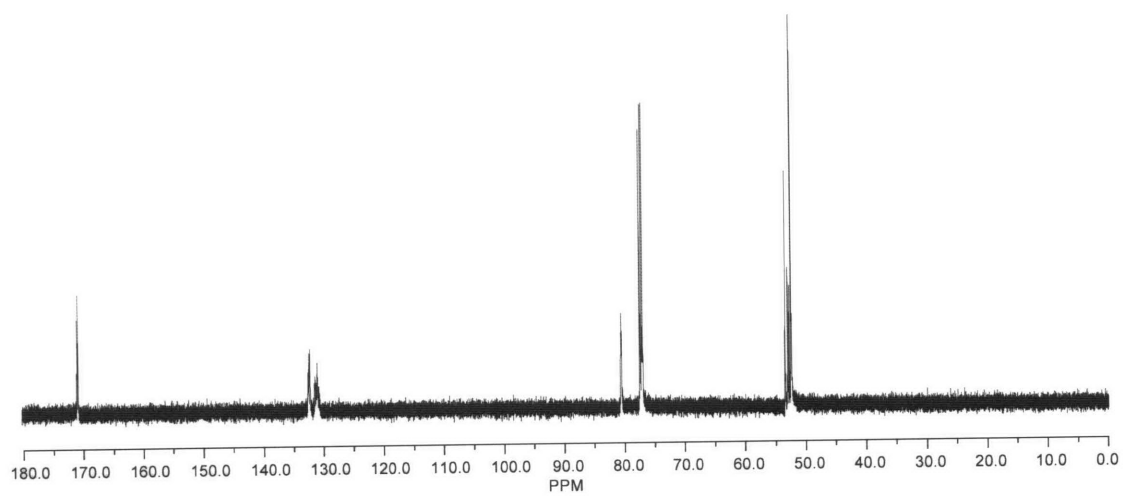
$^1\text{H}$  NMR spectrum of **P6** (500 MHz,  $\text{CDCl}_3$ )



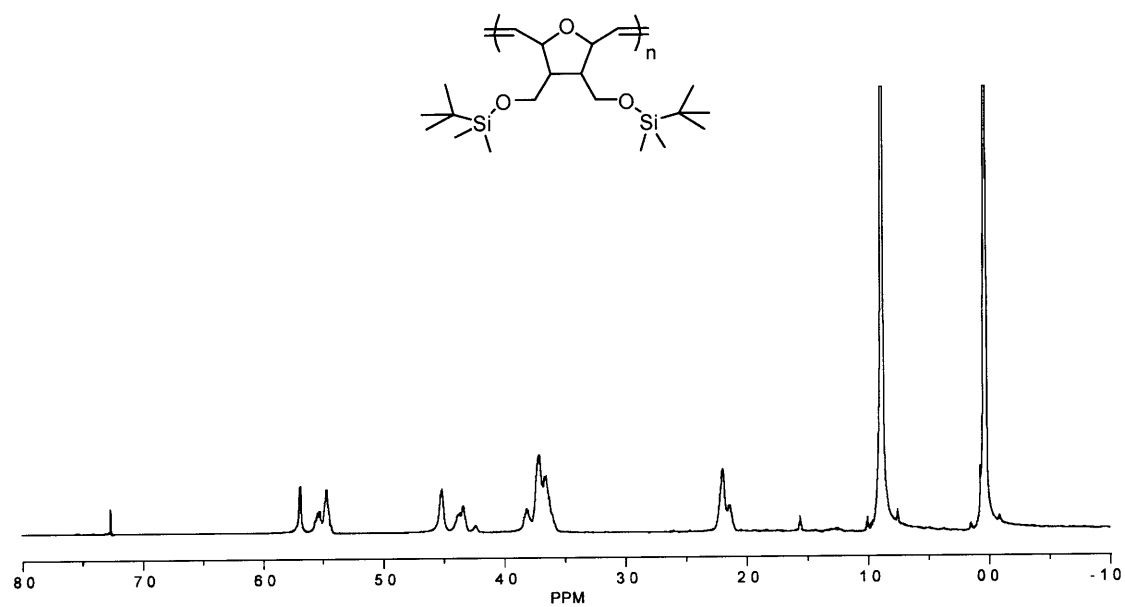
$^{13}\text{C}$  NMR spectrum of **P6** (125 MHz,  $\text{CDCl}_3$ )



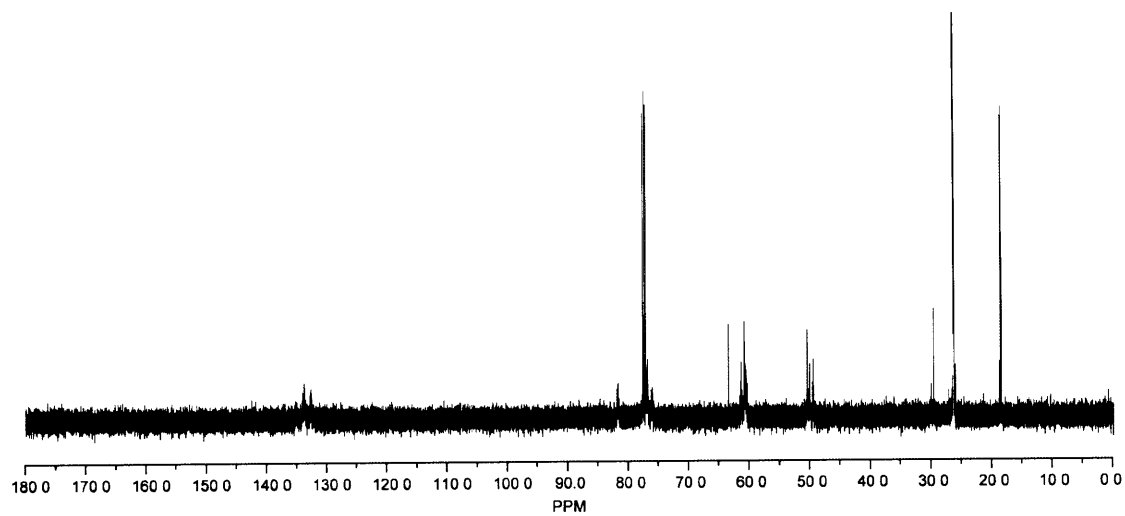
$^1\text{H}$  NMR spectrum of poly(**10**) by **G1** (500 MHz,  $\text{CDCl}_3$ )



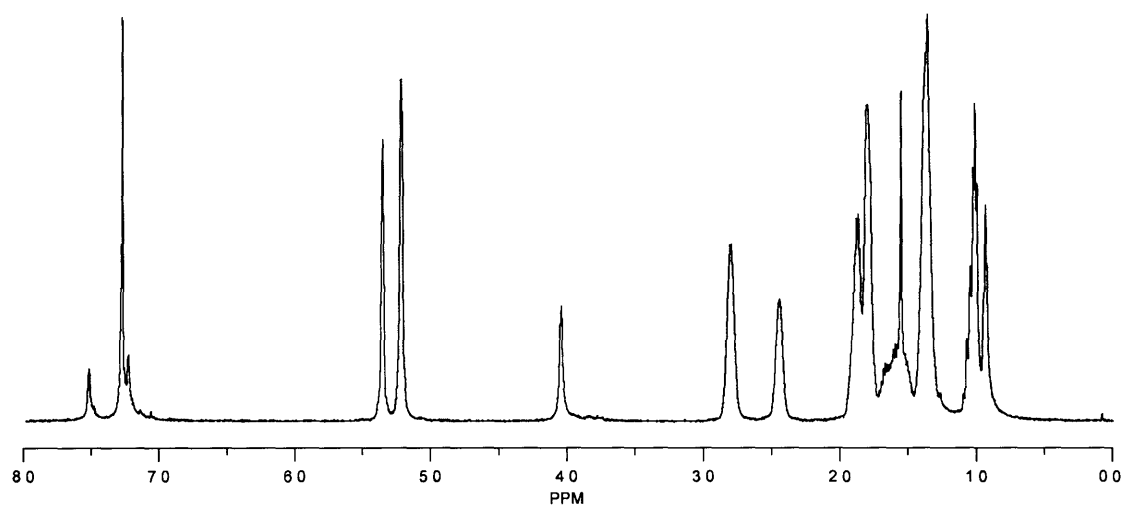
$^{13}\text{C}$  NMR spectrum of poly(**10**) by **G1** (125 MHz,  $\text{CDCl}_3$ )



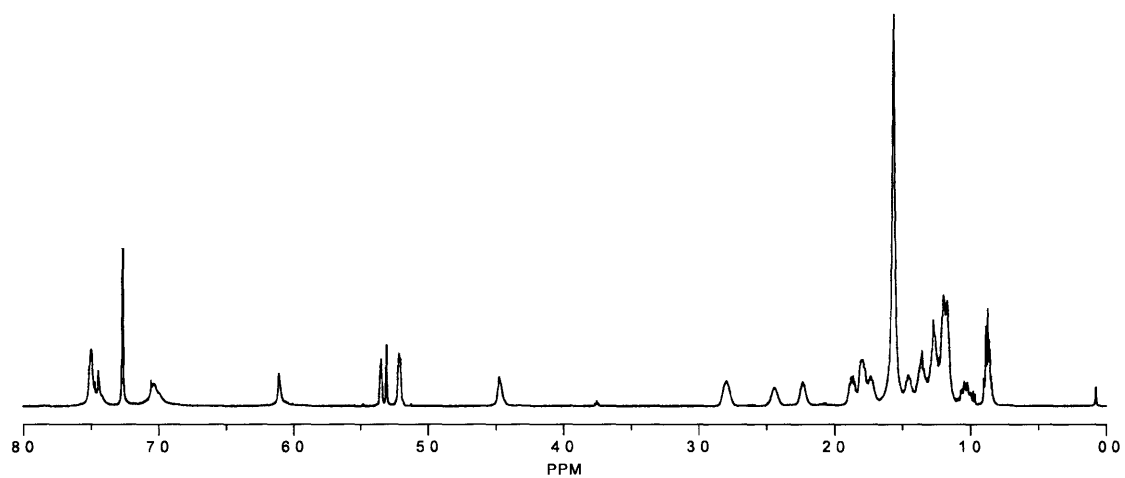
$^1\text{H}$  NMR spectrum of poly(11) by G2 (500 MHz,  $\text{CDCl}_3$ )



$^{13}\text{C}$  NMR spectrum of poly(11) by G2 (125 MHz,  $\text{CDCl}_3$ )

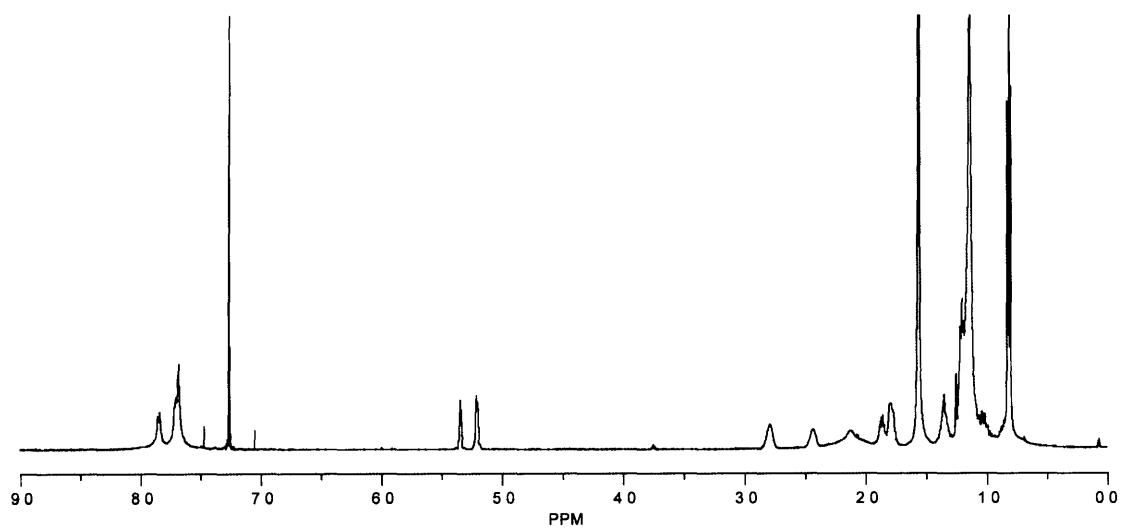


<sup>1</sup>H NMR spectrum of PNB-**P4**-PNB (500 MHz, CDCl<sub>3</sub>)

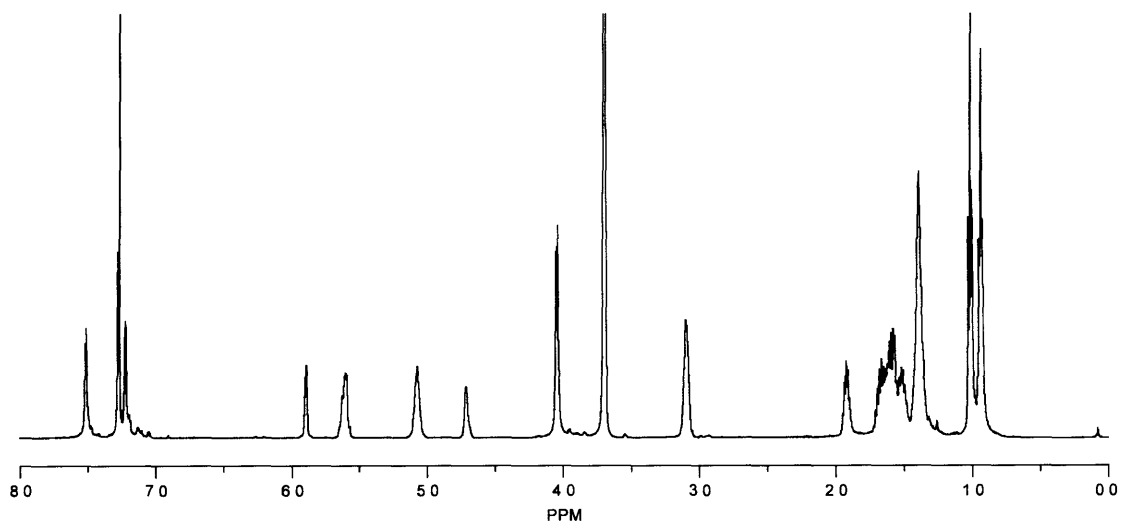


<sup>1</sup>H NMR spectrum of PNB-**P5**-PNB (500 MHz, CDCl<sub>3</sub>)

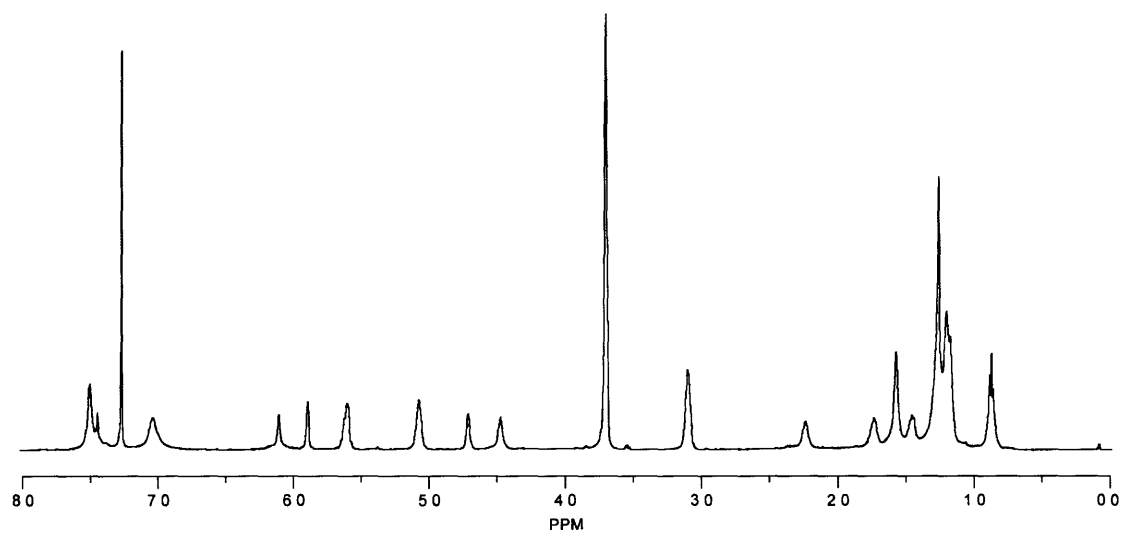




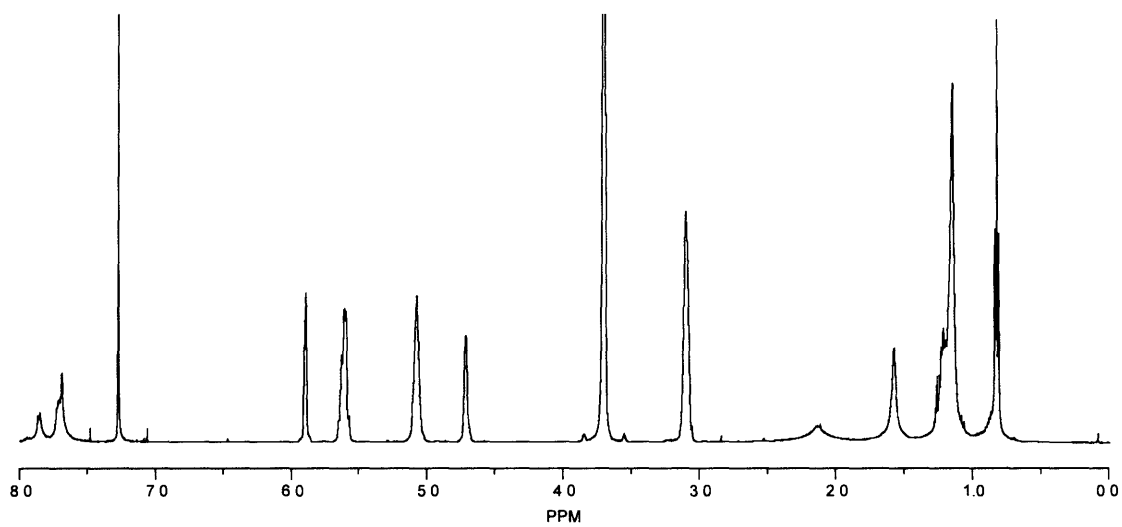
<sup>1</sup>H NMR spectrum of PNB-**P6**-PNB (300 MHz, CDCl<sub>3</sub>)



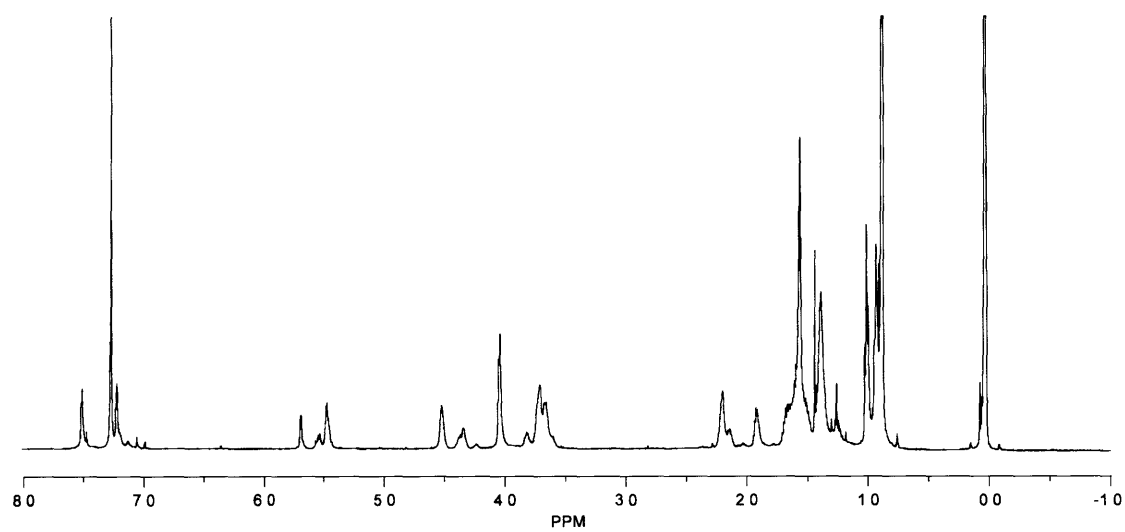
<sup>1</sup>H NMR spectrum of poly(**10**)-**P4**-poly(**10**) (500 MHz, CDCl<sub>3</sub>)



<sup>1</sup>H NMR spectrum of poly(10)-P5-poly(10) (500 MHz, CDCl<sub>3</sub>)

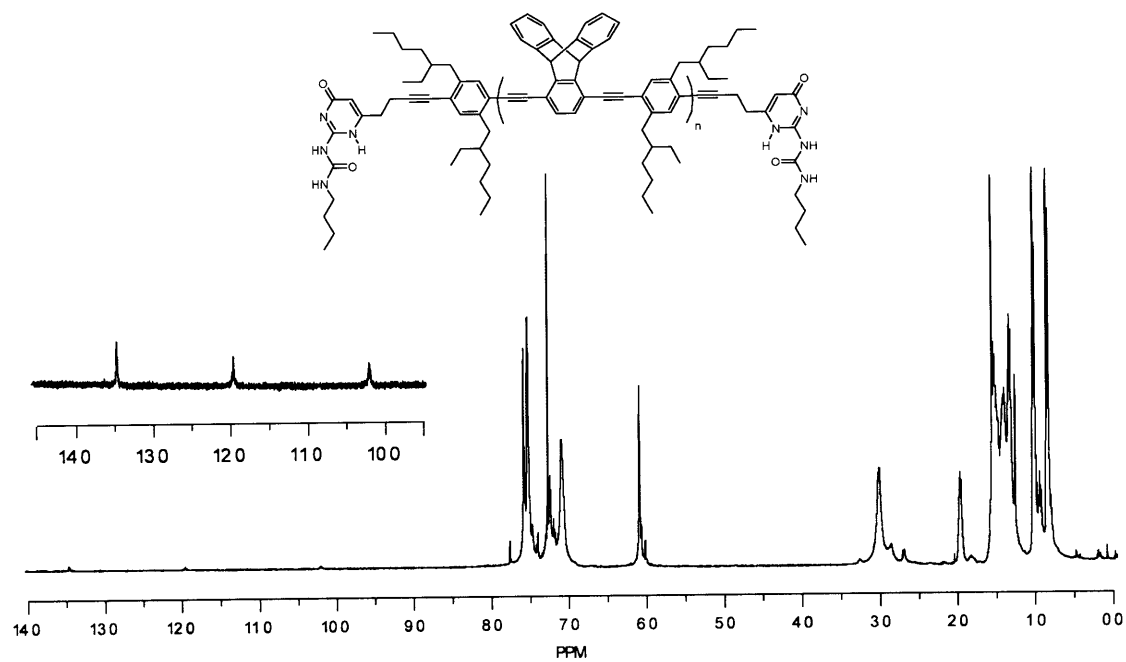


<sup>1</sup>H NMR spectrum of poly(10)-P6-poly(10) (500 MHz, CDCl<sub>3</sub>)

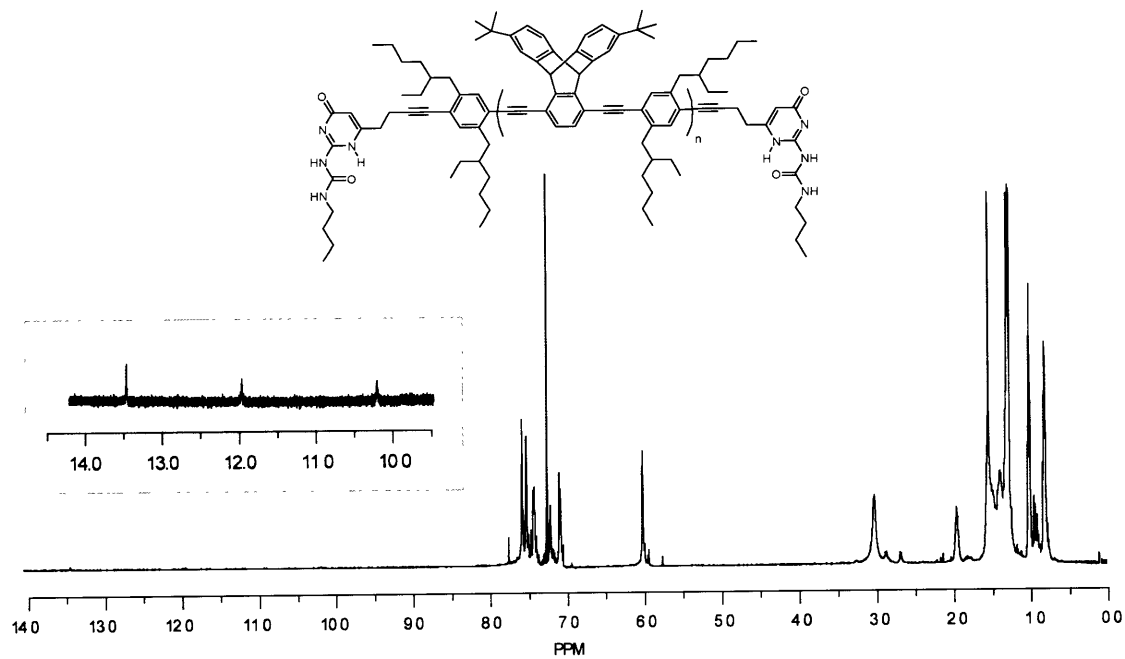


$^1\text{H}$  NMR spectrum of poly(11)-P4-poly(11) (500 MHz,  $\text{CDCl}_3$ )

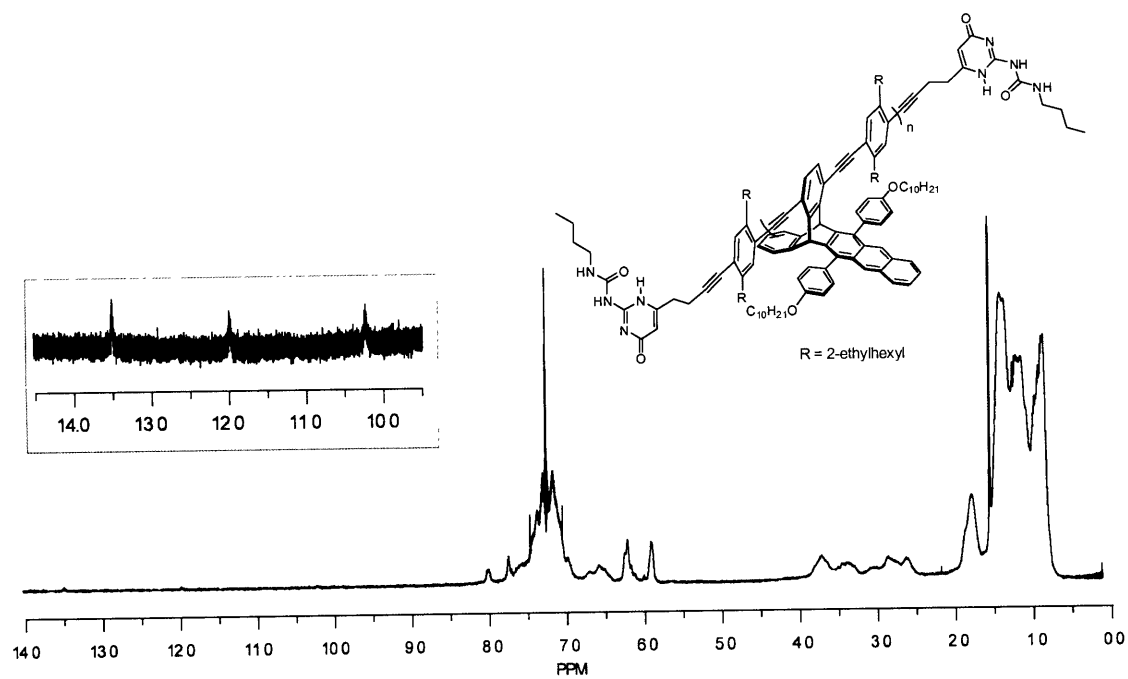
**Appendix 3**  
**NMR Spectra for Chapter 3**



<sup>1</sup>H NMR spectrum of P1 (500 MHz, CDCl<sub>3</sub>)



<sup>1</sup>H NMR spectrum of P2 (500 MHz, CDCl<sub>3</sub>)



$^1\text{H}$  NMR spectrum of **P3** (500 MHz,  $\text{CDCl}_3$ )